

**EFFECTS OF METHYL TERTIARY BUTYL ETHER AND DIESEL EXHAUST
PARTICLES ON *IN VITRO* AND *IN VIVO* VASCULAR FORMATION**

by

JOHN C. KOZLOSKY

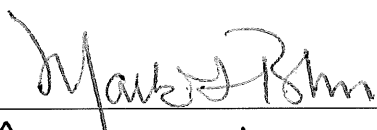
A dissertation submitted to the
Graduate School – New Brunswick
Rutgers, The State University of New Jersey
In partial fulfillment of the requirements

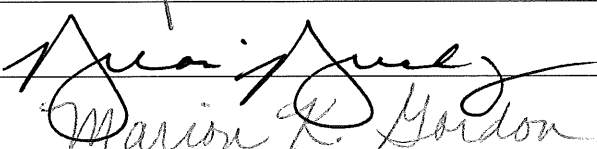
for the degree of

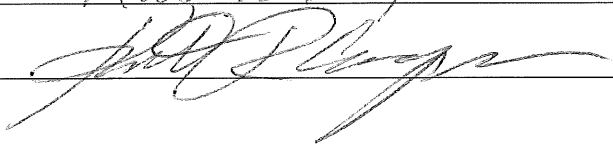
Doctor of Philosophy
Environmental Sciences
Written under the direction of

Professor Keith R. Cooper

and approved by







New Brunswick, New Jersey

January, 2010

ABSTRACT OF THE DISSERTATION

EFFECTS OF METHYL TERTIARY BUTYL ETHER AND DIESEL EXHAUST PARTICLES ON *IN VITRO* AND *IN VIVO* VASCULAR FORMATION

By JOHN C. KOZLOSKY

Dissertation Director: Professor Keith R. Cooper

Hazardous chemicals are released into the environment by a number of natural and anthropogenic activities and may cause adverse effects on human health and the environment. Air pollutants such as volatile organic compounds and respirable particulate material differ in chemical composition and reaction properties, but both can induce acute and chronic effects on human health. Methyl tertiary butyl ether (MTBE) and diesel exhaust particles (DP) are materials that are representative of these two classes of air pollutants. Although MTBE and DP differ physically and chemically, both have the potential to affect the vasculature.

Previous studies in this laboratory reported that exposure to MTBE halted embryonic vascular formation in the model teleost Japanese medaka (*Oryzias latipes*). The embryonic vasculature failed to develop while other non-vascular tissues developed normally. Based upon these findings, studies were undertaken to determine if MTBE would alter vascular formation in other model systems. Exposure of cultured rat brain endothelial cells to MTBE (0.34 - 34.0 mM) resulted in a dose-dependent reduction of microcapillary formation,

with the LOAEL at 0.34 mM. Tertiary butyl alcohol (TBA), a major metabolite of MTBE, was also tested. TBA (0.34 - 34.0 mM) had no effect on microcapillary formation. In a mouse Matrigel plug implantation assay, Matrigel plugs containing MTBE (34.0 mM) showed a complete lack of vessel formation compared to plugs containing Endothelial Cell Growth Supplement without MTBE. Treatment of HUVEC grown on Matrigel with 34 mM MTBE resulted in a decrease in phosphorylation of VEGFR-2 at both the Tyr⁹⁵¹ and Try⁹⁹⁶ phosphorylation sites. In addition, a rat reproductive study was used to test the antiangiogenic effects of MTBE *in vivo*. Timed-pregnant Fisher 344 rats were dosed orally by gavage with MTBE (500 - 1500 mg/kg) from implantation through gestation. Tissues from one half of the pups of each sex from each litter were examined histologically on post partum Day 1 for developmental vascular changes. The remaining pups from each litter continued to be dosed at the same level as the respective dam on post partum Days 1 to 10, and then were examined as described above. No vascular changes were observed in any of the tissues examined. The *in vitro* data demonstrated that the vasculature is a primary target of MTBE in several model systems if sufficiently high vascular concentrations are obtained and that the observed changes in vascular development may be in part due to inhibition of activation of VEGFR-2. However, in the rodent reproduction assay no histological vascular lesions were observed, which may reflect the inability to achieve high enough circulating MTBE levels.

In addition to the work with MTBE, studies were undertaken to explore the possible effects of DP on vascular formation. Exposure of human umbilical vein endothelial cells (HUVEC) *in vitro* to DP at concentrations of $\geq 25 \mu\text{g/mL}$ resulted in decreases in capillary-like tube formation. Additional *in vitro* studies in HUVEC determined that an organic extract derived from DP also inhibits vascular formation with a LOAEL of $20 \mu\text{g/mL}$ and complete inhibition of vascular formation at $40 \mu\text{g/mL}$ and that the effects are reversible except at the highest concentration of DP tested ($100 \mu\text{g/mL}$). Through the use of several assays and immunocytochemical staining techniques, it was determined that neither apoptosis nor chemical-induced cell death are responsible for the observed inhibitory effects. However, studies did indicate that decreases in activation of Rho GTPases may be involved in the inhibition of HUVEC vascular tube formation. Vascular formation would appear to be a sensitive target for both MTBE and organic compounds absorbed onto diesel exhaust particles. One of the mechanisms by which they prevent proper endothelial cell migration and tube formation may be due to disruption of the VEGF pathway in association with the cytoskeletal structure of the cells.

ACKNOWLEDGEMENTS

I would like to express my sincere thanks to Dr. Keith Cooper and Dr. Marion Gordon whose encouragement and understanding have guided me through this endeavor from the inception. I would also like to thank Dr. Greg Cosma and Dr. Raja Mangipudy for providing me with the support needed to see this project through to the end. In addition, I would like Dr. Carolyn Moyer for the endless hours of discussion over VEGF and immunocytochemistry. Finally, I would like to acknowledge my many colleagues at Bristol Myers Squibb, especially Lillie Penn, Julie Gerow, Toni Albanese, Katie Dubrow, Annette Pierri, Alicja Batog, Russ Gullo, and Laura Marthaler, for allowing me to tap into their extensive array of technical and scientific expertise.

DEDICATION

This dissertation is dedicated to my wife, Donna, whose love has supported me all of the way through my final goal and to my daughter Danielle who fills my life with joy every minute of every day.

TABLE OF CONTENTS

ABSTRACT OF THE DISSERTATION	ii
ACKNOWLEDGEMENTS	v
DEDICATION	vi
TABLE OF CONTENTS	vii
LIST OF ABBREVIATIONS	x
LIST OF TABLES	xiii
LIST OF FIGURES	xiv
INTRODUCTION.....	1

CHAPTER I:

Effects of Methyl Tertiary Butyl Ether on Capillary Endothelial Tube

Formation	25
INTRODUCTION	25
MATERIALS AND METHODS	27
Chemicals and cell culture supplies	27
Primary cultures of endothelial cells from rat brain and <i>in vitro</i>	
angiogenesis.....	27
Murine Matrigel plug implantation assay for <i>in vivo</i>	
angiogenesis	28
Chick chorioallantoic membrane (CAM) assay for <i>in vivo</i>	
angiogenesis.....	29
Reproductive vascular development in the rat.....	30

Immunofluorescence - Phosphorylated VEGFR-2.....	30
Statistics.....	31
RESULTS	32
SUMMARY OF THE DATA	36
FIGURES	38
CHAPTER II:	
Determination of the Possible Effects of Diesel Exhaust Particles on	
Capillary Endothelial Tube Formation.....	52
INTRODUCTION.....	52
MATERIALS AND METHODS.....	53
Cell culture.....	53
Diesel exhaust particles.....	54
Preparation of washed DP and organic extract from particulate material.....	54
Treatments - initial screening for possible effects of DP, DPE, and CB on capillary tube formation <i>in vitro</i>	55
Treatment - equivalent fraction.....	55
Capillary tube formation.....	56
Recovery assay.....	57
ECM cell adhesion assay.....	57
Caspase-9 and caspase-3 activity assays.....	58
Lactate dehydrogenase (LDH) assay.....	58
Annexin V and propidium iodide staining.....	59

Hoechst staining.....	59
DNA fragmentation assay.....	59
Actin cytoskeleton staining.....	60
RhoA, Rac1, and Cdc42 activation.....	60
Statistics.....	61
RESULTS.....	62
SUMMARY OF THE DATA.....	67
FIGURES AND TABLES.....	69
DISSERTATION DISCUSSION AND CONCLUSIONS.....	130
REFERENCES.....	141
VITA.....	156

LIST OF ABBREVIATIONS

α	alpha
β	beta
BETX	benzene, toluene, ethyl benzene, xylenes
CAM	chorioallantoic membrane
CB	carbon black
Cdc42	Cell division control protein 42 homolog
°C	degrees Celcius
CO ₂	carbon dioxide
DMSO	dimethyl sulfoxide
DP	diesel exhaust particles
DPE	diesel exhaust particle organic extract
ECGS	endothelial cell growth supplement
ECM	extracellular matrix
FBS	fetal bovine serum
GAP	GTPase-activating protein
GDP	guanosine diphosphate
GEF	guanine nucleotide exchange factor
GTP	guanosine triphosphate
GTPase	guanosine triphosphate hydrolase
HBSS	Hank's balanced salt solution
Hg	mercury
HUVEC	human umbilical vein endothelial cell

kg	kilogram(s)
L	liter(s)
LC ₅₀	lethal concentration 50 percent
LDH	lactate dehydrogenase
LOAEL	lowest observable adverse effect level
μm	micrometer
m ³	cubic meter(s)
mg	milligram(s)
mL	microliter(s)
mm	millimeter(s)
mM	millimolar
MTBE	methyl tertiary butyl ether
nM	nanomolar
NOAEL	no observable adverse effect level
NSTC	National Science and Technology Council
PAH	polycyclic aromatic hydrocarbon
PI	propidium iodide
PM ₁₀	particulate matter of 10 μ in diameter or less
PM _{2.5}	particulate matter of 2.5 μ in diameter or less
ppm	parts per million
%	percent
R	retardation factor
Rac1	Ras-related C3 botulinum toxin substrate 1

RhoA	ras homolog gene family member A
RFG	reformulated gasoline
TBA	tertiary butyl alcohol
TRITC	rhodamine
Tyr	tyrosine
μ	micron(s)
USEPA	United States Environmental Protection Agency
UV	ultraviolet
VEGF-A	vascular endothelial growth factor A
VEGF	vascular endothelial growth factor
VEGFR-1	vascular endothelial growth factor receptor 1
VEGFR-2	vascular endothelial growth factor receptor 2
WDP	washed diesel exhaust particles

LIST OF TABLES

Table 1. Initial Screen for Effects on *in vitro* Vascular Formation - 4 hours

Table 2. Screen for effects of DPE on *in vitro* vascular formation - 3 hours

Table 3. DPE range-finding - 3 hrs

Table 4. Exposure to DP, DPE, or WDP - 3 hours

Table 5. Recovery of Tube Formation - 18 hours

Table 6. HUVEC Attachment to Components of the ECM

Table 7. Summary of Evaluation of Apoptosis/Cell Death

LIST OF FIGURES

Figure 1. Formation of capillary-like structures by isolated rat brain endothelial cells grown on Matrigel following treatment with MTBE for 48 hours

Figure 2. Rat brain endothelial cell tube formation following 48 hour treatment with 0.34, 3.4, and 34 mM MTBE compared to control tube formation

Figure 3. Representative photographs of Matrigel plugs from the murine Matrigel plug implantation assay following exposure to saline or 34 mM MTBE

Figure 4. Representative photographs of chicken egg chorioallantoic membranes (CAM) following treatment with saline or 34 mM MTBE for 24 hours

Figure 5. Body weights in rat neonates from birth (Day 1) through Day 10 following exposure to 500 - 1500 mg/kg/day MTBE

Figure 6. Tissue weights in rat neonates following exposure to 500 - 1500 mg/kg/day MTBE

Figure 7. Representative images of HUVEC immunostained for phosphorylation of VEGFR-2 at both Tyr⁹⁵¹ and Try⁹⁹⁶ in untreated cells and following treatment with 34 mM MTBE for 4 hours

Figure 8. Preparation of an organic extract from diesel particles (DPE) and washed diesel particles (WDP)

Figure 9. Representative images of *in vitro* HUVEC tube formation following 4 hour exposure to 1, 10, or 100 $\mu\text{g/mL}$ diesel particles, 0.75 or 7.5 $\mu\text{g/mL}$ carbon black, or 1, 3, 10, or 20 $\mu\text{g/mL}$ diesel particle extract

Figure 10. Representative images of *in vitro* HUVEC tube formation following 3 hour exposure to 25, 50, 100, or 200 $\mu\text{g/mL}$ diesel particle extract

Figure 11. Representative images of *in vitro* HUVEC tube formation following 3 hour exposure to 10 - 100 $\mu\text{g/mL}$ diesel particle extract

Figure 12. Representative images of *in vitro* HUVEC tube formation following 3 hour exposure to 25, 50, or 100 $\mu\text{g/mL}$ diesel particles, 10, 20, or 40 $\mu\text{g/mL}$ diesel particle extract, or 15, 30, or 60 $\mu\text{g/mL}$ washed diesel particles

Figure 13. Representative images of *in vitro* HUVEC tube formation following 3 hour exposure to 25, 50, or 100 $\mu\text{g/mL}$ diesel particles, 10, 20, or 40 $\mu\text{g/mL}$ diesel particle extract, or 15, 30, or 60 $\mu\text{g/mL}$ washed diesel particles and subsequent 18-hour incubation with untreated fresh media

Figure 14. HUVEC adhesion to components of the ECM following 3 hour exposure to 10, 20, 30, or 40 $\mu\text{g/mL}$ DPE

Figure 15. Activation of caspase-9 or caspase-3 following 3 hour exposure of HUVEC to 10, 20, 30, or 40 $\mu\text{g/mL}$ DPE

Figure 16. LDH activity following 3 hour exposure of HUVEC to 10, 20, 30, or 40 $\mu\text{g/mL}$ DPE

Figure 17. Representative images of HUVEC immunostained for annexin V and propidium iodide following 3 hour exposure to 25, 50, or 100 $\mu\text{g/mL}$ diesel particles, 10, 20, or 40 $\mu\text{g/mL}$ diesel particle extract, or 15, 30, or 60 $\mu\text{g/mL}$ washed diesel particles

Figure 18. Representative images of HUVEC immunostained with Hoechst (H33342) following 3 hour exposure to 25, 50, or 100 $\mu\text{g/mL}$ diesel particles, 10, 20, or 40 $\mu\text{g/mL}$ diesel particle extract, or 15, 30, or 60 $\mu\text{g/mL}$ washed diesel particles

Figure 19. DNA fragmentation following 3 hour exposure of HUVEC to 10, 20, 30, or 40 $\mu\text{g/mL}$ DPE

Figure 20. Immunocytochemical staining of the actin cytoskeleton with TRITC-conjugated Phalloidin in HUVEC treated with 10, 20, 30 or 40 $\mu\text{g/mL}$ DPE

Figure 21. RhoA, Rac, and Cdc42 activity following exposure of HUVEC to 10, 20, 30, or 40 $\mu\text{g/mL}$ DPE

INTRODUCTION

Hazardous chemicals are released into the environment by a number of natural and anthropogenic activities and may cause adverse effects on human health and the environment. Combustion of fossil fuels is one of the major sources of pollutants in the atmosphere. Air pollutants such as volatile organic compounds and respirable particulate material differ in chemical composition and reaction properties, but both can induce acute and chronic effects on human health. Methyl tertiary butyl ether (MTBE) and diesel exhaust particles (DP) are materials that are representative of these two classes of air pollutants and were examined in this thesis.

Although MTBE and DP differ physically and chemically, both have the potential to affect the vasculature. The studies reported in this dissertation attempt to identify the mechanism by which vascular endothelial cells are the target for MTBE and DP. The physical, chemical, and biological properties of these compounds are discussed below.

MTBE - Overview of Use

MTBE is an organic solvent that has been used primarily as an octane booster since 1977 in the production of gasoline. More recently, MTBE has been added to gasoline to increase the oxygen content to meet certain requirements of the Clean Air Act (Hakansson, et al., 2001; Wang, et al., 2002). MTBE has historically ranked third as the most produced organic chemical in the United

States. In 1995 17.6 billion pounds were produced. Due to numerous reports of MTBE being detected in both surface and groundwater across the country, MTBE is being phased out within the United States. Wintertime oxygenated fuels contained as much as 15% by volume, while reformulated gasoline contained 11%. Levels in conventional grade gasoline ranged from 2 to 8%. MTBE is also approved for therapeutic use for dissolving cholesterol gallstones in the gallbladder (Leuschner, 1986).

With the increased use of MTBE over recent years by both the medical community and the petroleum industry there is potential exposure to organisms in the environment and the human population. Workers in the petroleum industry exposed to MTBE began reporting a high incidence of neurologic symptoms, including headaches, dizziness, and nausea (Moolenaar, et al., 1994; Prah, et al., 1994). While these symptoms are suggestive of vascular involvement, little information is available on the direct effects of MTBE on vasculature. Studies examining the effects of MTBE at concentrations from 10 – 300 ppm in the Japanese medaka (*Oryzias latipes*) developing embryo resulted in a unique lesion of the developing vasculature. The embryonic vasculature failed to develop, while other non-vascular tissues developed normally until vascularization became essential for further development (Kozlosky, et al., 1996). This initial observation was the justification for examining MTBE's effect on the vascular system in higher organisms and whether there was a risk of damage to developing blood vessels.

In the 1970's, MTBE started being used as an octane booster replacing tetraethyllead, primarily in mid and high grade gasoline. In this role MTBE has been added to gasoline at concentrations as high as eight percent by volume. In 1990, the Clean Air Act Amendments began requiring the use of reformulated and oxygenated gasoline in an attempt at reducing atmospheric carbon monoxide levels in areas that were not meeting National Ambient Air Quality Standards set by the USEPA. Since MTBE was already being used as an octane enhancer, use at even higher concentrations as an oxygenating agent was an easy solution toward meeting the new regulations.

The combustion of gasoline in motor vehicle engines is not complete. Products of this incomplete combustion include the emission of carbon monoxide, volatile organic compounds, and nitrous oxides. From these, and other emission products, hazardous chemicals are produced through reaction with ultra-violet light and other reactive substances. These compounds can cause a variety of health and air quality problems. The addition of oxygen in the form of MTBE promotes a more complete combustion of the gasoline resulting in the emission of carbon dioxide instead of carbon monoxide.

The Oxygenated Fuel (Oxyfuel) and Reformulated Gasoline (RFG) programs were initiated by the USEPA in 1992 and 1995 respectively to meet ambient air quality standards set by the 1990 Clean Air Act Amendments. The Oxyfuel Program requires the use of gasoline with 2.7% oxygen by weight in areas with high levels of carbon monoxide during the fall and winter seasons. The RFG Program, designed to reduce the emission of volatile organic

compounds and nitrogen oxides, requires 2.0% oxygen by weight throughout the year in those areas with the highest levels of air pollution. To meet the Oxyfuel oxygen weight requirement, MTBE has been added at a concentration of 15% by volume into gasoline, while to meet the RFG oxygen weight requirement, MTBE is added at a concentration of 11% by volume (USEPA, 1998).

In addition to use as a fuel oxygenate and octane enhancing agent, MTBE is used clinically as a cholesterol gallstone solvent. Patients treated in this way have MTBE delivered directly to their gall bladders through catheter tubes that are surgically inserted (Leuschner, 1986). It is also used in the manufacture of isobutene (Budavari, 1996).

MTBE - Physical and Chemical Properties

MTBE is a clear, colorless ether with a molecular weight of 88.15 g/mole, density of 0.7404 g/mL, and a structural formula of $(\text{CH}_3)_3\text{C}-\text{O}-\text{CH}_3$ (Budavari, 1996). It has a specific gravity of 0.744, a boiling temperature of 53.6-55.2°C, and a vapor pressure of 245 mm Hg at 25°C (NSTC, 1997).

MTBE has a high water solubility of approximately 50,000 mg/L (NSTC, 1997). This solubility can result in high concentrations of MTBE from gasoline in surface and ground water. For example, the water solubility of MTBE in gasoline containing 10% MTBE would be 5,000 mg/L whereas the total hydrocarbon solubility of non-oxygenated gasoline is approximately 120 mg/L (Poulsen, et al., 1992).

Taste and odor thresholds for MTBE range between 5 and 15 ug/L. Based upon these thresholds and animal toxicity data, a drinking water advisory for MTBE has been set by the USEPA in the range of 20 to 40 ug/L (USEPA, 1997). A drinking water advisory is a recommended guideline but it is not enforceable by the USEPA.

In a USEPA fact sheet (USEPA, 1998), several reasons were listed to demonstrate why MTBE is preferred as a gasoline oxygenate over others such as ethanol. MTBE is especially favorable in warm weather because it produces a reduction in the vapor pressure of gasoline. This reduction decreases the volatility of the components which leads to a reduction in smog producing chemicals. MTBE is also less expensive to distribute and is easier to blend than other oxygenates. It can be produced at the refinery and the gasoline can be transferred through existing pipelines (Squillace, et al., 1997).

MTBE - Environmental Fate and Transport

Releases of MTBE into the environment can occur from many sources. The sources can be classified into two categories, point sources and non-point sources. A point source is a discharge from a discrete point location such as a pipe or a leaking underground fuel storage tank. Non-point sources are more extensive and include urban runoff, automotive emissions, and atmospheric deposition. Some of the major release sources for MTBE include industrial manufacturing or gasoline blending sites; spills during the storage, distribution, and transfer of blended gasoline; from spills, leaks, and emissions at service

stations; and from incomplete combustion (Brown, 1997). Petroleum refineries account for approximately 1.4 million kilograms of the MTBE released into the atmosphere each year. Amounts from sources such as vehicle emissions and evaporative loss were estimated to have totaled approximately 43 tons of MTBE per day in California alone (USEPA, 1998).

If MTBE is released into the atmosphere it will exist almost entirely in the vapor phase. The fate of most of the MTBE in the atmosphere will be dispersion and dilution in the troposphere where it will then be photooxidized. The half-life of MTBE in the atmosphere has been calculated to be between 2.8 and 6.1 days depending upon the hydroxyl radical concentration in the air (Bennett, et al., 1990). Direct photolysis by UV absorption is not expected to be an important removal process because MTBE will not absorb light above 290 nm (Calvert, et al., 1966).

MTBE in the atmosphere tends to partition into atmospheric water, including precipitation (Squillace, et al., 1997). MTBE removed from the atmosphere by precipitation will be directly introduced into surface water and shallow ground water (Pankow, et al., 1997). If MTBE-contaminated air comes into contact with uncontaminated water, the MTBE will be expected to condense from the atmosphere into the water. Volatilization and condensation are complementary processes that allow the exchange of MTBE across an air-water interface. Volatilization refers to the movement of MTBE from water into the atmosphere, while condensation refers to the movement of MTBE from the

atmosphere into water. Both processes are driven by the concentration gradient between the air and the water.

MTBE is expected to volatilize into the atmosphere when contaminated surface water comes in contact with uncontaminated air. The rate of volatilization from surface water is affected by several factors including the flow rate of the water, air and water temperature, wind velocity, and water depth (Pankow, et al., 1996). The estimated half-life of MTBE from streams, rivers, and lakes are 2.5 hours, 9.5 hours, and 137 days respectively (USEPA, 1993). Summer conditions of air and water temperatures can decrease the half life of MTBE in a body of water by a factor of two or three (Pankow, et al., 1996). MTBE is not expected to significantly adsorb to sediment or suspended particulate matter (Fujiwara, et al., 1984).

In groundwater, the mobility of MTBE is high. The mobility of a compound in groundwater can be described through that compounds retardation factor (R). The retardation factor is the ratio of the velocity of the water to the velocity at which a compound is being transported within that water. MTBE exhibits a retardation coefficient of 1.0 which indicates the compound will migrate through the soil at the same rate as groundwater (Hubbard, et al., 1994). Other compounds commonly found in groundwater contaminated with gasoline, such as members of the BTEX group (benzene, toluene, ethyl benzene, and xylenes) all exhibit retardation coefficients higher than 1.0 and tend to move slower than the flow of groundwater. Should groundwater become contaminated with fuel containing MTBE, the leading edge of the plume will contain mainly MTBE with

little or no BTEX contamination. Also, the vertical distribution of MTBE within the plume will be slightly deeper and wider than BTEX compounds (Davidson, et al., 1996). MTBE will be one of the first contaminants to be detected in drinking water wells following a gasoline leak or spill.

MTBE is very water soluble compared to the BTEX compounds and other components in gasoline. The solubility of pure liquid MTBE in water is about 50,000 mg/L whereas the next most-soluble component of gasoline, benzene, has a water solubility of 1,780 mg/L (Mancini & Stubblefield, 1997). However, the water solubility of MTBE is reduced when it is present in a mixture such as gasoline. This is due to a cosolvency effect for MTBE with the remaining components of the gasoline mixture. With a gasoline-water partitioning coefficient of 15.7, MTBE will tend to partition preferentially to the gasoline (Poulsen, et al., 1992). A gasoline that is 10 percent by weight MTBE, reduces the solubility of MTBE in water to about 5,000 mg/L (Squillace, et al., 1997).

Water solubility is the most important chemical property affecting the partitioning of organic compounds between water and subsurface solids. In a sand aquifer having an organic carbon content of 0.1% and assuming a MTBE concentration in the groundwater of 3.0 µg/mL, only about 8% of the total MTBE present would adsorb to the aquifer organic material. In contrast, under the same conditions, about 40% of the total benzene would be adsorbed to the subsurface solids (Squillace, et al., 1997).

MTBE released into the soil will be expected to volatilize rapidly. It will be expected to exhibit very high mobility and may leach into ground water. It will not

be expected to hydrolyze in soil and sorbs only weakly to subsurface solids (Fujiwara, et al., 1984). In one study by Shaffer and Uchrin (1997), the sorptive and degradative characteristics of MTBE were examined in three (Cohansey sand, acid washed sand, and Neshaminy clay) water/soil systems under both oxic and anoxic conditions. All three soil systems exhibited uptake of MTBE under oxic conditions. This uptake was attributed to aerobic activity in the acid washed sand and clay samples. The only soil to exhibit uptake under anoxic conditions was the Cohansey sand sample. This uptake was attributed to sorption because the Cohansey soil also readily adsorbs to other gasoline components (Uchrin, et al., 1992).

The biodegradability of MTBE in the subsurface soil is substantially slower than BTEX fuel components. MTBE will persist in the groundwater under both aerobic and anaerobic conditions because of its resistance to physical, chemical, and microbial degradation (Squillace, et al., 1996). This slower degradation is due, in part, to the relatively unreactive tertiary carbon bond structure of the molecule (Sulflita and Mormile, 1993).

MTBE - Exposure

For the general population, the activities that lead to the highest possibility for exposure to MTBE were those involving the use of automobiles. Refueling, commuting to work, and operating an automobile as part of employment accounted for the highest MTBE exposure levels (Lioy, et al., 1994). In one study, during refueling, the highest concentrations of MTBE in the personal

breathing zone of the individuals tested were found to be 0.11 ppm (Lindstrom, et al., 1996) while in a similar study, Lioy, *et al.* (1994) found the mean MTBE concentrations to be 0.3 ppm. In automobile cabin interiors, Vayghani and Weisel (1999) found the MTBE concentration during refueling exceeded 1 ppm. The estimated mean dose for the general population exposed through the air while commuting, refueling, and during residential exposure was found to be in the range of 0.004 – 0.06 mg/kg-day (Lin, et al., 2005; Hakkola and Saarinen, 2000).

The general public may also be exposed to MTBE through the use of contaminated water (Ayotte, et al., 2005; Moran, et al., 2005; Kolb and Puttmann, 2006). The mean dose through ingestion of drinking water, inhalation during showering, and dermal absorption while bathing was found to be 0.0014 mg/kg-day (Brown, 1997). Exposure levels to MTBE were 1.2 to 4 times higher in individuals living in close proximity to gasoline stations than the levels experienced by the general population. It has also been estimated that the daily dose levels to young children are 10 to 20% higher than the doses to adults living in the same area due to differences in their levels of activity such as breathing and drinking rates (Froines, et al., 1998).

Working with MTBE or gasoline containing MTBE in occupations such as gas station attendant, automobile mechanic, or fuel production and distribution worker can lead to inhalation or dermal exposures at the ppm level throughout the entire work shift (Vainiotalo and Ruonakangas, 1999). In Stamford, Connecticut, auto mechanics were found to have daily MTBE exposures ranging

from 0.03 ppm to as high as 12.0 ppm (White, et al., 1995). The exposure of Finnish tanker drivers to MTBE during loading and delivery was between 13 and 91 mg/m³ (Hakkola and Saarinen, 1996). Predicted doses of MTBE for tanker drivers in California were found to be approximately two-fold higher than the estimated values listed above for the general population (Froines, et al., 1998). Lifetime doses for workers in areas of the United States where MTBE is used were calculated to be in the range of 0.01 to 0.1 mg/kg-day (Brown, 1997).

MTBE - Affect on Reproduction and Development

In one- and two-generation reproductive studies, rats exposed to MTBE via inhalation showed no adverse effects at dose levels up to 3000 ppm (Biles, et al., 1987; Bevan, et al., 1997). No reproductive or developmental effects were seen in rats dosed via inhalation at concentrations up to 2500 ppm (Conaway, et al., 1985). The results of one *in vitro* study showed that MTBE inhibited cell growth in rat fibroblasts by causing an accumulation of cells in the s-phase of the cell cycle (Sgambato, et al., 2009).

In mice, inhalation exposure levels of 4000 and 8000 ppm produced a reduction in implantations. Embryotoxic effects were also seen including decreased pup viability and skeletal malformations such as cleft palate, scrambled and fused sternebra, and angulated ribs. In this study, the NOAEL for parental and developmental toxicity was 400 ppm and for reproductive toxicity was at least 8000 ppm (Conaway, et al., 1985). Mice exposed to 8000 ppm MTBE via inhalation for 4 and 8 months exhibited decreases in relative uterine

and ovarian weight compared to controls (Moser, et al., 1998). Human exposures are expected to be 1000 to 10,000 times lower than the NOAEL's found in these studies; therefore, it is unlikely MTBE will cause reproductive or developmental toxicity in humans.

Diesel Exhaust Particles (DP) - Physical and Chemical Properties

Epidemiological studies have shown that, in addition to liquid air pollutants like MTBE, particulate pollution has become a major concern both in occupational settings and for the population in general. Exposure to particulate matter in ambient air, especially with a diameter less than 10 μm (PM_{10}), is associated with increased morbidity and mortality caused by respiratory diseases, however, particles with a diameter less than 2.5 μm ($\text{PM}_{2.5}$) have recently been shown to be more closely related to the respiratory effects and subsequent mortality (Pope, et al., 1995; Pope, et al., 2004; Samet, et al., 2000; Peters, et al., 1997; Kappos, et al., 2004).

A predominant constituent of $\text{PM}_{2.5}$ in urban and industrial areas is diesel exhaust (Vogt, et al., 2003; Almeida, et al., 2006; Yue, et al., 2006). Diesel exhaust particles (DP) consist of carbon nuclei resembling carbon black that absorb a wide array of organic compounds including a variety of polycyclic aromatic hydrocarbons (PAH), heterocyclic organic compounds, quinones, aldehydes, aliphatic hydrocarbons, and nitro-PAHs (Akiyama, 2006; Bayona, et al., 1988; Draper, 1986; Li, et al., 2000; Schuetzle, et al., 1981; Schuetzle, 1983). In the diesel engine and exhaust system, particles form in three stages. In the

first stage, particles are formed from cracking, pyrolysis, dehydrogenation, and pyrosynthesis. These primary particles range in size from 0.001 to 0.01 μm in diameter and represent the carbon nuclei mentioned above. In the second phase, spherical particles of 0.01 to 0.05 μm in diameter form through condensation where organic and other compounds condense on the surface of the carbon nuclei. In the last phase, the soot particles form clusters and chains in a process termed coagulation forming particles reaching 0.1 to 0.2 μm in diameter (Kim, et al, 2002; Kittleson, 1998). These are the particles that are primarily released from diesel engines.

DP - Partitioning in the Environment

Source appointment studies of $\text{PM}_{2.5}$ report diesel and gasoline vehicles are the major source of particulate matter (Maykut, et al., 2003; Schauer, et al., 1996; Watson and Chow, 2001; Palmgren, et al, 2003); however, diesel engines emit as much as 100 times the elemental carbon and 20 times the organic carbon as compared to gasoline engines (U.S. EPA, 2004). Additional emissions result from numerous off-road sources such as lawn mowers, tractors, snow mobiles, construction equipment, trains, and marine vessels (U.S. EPA, 2002).

Diesel exhaust particles released from a source are immediately diluted into the atmosphere. Diffusion and transport processes occur simultaneously to dilute the particles up to 1000 times the concentration exiting from the source under typical roadway conditions (Zielinska, 2005). In the atmosphere, organic compounds bound to particles can chemically react with the environment.

Important reactions for these particle-bound organics include photolysis, reactions with ozone, and nitration with NO_2 , HNO_3 , and N_2O_5 . Examples of these reactions are shown through laboratory studies performed using PAHs. PAHs and nitro-PAHs are known constituents of the organic layer of diesel particles (Akiyama, 2006; Bayona, et al., 1988; Draper, 1986; Li, et al., 2000; Schuetzle, et al., 1981; Schuetzle, 1983). These compounds are also known toxicants and may be responsible for many of the toxicities observed with diesel particles.

Photolysis studies performed by Behymer and Hites, showed that the extent of photodegradation of PAH absorbed to different types of particulate matter varied with the nature of the particle to which they were absorbed. PAH were stabilized if the carbon black content of the particle was greater than 5%. On black particles, the half-life of PAHs was on the order of several days (Behymer and Hites, 1985, 1988). Since diesel particles consist of a carbon nuclei resembling carbon black, the PAH absorbed to these particles should be stable under normal atmospheric conditions.

Studies have reported the reaction of particle-bound PAHs with ozone. Using simulated atmospheric conditions, reactions with ozone were shown to occur quickly. Half-lives of one to several hours were determined (Pitts, et al., 1980, 1986). In an animal study, instillation of diesel particles that had been exposed to ozone for 48 hours prior to dosing into the lung of rats potentiated the inflammatory and cytotoxic effects observed with untreated particles (Madden et al., 2000). In addition to reactions with ozone, several studies by Pitts and co-

workers have shown that nitration reactions occur when PAHs absorbed to various substrates are exposed to different simulated atmospheres (Pitts, et al., 1978; Pitts, et al., 1985a; Pitts, et al., 1985b; Pitts, et al., 1985c).

Removal of diesel particles from the atmosphere can occur through either dry or wet deposition. Dry deposition is the settling or impacting of particles from the atmosphere on to surfaces such as soil, vegetation, water, or man-made structures, and the subsequent physical attachment to, or chemical reaction with, these surfaces. Wet deposition refers to the removal of particles from the air by rain, snow, clouds, or fog. Larger particles can be removed from the air within a few hours; however, particles of less than 1 micron are removed less efficiently. These smaller particles can have atmospheric residence times of up to several days making them readily breathable (Dolske and Gatz, 1985; Zielinska, 2005).

DP - Exposure

Fine particles penetrate deep in the lung and deposit in the alveolar space where the toxic organic compounds can leach from the particles, reach the endothelium, and cause direct damage to endothelial cells or be absorbed into the blood (Gerde, et al., 2001). The particles as a whole can also translocate from the lungs into the blood where they are barely recognized by phagocytic cells (Borm and Kreyling, 2004; Geiser, et al., 2005; Nemmar, et al., 2002; Nemmar, et al., 2004). In the blood, both the organic and particulate components can be transported to organs and tissues far removed from the point

of initial exposure where they may play a role in diesel particle induced toxicity (Elder and Oberdorster, 2006; Ma and Ma, 2002).

DP - Affects on Reproduction and Development

Examples of extrapulmonary toxicity can be found in epidemiologic studies conducted in North and South America, Asia, and Europe where exposure to particulate air pollution during pregnancy can be linked with low term birth weight, intrauterine growth retardation, preterm birth, perinatal mortality, and birth defects (Wang, et al., 1997; Dejmek et al, 1999; Dejmek, et al., 2000; Xu, et al., 1995; Pereira, et al., 1998; Ha, et al., 2001; Loomis, et al., 1999; Lipfert, et al., 2000). In animal studies, female mice exposed to DP during pregnancy had significantly lower uterine weights than the control mice (Tsukue, et al., 2002). Prenatal exposure to diesel exhaust has also been associated with decreases in offspring body weight in mice (Fujimoto, et al., 2005). These findings may be indicative of an impairment of blood flow between mother and fetus as a result of altered angiogenesis.

Pregnancy causes changes in maternal circulation that are necessary for the supply of nutrients, the excretion of embryonic metabolic products, gas exchange, protective immunity, and cardiopulmonary function to support growth of an embryo. In the early stages of pregnancy, the blood vessels that link the maternal and fetal circulation are not yet formed. Both DP and organic fractions extracted from particulate material have been shown to have direct effects on endothelial cells *in vitro*, possibly due to oxidative stress resulting from the

formation of active oxygen species (Bai, et al., 2001; Sumanasekera, et al., 2007; Hirano, et al., 2003; Ying, et al., 2009). In the lungs of mice treated with DP, histopathologic evaluations have shown disruption of capillary endothelial cells and detachment of endothelium from the basement membrane. (Ichinose, et al., 1995). In addition, treatment of cultured human umbilical vein endothelial cells (HUVEC) with carbon black, a mimetic for the nuclei of diesel exhaust particles, inhibited the formation of gap junctions, induced vacuole formation, and inhibited cell proliferation (Yamawaki and Iwai, 2006). Since an adequate blood supply is required for normal development of the fetus, these studies suggest that exposure to DP during gestation may impair the early development of the placental boundary through the inhibition of blood vessel formation or angiogenesis.

Development of Hypothesis

Workers in the petroleum industry exposed to MTBE began reporting a high incidence of symptoms suggestive of vascular involvement, including headaches, dizziness, and nausea (Moolenaar, et al., 1994; Prah, et al., 1994). *In vivo* and *in vitro* experimental studies indicate exposure to MTBE can induce production of reactive oxygen species and lipid peroxidation (Li, et al., 2007; Li, et al. 2008; Li, et al., 2009; Sgambato, et al., 2009). Exposure to particulate matter in ambient air, especially with a diameter less than 10 μm (PM_{10}), is associated with increased morbidity and mortality caused by respiratory diseases (Pope, et al., 1995; Pope, et al., 2004; Samet, et al., 2000; Peters, et al., 1997;

Kappos, et al., 2004). As with MTBE, proposed mechanisms for the effects associated with particulate matter are related to oxidative stress including production of reactive oxygen species (Bai, et al., 2001; Becker, et al., 2005), initiating inflammatory responses (Salvi, et al., 1999), and disrupting vascular function (Hansen, et al., 2007). Subsequent to the damage caused to the lung and other tissues by these reactive processes, tissue repair mechanisms will be initiated. Angiogenesis is essential for this type of tissue repair and remodeling, and chemicals which inhibit this process may result in a prolonged disease state.

Tissue damage is repaired through replacement of the injured tissue by regeneration of native parenchymal cells. This mechanism involves the close coordination and interaction between the various cell types of the tissue, including the vasculature to supply essential nutrients. The tightly regulated repair response can be disrupted if toxic agents such as MTBE or DP persist in the damaged area. Chronic exposure to sufficiently high concentrations of these toxicants may impair normal revascularization of damaged tissues or normal angiogenesis.

Angiogenesis is a key factor in many human diseases such as cancer, diabetic retinopathy, arthritis, and atherosclerosis (Folkman, 1995; Carmeliet and Jain, 2000). The process of angiogenesis is a highly organized sequence of events that include initiation, protease production, and the migration and differentiation of endothelial cells. Each step is controlled to meet the requirements of the tissue into which the vessel is growing. Angiogenesis can be mediated by growth factor stimulation of endothelial cells. Vascular endothelial

growth factor A (VEGF-A) is one of the most potent pro-angiogenic growth factors identified. VEGF-A is essential for the formation of a normal vascular network during embryonic development and the continued development of blood vessels during the neonatal period (Dunan, et al., 2003; Carmeliet, et al., 1996; Ferrara, et al., 1996; Gerhardt, et al., 2003; Gerber, et al., 1999). Specific VEGF-A isoforms and concentration gradients are important for neovessel pattern formation as is molecular cross-talk between different cell types for vessel maturation (Gerhardt, et al., 2004; Gerhardt, et al., 2003; Benjamin, et al., 1998).

Two growth factor receptors, vascular endothelial growth factor receptor-1 (VEGFR-1 or flt-1) and vascular endothelial growth factor receptor-2 (VEGFR-2, flk-1, or KDR), participate in VEGF-A signal transduction in vascular endothelial cells. Both receptors are membrane-spanning receptor tyrosine kinases that bind VEGF-A, but their effects on signaling are very different. Mice lacking VEGFR-2 have little or no blood vessel formation, suggesting that many downstream effects of VEGF on endothelial cells are mediated through this receptor (Shalaby, et al., 1995). In contrast, mice lacking VEGFR-1 show vascular overgrowth and disorganization (Fong, et al., 1995).

Microcapillary formation also relies on cell adhesion events mediated by cell surface receptors for extracellular matrix (ECM) proteins. Of these receptors, the integrins, have a vital function in the process of angiogenesis. On the outside of the cell, integrins bind to ECM proteins like fibronectin, vitronectin, laminin I, and collagen IV. Inside the cell, integrins bind elements of the cytoskeleton as well as various signaling proteins (Vouri, 1998). Integrins are heterodimeric

proteins consisting of one α and one β subunit. At least 20 combinations of these subunits are possible with each recognizing one or several ECM proteins (Eliceiri and Cheresh, 1998). Of these possible combinations, integrin $\alpha_v\beta_3$ is of special interest in the process of angiogenesis.

Integrin $\alpha_v\beta_3$ is a receptor for ECM ligands with an exposed Arg-Gly-Asp peptide sequence including vitronectin and fibrinogen (Cheresh, 1987; Leavesky, et al., 1992; Cheresh, 1993). In non-dividing endothelial cells integrin $\alpha_v\beta_3$ is expressed only at low levels. Initiation of angiogenesis promotes expression of integrin $\alpha_v\beta_3$ on the proliferative endothelial cells but not in the pre-existing, quiescent cells (Brooks, et al, 1994a). Antibodies against the integrin $\alpha_v\beta_3$ will inhibit normal vessel growth but do not disrupt pre-existing vessels (Brooks, et al., 1994a). Inhibition of attachment of integrins to the ECM may be one mechanism by which compounds disrupt angiogenesis.

Antagonists of integrin $\alpha_v\beta_3$ have been shown to selectively activate endothelial cell p53 and increase the expression of the p53-inducible cell cycle inhibitor p21^{WAF1/CIP1} (Stromblad, et al., 1996). Induction of p53 activity in cells undergoing DNA synthesis can lead to apoptosis. Administration of $\alpha_v\beta_3$ antagonists has also been shown to induce apoptosis in growth factor- or tumor cell-activated blood vessels (Brooks, et al., 1994b). If integrin binding to the ECM is disrupted in endothelial cells leading to the inhibition of angiogenesis, investigations into the events involved in the apoptotic cascade can be used as a link to identifying this mechanism.

During the development of the vascular network, endothelial cells first form a solid cord of cells. These cells eventually form a lumen and become capable of carrying blood. Studies using *in vitro* models where endothelial cells are plated on reconstituted basement membrane or embedded in three dimensional collagen gels form cell networks that resemble capillary structures *in vivo*. These studies indicate that interactions between the extracellular matrix and integrins, and signaling events involving cytoskeletal elements, control endothelial cell migration and shape and drive the capillary morphogenesis of endothelial cells (Davis, et al., 2002; Davis, et al., 2000; Davis and Camarillo, 1995; Kniazeva and Putnam, 2009).

The morphogenic changes observed in endothelial cells during capillary formation, along with the associated changes in cell shape and migration, have been shown to be related to the actin cytoskeleton (Davis, et al., 2002). Remodeling of the actin cytoskeleton is controlled by actin binding proteins including those involved in monomer sequestering, nucleating, filament severing, depolymerizing, and capping activities (Pollard and Borisy, 2003). Of these proteins, the Rho family of GTPases is of major importance. The Rho GTPases cycle between GTP-bound active states and GDP-bound inactive states. The activation is controlled by guanine nucleotide exchange factors (GEFs) that catalyze the exchange of GDP for GTP (Schmidt and Hall, 2002). Inactivation is controlled through GTPase-activating proteins (GAPs) that stimulate intrinsic GTPase activity (Etienne-Manneville and Hall, 2002). In endothelial cells, VEGF-A has been shown to be responsible for regulation of Rho GTPases and

organization of the cytoskeleton. VEGF-stimulated Rho GTPase activation is very short-lived with the levels of the active proteins falling back to baseline within minutes (Lamallice, et al., 2004; van Nieuw Amerongen, et al., 2003, Zeng, et al., 2002, Ren, et al., 1999).

Studies indicate that cytoskeletal contractile forces established through the actin cytoskeleton may be responsible for the organization of endothelial cells into pre-capillary cords and eventually into tubes with a lumen. During morphogenesis, contractility of the cytoskeleton allows endothelial cells to transmit mechanical forces through the extracellular matrix. These forces form tension-based guidance pathways that allow for the organization of endothelial cells into interconnecting cords and provide pattern organization without the requirement of cell to cell contact (Vernon and Sage, 1995; Davis and Camarillo, 1995; Korff and Augustine, 1999). These contractile forces can also regulate the size and diameter of lumen formation (Sieminski, A.L., et al., 2004).

The contractile forces generated within endothelial cells and transmitted through the extracellular matrix are mediated by actin filaments. The forces are controlled through actin polymerization and bundling of polymerized actin into stress fibers (Whelan and Senger, 2003; Hong, et al., 2004). Bundling of polymerized actin into stress fibers is induced by the GTPase RhoA (Liu and Senger, 2004; Hong, et al., 2004). Inhibition of RhoA activity inhibited VEGF-A induced organization of endothelial cells into blood vessels and resulted in disorganized growth patterns and disruption of capillary blood vessels (Hoang, et al., 2004; Cascone, et al., 2003).

Other members of the Rho GTPase family have been shown to be involved in endothelial cell and capillary vessel morphogenesis and stability. Rac1 promotes assembly of the VE cadherin-catenin-actin complex to stabilize endothelial cell-cell junctions and stimulates motility through formation of lamellipodia, Cdc42 regulates the polymerization of actin to produce hair-like protrusions called filopodia, and both Rac1 and Cdc42 are required for lumen formation (Bayless and Davis, 2002; Cascone, et al., 2003). Inhibition of Rac1 function in endothelial cells *in vivo* inhibited growth factor-induced angiogenesis *in vivo* and activated Rac1 promotes recruitment of integrin $\alpha_v\beta_3$ to lamellipodia (Dormond, et al, 2001; Kiosses, et al, 2001). Compounds that disrupt the proper assembly of the actin cytoskeleton can play a role in inhibition of endothelial cell migration and vascular tube formation.

From the discussion above, one can deduce that VEGF, VEGF receptors, integrins, integrin binding to the extracellular matrix and cytoskeleton, the cytoskeleton itself, and the Rho family of GTPases all provide possible target mechanisms for antiangiogenic effects of toxicants. In addition to the earlier discussion of the involvement of angiogenesis in tissue repair, inhibition of vascular development is also important in regard to the developing fetus. Fetal growth and development can be altered by maternal exposures to air pollutants (Maisonet, et al., 2001; Rogers, et al., 2000; Dejmek, et al., 2000). MTBE and DP are two environmental pollutants that have received a considerable amount of attention during the past decade. Epidemiologic and experimental studies have shown that both MTBE and DP have the potential to affect vasculature as a

target of toxicity. This has led to formulation of the following hypothesis to direct this research: MTBE and DP alter angiogenesis through VEGF-related pathways leading to disruption of the endothelial cytoskeleton. A series of studies were carried out to examine whether MTBE, DP, or the extractable organic components from DP result in disrupted vascular tube formation. The hypothesis was tested by the following specific aims: (1) MTBE and DP disrupt vascular formation in *in vitro* models of endothelial cell tube formation; (2) inhibition of vascular formation observed following exposure to MTBE *in vitro* can be duplicated *in vivo* and result in vascular lesions in the rat; (3) inhibition of vascular formation observed following exposure to MTBE *in vitro* in rat endothelial cells can be duplicated using alternate models and species; (4) inhibition of vascular formation observed following exposure to MTBE is mediated through the VEGFR-2; (5) inhibition of vascular tube formation observed following exposure to DP observed *in vitro* is due to the extractable organic component, not the carbon core; (6) inhibition of vascular tube formation observed following exposure to DPE is due to cells undergoing apoptosis or cell death; and (7) inhibition of vascular tube formation observed following exposure to DPE is due to effects on the organization of the actin cytoskeleton which can be mediated through VEGF.

CHAPTER I:
Effects of Methyl Tertiary Butyl Ether on Capillary Endothelial Tube
Formation

INTRODUCTION

MTBE is an organic solvent that has been used primarily as an octane booster since 1977 in the production of gasoline. More recently, MTBE has been added to gasoline to increase the oxygen content to meet certain requirements of the Clean Air Act. MTBE has historically ranked third as the most produced organic chemical in the United States. In 1995 17.6 billion pounds were produced. Due to numerous reports of MTBE being detected in both surface and groundwater across the country, MTBE is being phased out within the United States. Wintertime oxygenated fuels contained as much as 15% by volume, while reformulated gasoline contained 11%. Levels in conventional grade gasoline ranged from 2 to 8%. MTBE is also approved for therapeutic use for dissolving cholesterol gallstones in the gallbladder (Leuschner, 1986).

With the increased use of MTBE over recent years by both the medical community and the petroleum industry come parallel increases in the potential for exposure of the environment and the human population to MTBE. Workers in the petroleum industry exposed to MTBE began reporting a high incidence of neurologic symptoms, including headaches, dizziness, and nausea (Moolenaar, et al., 1994; Prah, et al., 1994). While these symptoms are suggestive of vascular involvement, little information is available on the direct effects of MTBE

on vasculature. Studies examining the effects of MTBE at concentrations from 10 – 300 ppm in the Japanese medaka (*Oryzias latipes*) developing embryo resulted in a unique lesion of the developing vasculature. The embryonic vasculature failed to develop, while other non-vascular tissues developed normally until vascularization became essential for further development (Kozlosky, et al., 1996). The resulting unique lesion found in piscine embryonic vasculature prompted further investigation to determine if MTBE would alter rat brain microvessels and blood vessel growth and development *in vivo*.

As a part of the present study, primary cultures of rat brain endothelial cells were used to evaluate the effect of MTBE on angiogenesis *in vitro*. Isolated endothelial cells from rat brain grown on Matrigel elaborate cytoplasmic processes which, after two days in culture, form microcapillaries (Doron, et al., 1991). Pregnant Fisher 344 rats and a mouse Matrigel plug implantation assay were used to examine the effects of MTBE on vascular development *in vivo*. In addition, HUVEC grown on Matrigel were used to evaluate the contribution of the VEGFR-2 to the effects on vascular formation observed following treatment with MTBE. The results of these studies provide evidence that exposure of vascular endothelial cells to MTBE results in a decrease in vascular tube formation *in vitro* and angiogenesis *in vivo* and that these effects may be due in part to decreased activation of the VEGFR-2.

MATERIALS AND METHODS

Chemicals and cell culture supplies

Methyl tertiary butyl ether (MTBE), tertiary butyl alcohol (TBA), sodium heparin, collagenase (type II), percoll, Triton X-100, and dextran were purchased from Sigma-Aldrich (St. Louis, MO). M-199 media, penicillin/streptomycin, and fetal bovine serum (FBS) were purchased from Gibco (Invitrogen, Carlsbad, CA). EGM-2 culture media and supplements (EBM-2 BulletKits) were purchased from Clonetics (Lonza Walkersville, Inc., Walkersville, MD). Matrigel (phenol red free) and Endothelial Cell Growth Supplement (ECGS) were purchased from BD Biosciences (San Jose, CA). Tissue culture plates were from Falcon (Becton Dickinson Labware, Franklin Lakes, NJ).

Primary cultures of endothelial cells from rat brain and *in vitro* angiogenesis

Endothelial cells from the brains of Fisher-344 rats (3 to 4 days old) were isolated by centrifugation on dextrose and percoll density gradients following enzymatic treatment with collagenase type-2 and maintained in culture following the procedures described by Doron, *et al.* (1991). Primary cultures were maintained in Medium 199 containing HEPES (10 mM), L-glutamine (2 mM), 20% FBS, sodium heparin (90 $\mu\text{g/mL}$), ECGS (20 $\mu\text{g/mL}$), and 1X penicillin/streptomycin in 24-well culture plates containing glass cover slips precoated with Matrigel. Primary cultures of endothelial cells grown on Matrigel elaborate cytoplasmic processes which, after two days in culture, form capillary-

like tubes. A sterile, round, glass cover slip was placed in each well of a twenty-four well culture plate. Each cover slip was then coated with 100 μ L Matrigel and the plate was placed at 37°C for 30 minutes to allow the Matrigel to polymerize. Immediately following the isolation procedure, endothelial cells were seeded into the prepared plates at 5×10^4 cells/well. After 48 hours at 37° C in a humidified, 5% CO₂ atmosphere, the treated cells were fixed in 4% paraformaldehyde, immunostained for α -tubulin, and each cover slip was mounted to a microscope slide. Images were acquired from random fields on each slide at 200X magnification. Cord formation was quantified by counting the number of tubes in random photos from each treatment. Statistical significance from control was determined by Dunnett's Test and the results were expressed as means \pm SEM. A value of $P < 0.05$ was considered statistically significant.

Murine Matrigel plug implantation assay for *in vivo* angiogenesis

The Matrigel plug implantation assay was based on the method of Passaniti, et al. (1992). The assay was performed using two groups of five female mice (C57BL/6NCr Charles River) 6 to 8 weeks of age. A test group was implanted with plugs of Matrigel premixed with 100 ng/mL ECGS to which 34.0 mM MTBE was added. A control group received plugs of Matrigel containing 100 ng/mL ECGS only. The Matrigel (0.5 mL) was injected between the skin and abdominal muscle of each mouse in the groin area close to the dorsal midline. After 10 days, the plugs were dissected from the mice, embedded and sectioned in paraffin, and the sections were stained using

hematoxylin-eosin. Angiogenesis was considered to be indicated by the growth of blood vessels into the solid plug of Matrigel.

Chick chorioallantoic membrane (CAM) assay for *in vivo* angiogenesis

The CAM assay is one of the most widely used methods to study angiogenesis *in vivo*. Through the use of this assay, changes in the growth of capillary vessels can be observed. Fertile hens' eggs were prepared for sample application by first removing approximately 2 mL of albumen from the egg using a 21G needle. A small hole is then cut in the shell to puncture the air sac. Finally, a 1-cm square hole is cut in the shell. This procedure causes the CAM to drop as the remaining egg contents fill the void left by the collapse of the air sac and removal of the albumen. The square hole was covered with adhesive tape and the eggs were placed in a 37°C incubator until sample application.

On day 10, surviving eggs were organized into dose groups and 0.3 mL of 34.0 mM MTBE in sterile saline or sterile saline alone (control) was administered through the adhesive tape using a needle and syringe. The treated eggs were then returned to the 37°C incubator. After 24 hr of exposure, the CAM from each egg was fixed using ice-cold 4% paraformaldehyde. Each CAM was then excised and mounted on a microscope slide. Angiogenesis was considered to be indicated by an increase in the vascular network covering the CAM.

Reproductive vascular development in the rat

MTBE in corn oil was given to four groups of five pregnant female rats (Harlan Sprague-Dawley), orally by gavage, once daily from implantation (day 6 of pregnancy) through gestation at 500, 1000, 1200, or 1500 mg/kg/day. An additional group of five pregnant rats given corn oil alone served as a control. At birth, approximately one half of the animals of each sex from each litter were sacrificed and necropsied, and any gross observations were recorded. Representative samples of brain, lung, liver, kidney, heart, and stomach from these animals were collected and fixed in 10% neutral buffered formalin. Tissues were processed, sectioned, stained with hematoxylin and eosin, and subsequently examined by light microscopy for deviations in vascular development. The remaining animals from each litter were given MTBE in corn oil orally by gavage once daily from birth through post partum Day 10 at the same level as their respective dam. These animals were then sacrificed on post partum Day 11 and examined as described above. Statistical significance from control was determined by Dunnett's Test and the results were expressed as means \pm SEM. A value of $P < 0.05$ was considered statistically significant.

Immunofluorescence - Phosphorylated VEGFR-2

HUVECs (2.5×10^5) were incubated at 37°C in a humidified 5% CO₂ atmosphere following treatment with 34 mM MTBE and without treatment in 4-chamber glass cell culture slides (100 μ L Matrigel/chamber) for 4 hours. After 4 hours, the cells were fixed with 4% paraformaldehyde for 10 min, and then

permeabilized with 0.05% Triton X-100 for 10 min at room temperature. Nonspecific reactivity was blocked by incubation with 5% normal goat serum in PBS for 1 hr at room temperature. Endothelial tubes were incubated with the either Phospho-VEGF Receptor-2 (Tyr⁹⁹⁶) or Phospho-VEGF Receptor-2 (Tyr⁹⁵¹) primary antibody (Cell Signaling #2474 or #2471) at a 1:200 dilution for 1 hr at room temperature, followed by a 1 hr room temperature incubation with goat anti-rabbit secondary antibody labeled with Alexa 488 (Molecular Probes/ Invitrogen cat # A11008), diluted 1 to 200. Representative photographs were acquired following staining.

Statistics

For statistical analysis, each *in vitro* experiment was performed at least 2 times. The results were expressed as means \pm SEM and analyzed by using Dunnett's tests. A value of $P < 0.05$ was considered statistically significant.

RESULTS

***In vitro* rat brain capillary-like tube formation**

To evaluate the effect of MTBE on angiogenesis *in vitro*, primary cultures of rat brain endothelial cells were isolated and maintained in culture. When grown on Matrigel, the freshly-isolated endothelial cells elaborated cytoplasmic processes which, after two days in culture, formed capillary-like tubes. Cord formation was quantified by counting the number of tubes in random photos from each treatment using the National Institute of Health (NIH) ImageJ software. Exposure of cultured rat brain endothelial cells to MTBE (0.34 – 34.0 mM) resulted in a dose-dependent reduction of capillary tube formation (Figures 1 and 2). Treatment with tertiary butyl alcohol (0.34 - 34.0 mM), a major metabolite of MTBE, had no effect on microcapillary tube formation when compared to control (data not shown). These data suggest that microcapillaries may be a primary target of MTBE and that toxicity may be mediated by endothelial cells *in vivo*. MTBE completely inhibited rat brain endothelial cells from forming capillary-like tubes *in vitro* at 34.0 mM with a LOAEL of 0.34 mM.

***In vivo* murine Matrigel plug assay**

The effect of MTBE on angiogenesis *in vivo* was also tested using the Matrigel plug implantation assay. Matrigel plugs, premixed with 100 ng/mL ECGS, were implanted between the skin and abdominal muscle of each mouse in the groin area close to the dorsal midline. After 10 days, the plugs were dissected from the mice, embedded and sectioned in paraffin, and the sections

were stained using hematoxylin-eosin. Angiogenesis was considered to be indicated by the growth of blood vessels into the solid plug of Matrigel. Matrigel plugs supplemented with ECGS showed a robust angiogenic response (Figure 3A). The addition of 34.0 mM MTBE to the ECGS-supplemented plug resulted in near complete inhibition of angiogenesis (Figure 3B).

***In vivo* chick chorioallantoic membrane (CAM) assay**

The effect of MTBE on angiogenesis *in vivo* in a non-mammalian system was tested using the CAM assay. The chorioallantoic membrane in fertile hens' eggs was treated with either 34.0 mM MTBE in sterile saline or sterile saline alone. Following 24 hr of exposure, the addition of 34.0 mM MTBE resulted in a substantial decrease in the development of small blood vessels and branching off the larger vessels (Figure 4).

***In vivo* rat developmental study**

In an effort to determine if MTBE would affect developing microcapillaries *in vivo*, pregnant female rats were dosed orally by gavage with MTBE in corn oil at 500 to 1500 mg/kg/day, from implantation (day 6 of pregnancy) through gestation. Rats receiving 500 or 1000 mg/kg/day MTBE showed no adverse clinical signs; however, those animals receiving 1200 or 1500 mg/kg/day collapsed approximately 30 seconds following dosing and recovered within 2 minutes.

At birth, one half of the animals of each sex from each litter were necropsied and any gross observations were recorded. Tissues from these animals were then examined histologically for deviations in vascular development. The remaining animals from each litter were dosed orally by gavage through post partum Day 10 with MTBE in corn oil at the same dose as their respective dam. Narcotic effects, similar to those observed in the dams, were also observed in the pups receiving 1200 or 1500 mg/kg/day MTBE. These animals were necropsied on post partum Day 11 and examined in an identical manner to that described above. No changes in body weight or organ weights were observed (Figures 5 and 6). In addition, no changes in vascular development were observed in any of the rats following either gross or histological examination at the light level.

Immunofluorescence - Phosphorylated VEGFR-2

Preliminary studies were carried out to examine the ability of MTBE to inhibit phosphorylation of the VEGFR-2. During immunostaining, HUVEC were very easily washed off the Matrigel. In addition, placement of a coverslip on the slides caused the cells to release from the Matrigel and move to the edges of the field. It was observed that during the process of tube formation, HUVEC are not strongly attached to the soft Matrigel matrix. Several slides did show that treatment with 34 mM MTBE resulted in a decrease in phosphorylation of VEGFR-2 at both the Tyr⁹⁵¹ and Try⁹⁹⁶ phosphorylation sites (Figure 7).

Additional studies are needed to further characterize the dose response and reproducibility of these findings.

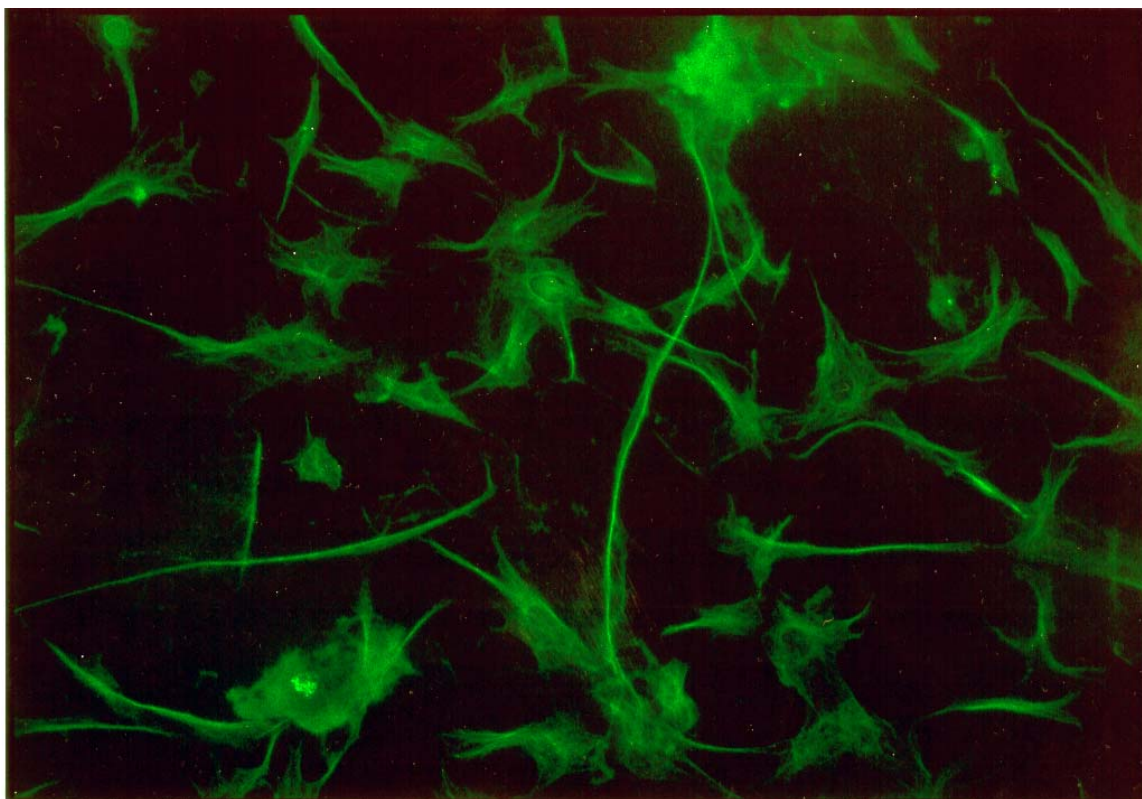
Summary of the Data

MTBE at sufficiently high concentrations can prevent angiogenesis in several *in vitro* (rat isolated vascular endothelial cells grown on Matrigel, avian CAM assay) and *ex vivo* (Matrigel plug in mice) model systems. Exposure of cultured rat brain endothelial cells to MTBE (0.34 – 34.0 mM) resulted in a dose-dependent reduction of capillary tube formation when grown on Matrigel for 48 hours (Figures 1 and 2). The LOAEL was at 0.34 mM, and this resulted in approximately a 50% decrease in branching. The addition of 34.0 mM MTBE to ECGS-supplemented Matrigel plugs inserted under the skin of mice resulted in near complete inhibition of angiogenesis (Figure 3B). Following 24 hr of exposure, the addition of 34.0 mM MTBE resulted in a substantial decrease in the development of small blood vessels and branching off the larger vessels in the chicken egg CAM (Figure 4). In addition, treatment of HUVEC grown on Matrigel with 34 mM MTBE resulted in a decrease in phosphorylation of VEGFR-2 at both the Tyr⁹⁵¹ and Try⁹⁹⁶ phosphorylation sites (Figure 7). This would support the hypothesis that MTBE can interfere with angiogenesis by disrupting the VEGFR-2 which likely alters actin and cytoskeleton formation that are critical in angiogenesis. However, when MTBE (500 - 1500 mg/kg/day) was given by gavage to pregnant rats and then their offspring for 10 days post parturition no morphological effects were observed. There were no observed changes in body weight, organ weights, or relative organ weights (Figures 5 and 6). In addition, no changes in vascular development were observed in any of the rat pups following either gross or histological examination at the light level. The striking

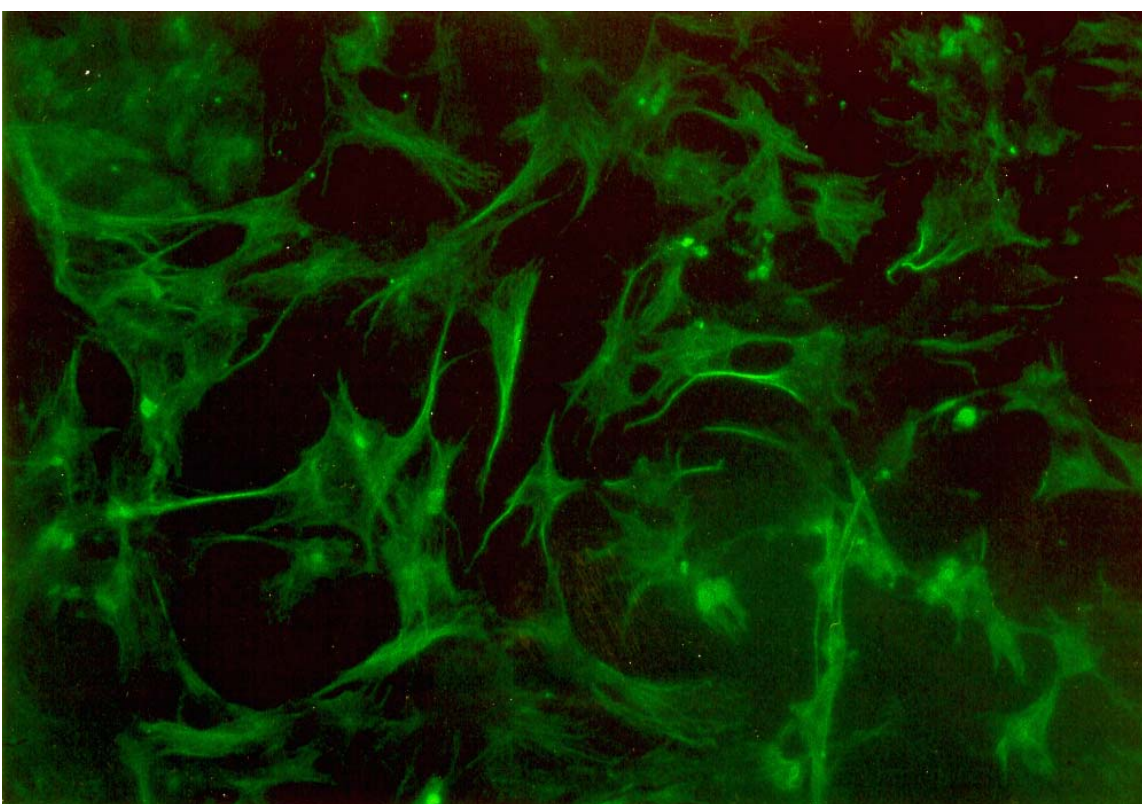
difference observed between the *in vitro* and *in vivo* effects are likely due to the inability to achieve high enough circulating levels of MTBE in the pups. This is likely a result of both the exhalation of MTBE and the metabolism in the liver converting the MTBE into TBA, a non-toxic metabolite. Future reproductive studies should concentrate on lower doses given in a more chronic dosing regiment.

FIGURES

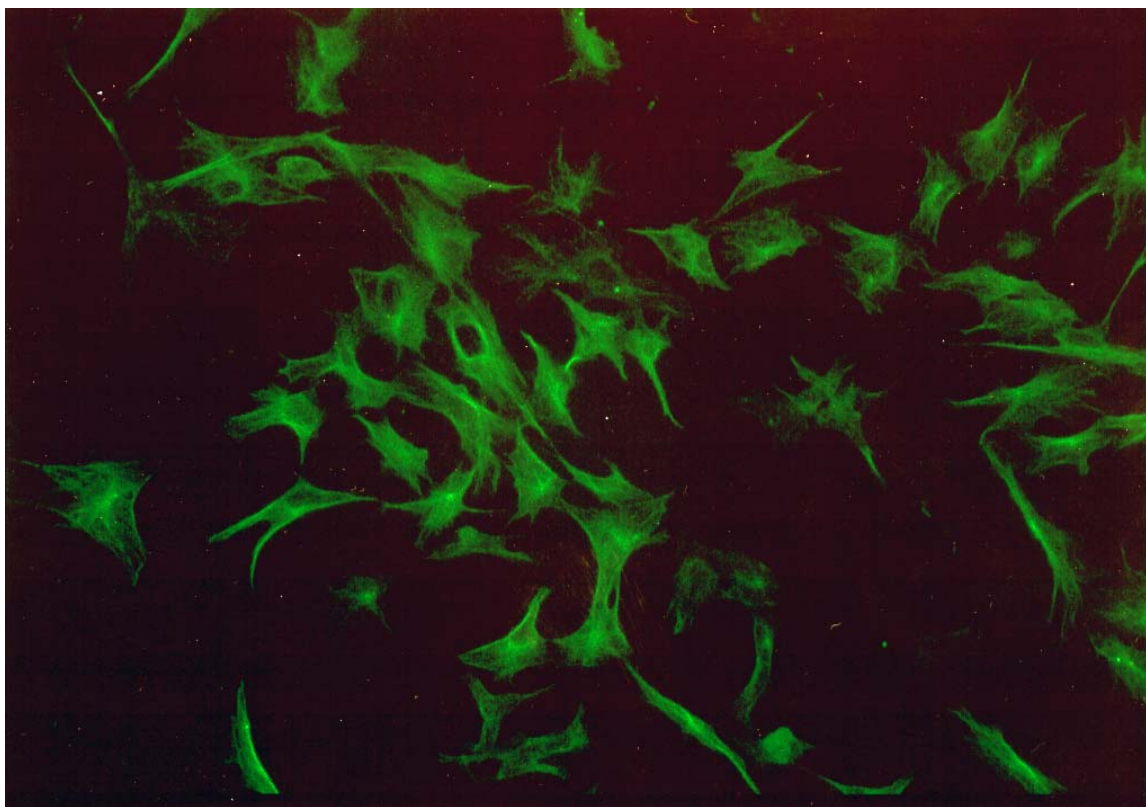
Figure 1. Formation of capillary-like structures by isolated rat brain endothelial cells grown on Matrigel following treatment with MTBE for 48 hours: Representative photographs (200X) of (A) untreated rat brain endothelial cells seeded on Matrigel-coated glass cover slips after 48 hours and following treatment with (B) 0.34 mM MTBE, (C) 3.40 mM MTBE, or (D) 34.0 mM MTBE for 48 hours. Cells were fixed in 4% paraformaldehyde and immunostained for α -tubulin.



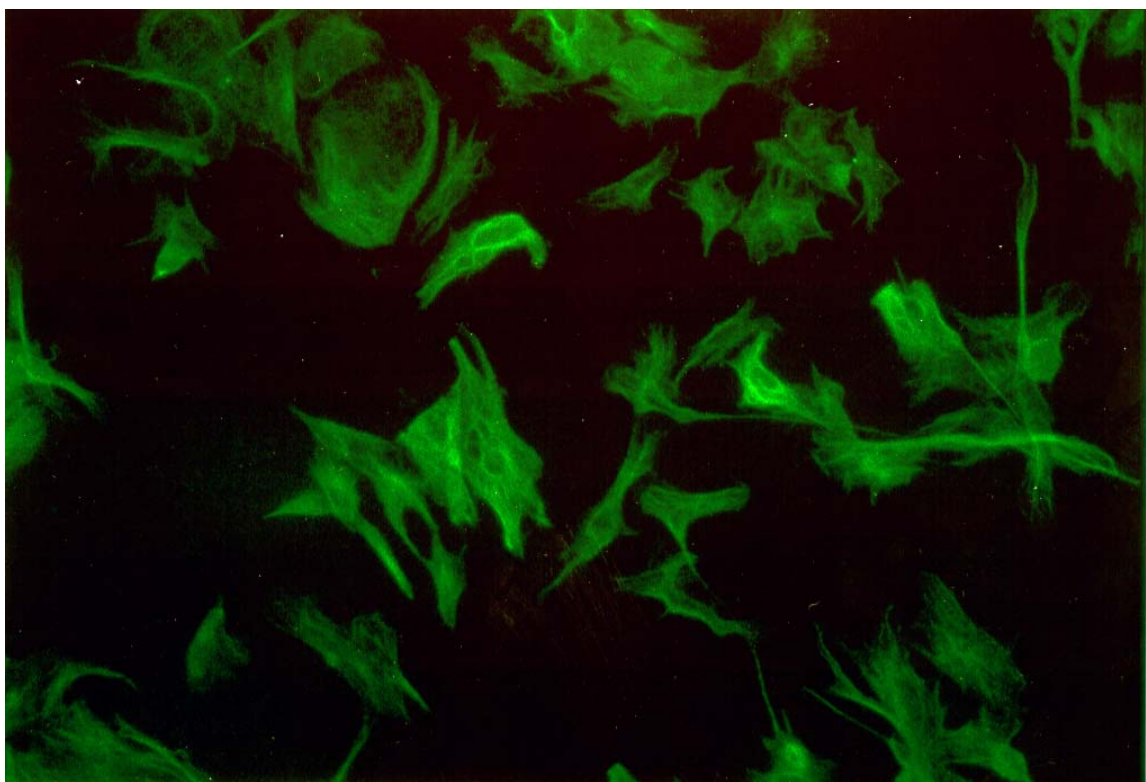
A



B



C



D

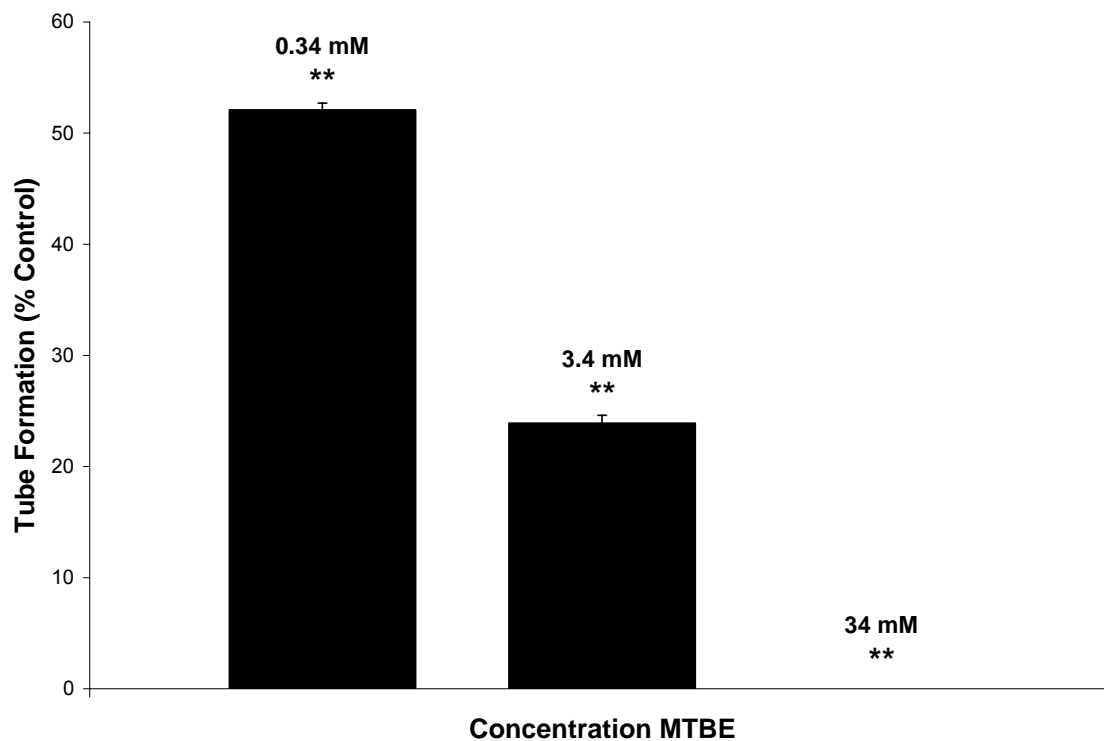
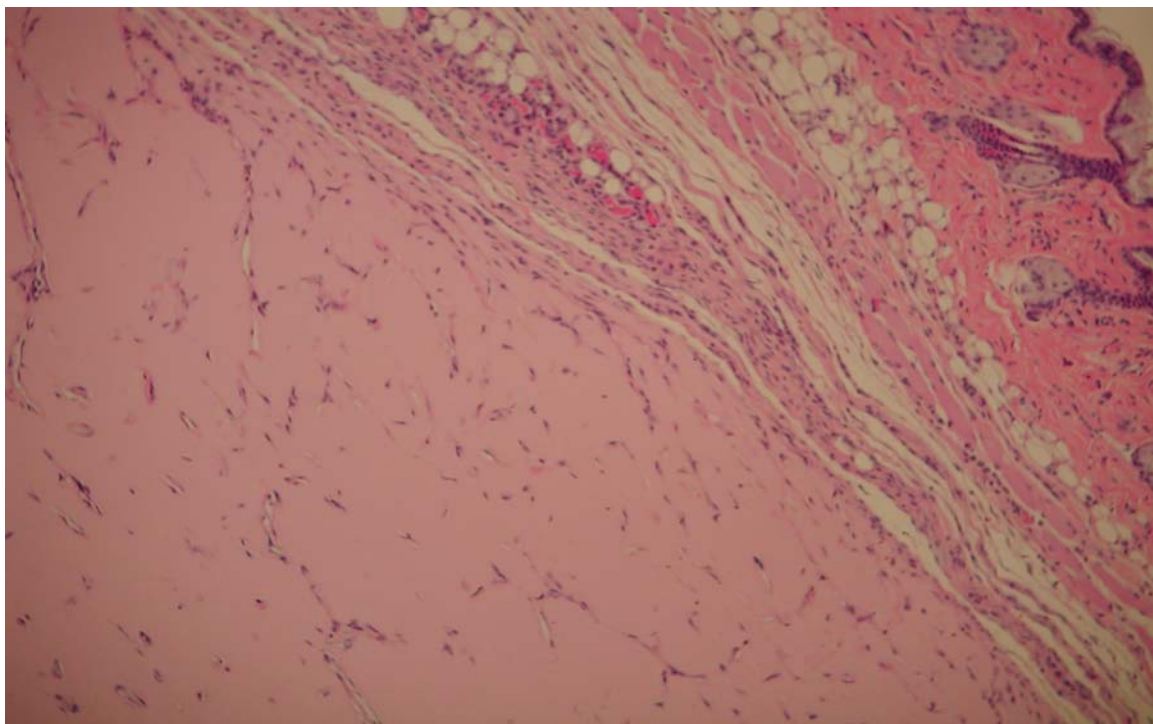
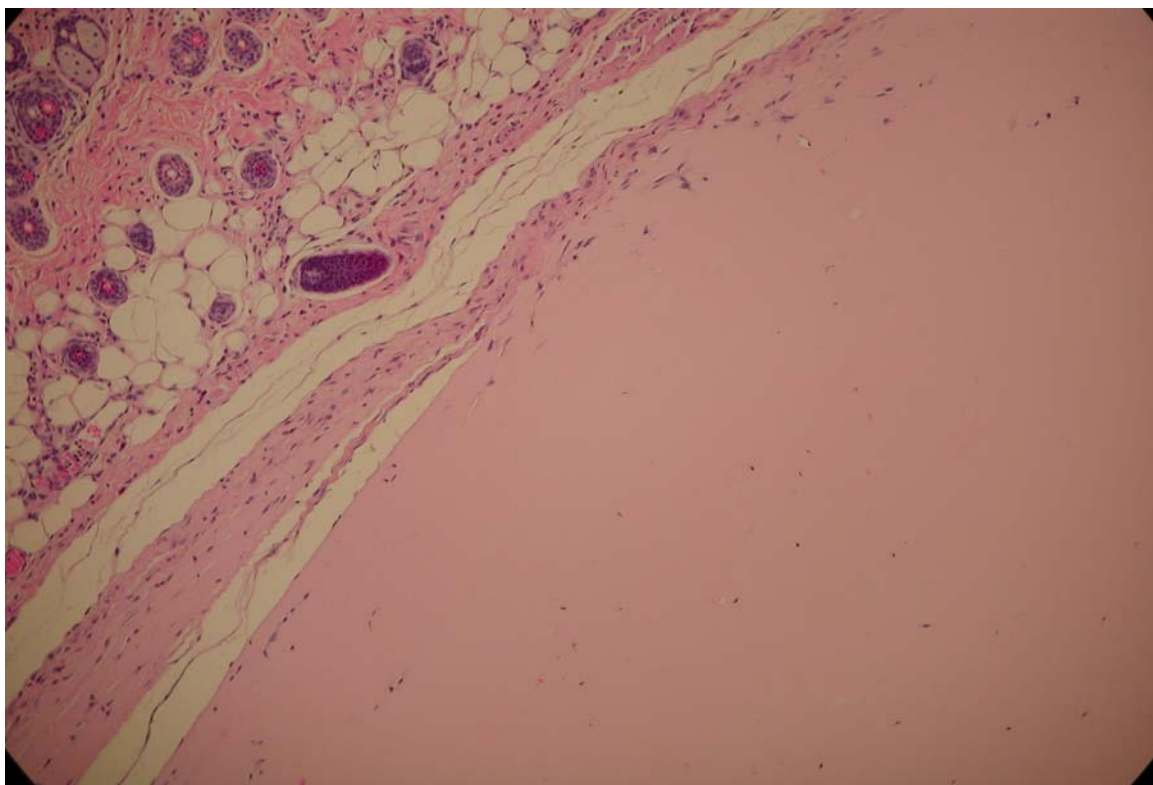


Figure 2. Rat brain endothelial cell tube formation following 48 hour treatment with 0.34, 3.4, and 34 mM MTBE compared to control tube formation. Images were acquired from random fields at 200X magnification. Cord formation was quantified by counting the number of tubes in random photos from each treatment using the National Institute of Health (NIH) ImageJ software. Statistical significance from control was determined by Dunnett's Test. Error bars denote standard deviation. ** $P < 0.01$ relative to control.

Figure 3. Representative photographs of Matrigel plugs from the murine Matrigel plug implantation assay following exposure to saline or 34 mM MTBE: Images are hematoxylin and eosin stained cross sections of Matrigel plugs at the boarder of the skin at 100X magnification. Matrigel plugs containing the indicated amount of MTBE and/or endothelial cell growth supplement (ECGS) were embedded between the skin and abdominal wall of mice for 10 days, then collected and sectioned. (A) Matrigel plugs supplemented with 100 ng/mL ECGS. (B) with addition of 34.0 mM MTBE to the ECGS-supplemented plug.

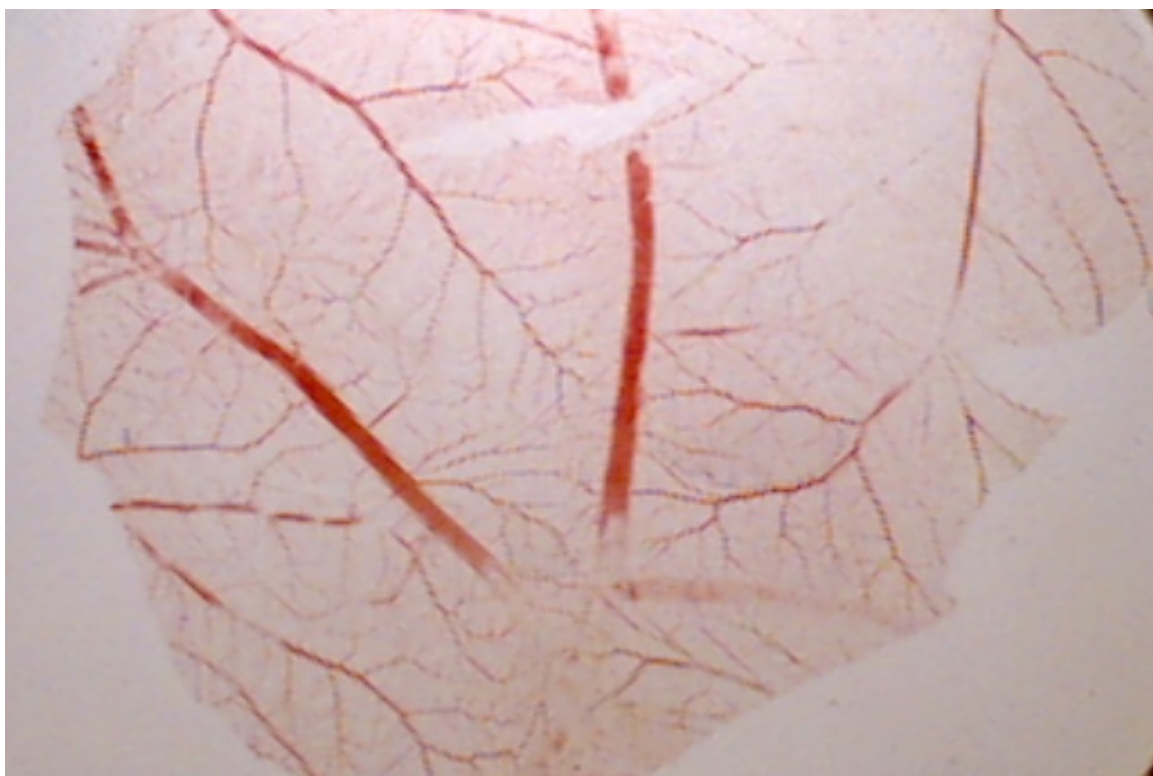


A

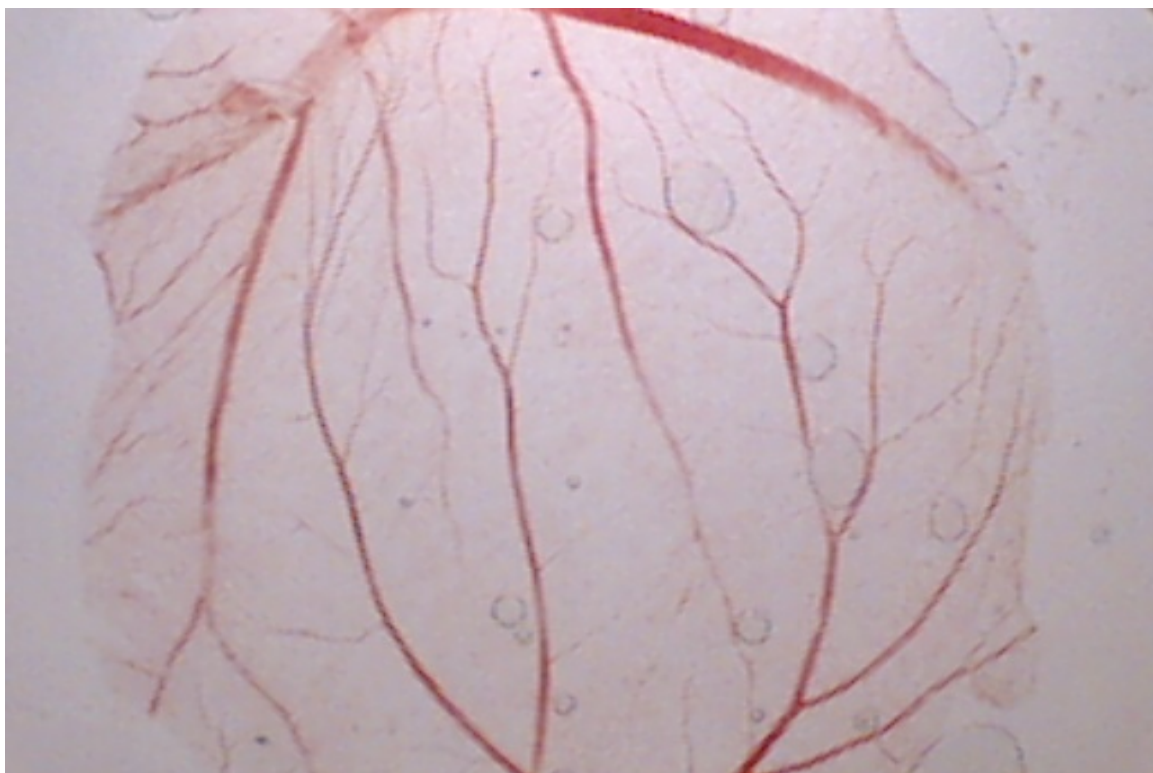


B

Figure 4. Representative photographs of chicken egg chorioallantoic membranes (CAM) following treatment with saline or 34 mM MTBE for 24 hours: (A) CAM treated with sterile saline. (B) CAM following exposure to 34.0 mM MTBE for 24 hours. The images are 10X magnification.



A



B

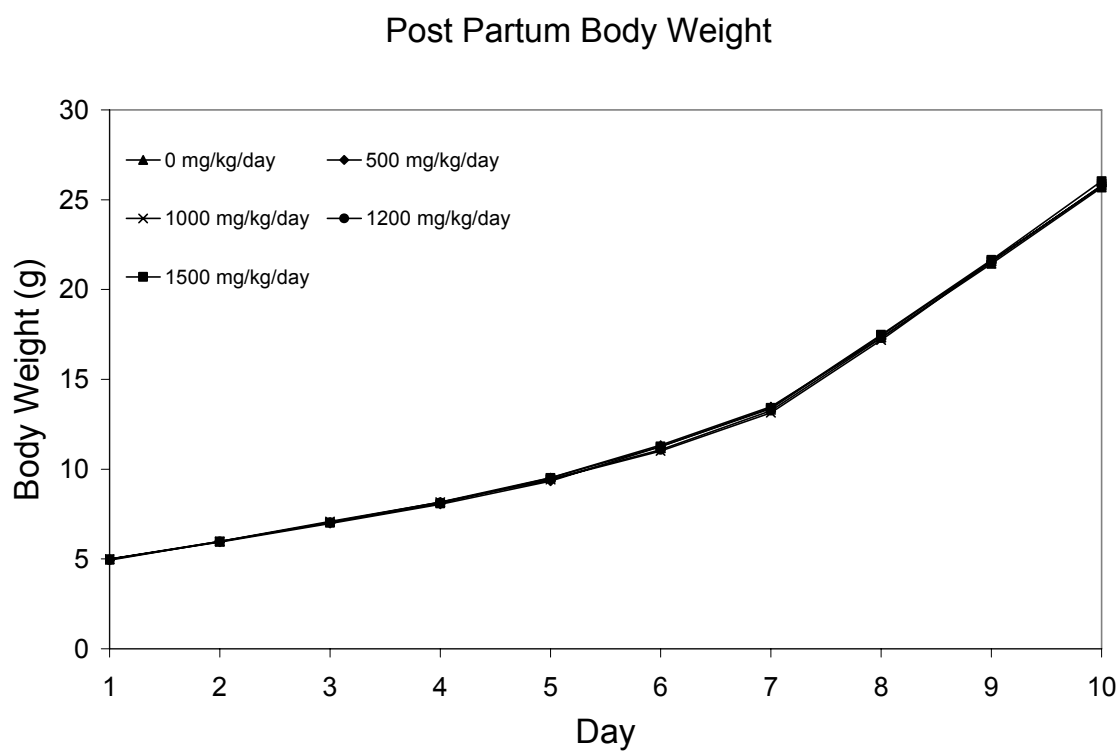


Figure 5. Body weights in rat neonates from birth (Day 1) through Day 10 following exposure to 500 - 1500 mg/kg/day MTBE: Mean of 47 - 53 pups per time point.

Figure 6. Tissue weights in rat neonates following exposure to 500 - 1500 mg/kg/day MTBE: Mean of 22 - 29 pups per time point. Tissue weights include liver (A), brain (B), kidney (C), stomach (D), lung (E), and heart (F) from Day 1 (birth) and Day 11. Statistical significance from control was determined by Dunnett's Test. Error bars denote standard deviation.

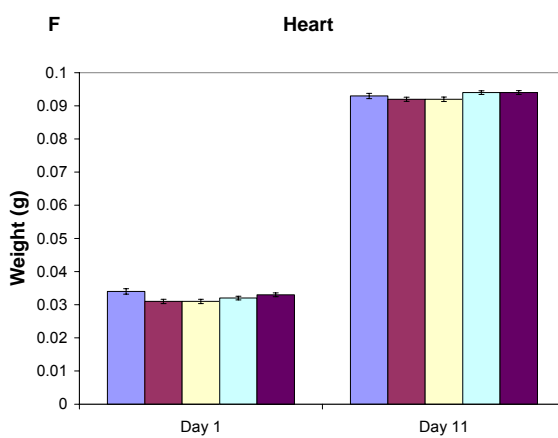
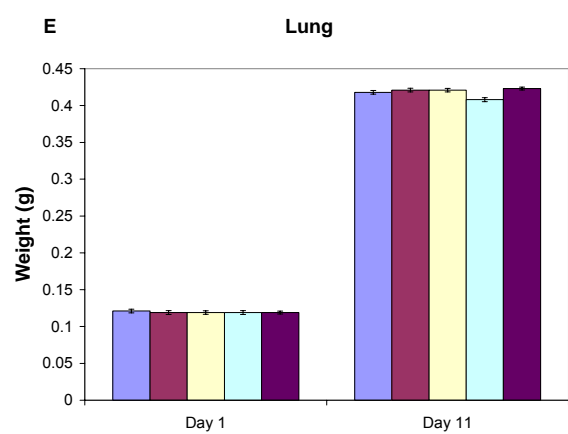
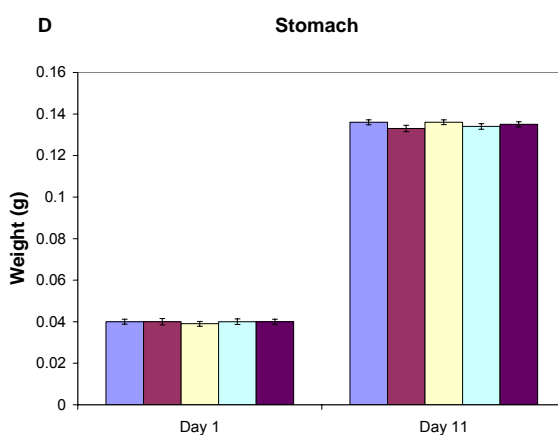
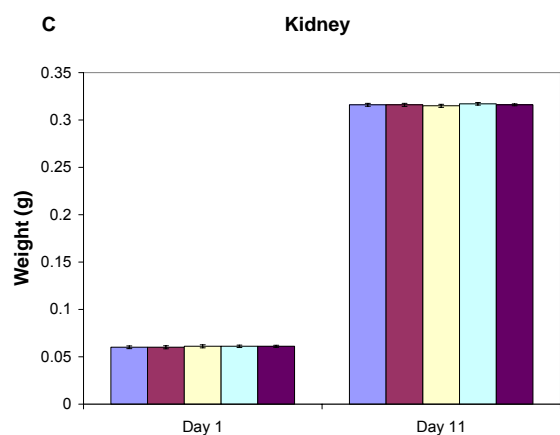
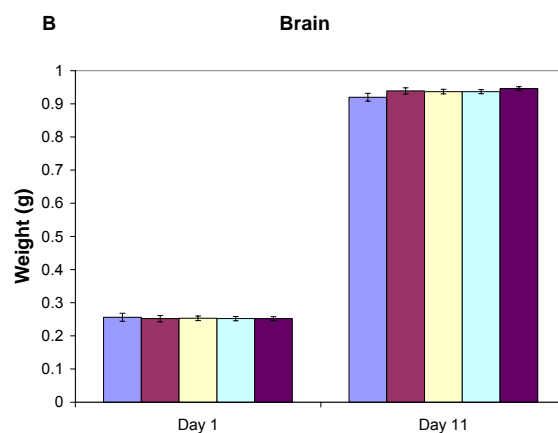
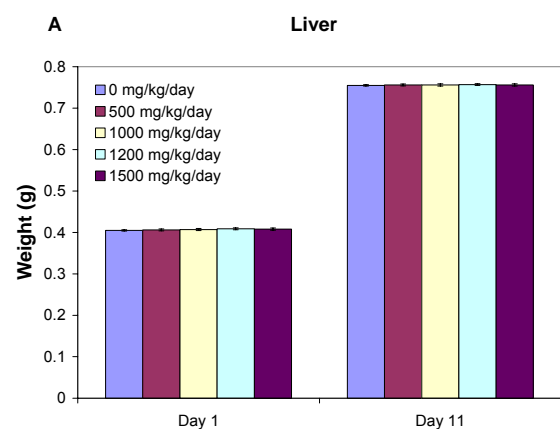
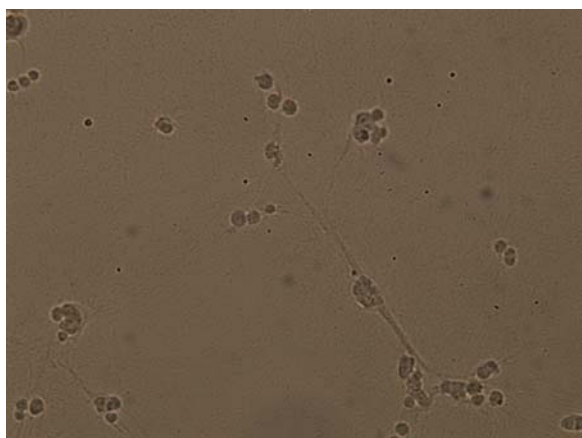
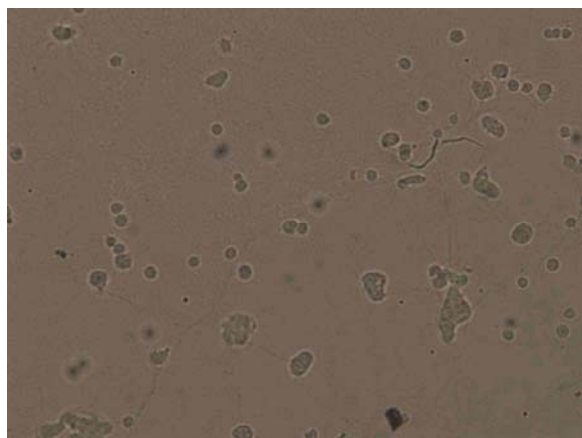
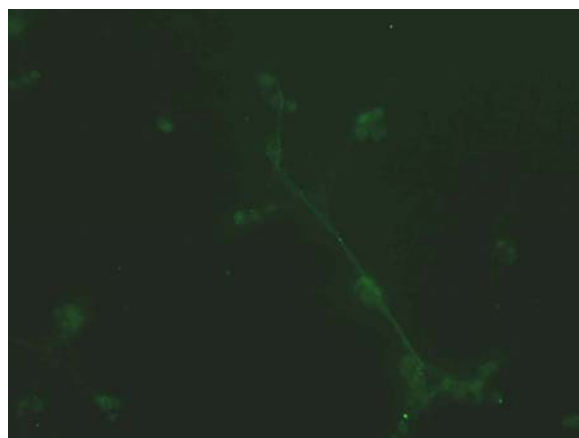


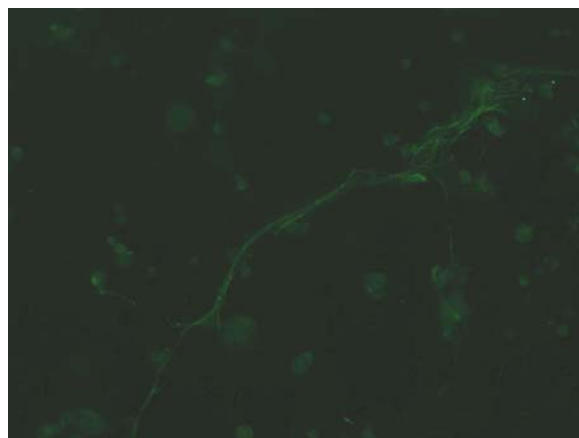
Figure 7. Representative images of HUVEC immunostained for phosphorylation of VEGFR-2 at both Tyr⁹⁵¹ and Tyr⁹⁹⁶ in untreated cells and following treatment with 34 mM MTBE for 4 hours: Representative bright field (left) and immunostained (right) photographs (200X) of (A) untreated HUVEC stained for VEGFR-2 phosphorylated at Tyr⁹⁵¹; (B) untreated HUVEC stained for VEGFR-2 phosphorylated at Tyr⁹⁹⁶; (C) HUVEC treated with 34 mM MTBE for 4 hours then stained for VEGFR-2 phosphorylated at Tyr⁹⁵¹; (D) HUVEC treated with 34 mM MTBE for 4 hours then stained for VEGFR-2 phosphorylated at Tyr⁹⁹⁶.

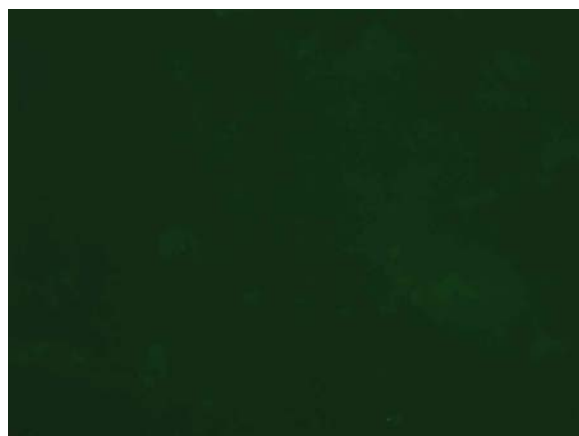
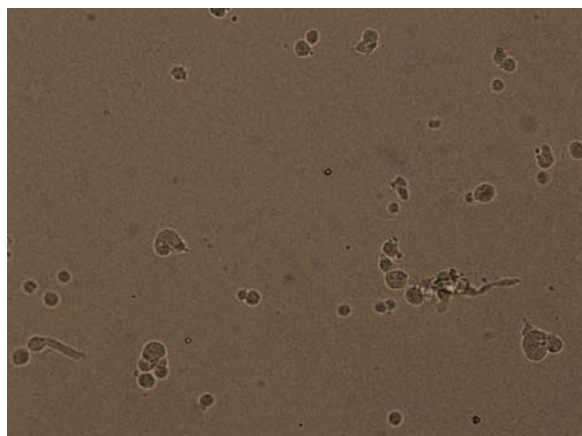


A

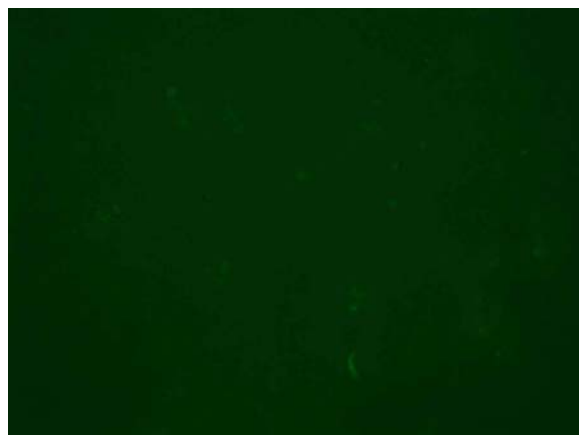
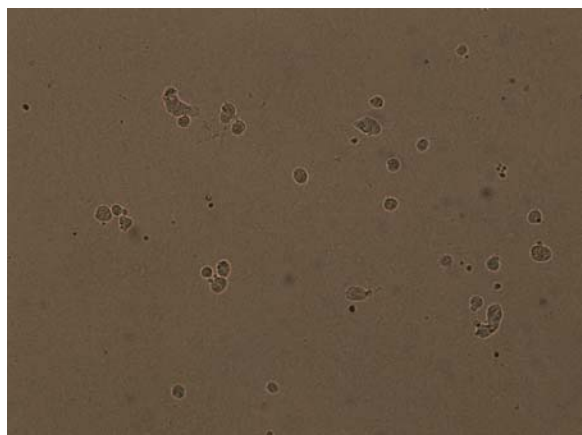


B





C



D

Chapter II:

Determination of the Possible Effects of Diesel Exhaust Particles on Capillary Endothelial Tube Formation

INTRODUCTION

The studies described in Chapter II deal with the effects of DP on endothelial cell tube formation. The hypothesis was that DP disrupt endothelial tube formation through direct effects on endothelial cells. The potential effects of DP on angiogenesis were investigated with an *in vitro* capillary tube-forming model using primary cultures of HUVEC. Four treatments were evaluated; the DP as a whole, carbon black to represent the core or nucleus of the diesel particle, an organic component derived from extraction of DP using dichloromethane, and the washed particles resulting from the extraction in order to determine the contribution of either the particle or the absorbed organic component. The studies described in this chapter include an evaluation of *in vitro* tube formation in HUVEC grown on Matrigel and the ability of the HUVEC to recover from the effects observed following treatment with DP and DPE. Also investigated were the possible involvement of apoptosis and the organization of the actin cytoskeleton.

The results of these studies provide evidence that DP inhibit capillary tube formation *in vitro* and it appears to be the organic component of these particles, not the carbon core, producing this effect. These studies also show that the inhibition of tube formation is not mediated through apoptosis or cell death, but may be caused by disorganization of the cytoskeleton mediated through the Rho GTPases Rac1 and

Cdc42. In addition, results of the recovery assay indicate that the effects produced by DP and DPE are reversible.

MATERIALS AND METHODS

Chemicals and culture supplies

Dimethyl sulfoxide (DMSO), dichloromethane, Neutral Red Solution, Neutral Red Assay Solubilization Solution, Triton X-100, Tween-20, and Tween-80 were purchased from Sigma-Aldrich (St. Louis, MO). EGM-2 Culture media and supplements (EBM-2 BulletKits) were purchased from Clonetics (Lonza Walkersville, Inc., Walkersville, MD). Phosphate buffered saline (PBS) and was purchased from Gibco (Invitrogen, Carlsbad, CA). Matrigel (phenol red free), Matrigel (reduced growth factor), and Matrigel-coated culture plates were obtained from BD Biosciences (San Jose, CA). Tissue culture T-75 flasks, 100 mm cell culture plates, and chamber tissue culture glass slides were from Falcon (Becton Dickinson Labware, Franklin Lakes, NJ).

Cell culture

Human umbilical vein endothelial cells (HUVEC) were purchased from Clonetics (Lonza Walkersville, Inc., Walkersville, MD) and passages 3 to 6 were used for all experiments. HUVECs were expanded; frozen overnight at -80°C in 50% EGM-2 media and 50% Cryoprotective Freezing Media (Lonza), then stored in liquid nitrogen for future use. To prepare for experiments, HUVECs were cultured in monolayers in T-75 tissue culture flasks and expanded in EGM-2. The cells were maintained at 37°C in a humidified 5% CO₂ atmosphere. Culture medium was changed every 2 - 3 days and the

cells were examined daily with an inverted microscope (type). Subculturing was performed when cell confluence reached approximately 80%.

Diesel exhaust particles

Diesel exhaust particles (DP) were obtained from M. Sagai (Aomori University of Health and Welfare, Aomori, Japan) and were prepared as previously described (Sagai et al, 1993). The particles were suspended by vortexing and ultrasonication at 10 mg/mL in PBS containing 0.05% Tween-80 and stored at 4°C.

Preparation of washed DP and organic extract from particulate material

Organic extracts from DP were prepared by extraction of particulate material with dichloromethane (Figure 8). One gram of DP was extracted 4 times in 10 mL of dichloromethane by ultrasonication. All four dichloromethane fractions were combined, evaporated to dryness, and weighed. This procedure yielded approximately 400 mg of residue from the 1 g of dry DP sample. The evaporated diesel exhaust particle extract (DPE) was dissolved in DMSO (500 mg/mL) and stored at -80°C. Following the extractions, the washed DP (WDP) remaining were evaporated to dryness and suspended by vortexing and ultrasonication at 10 mg/mL in PBS containing 0.05% Tween 80 and stored at 4°C.

Treatments - initial screening for possible effects of DP, DPE, and Carbon Black (CB) on capillary tube formation *in vitro*

HUVECs were treated with DP or CB suspended in a vehicle of 0.05% Tween 80 in PBS or DPE dissolved in DMSO. Each treatment was further diluted in EGM-2 media to the final concentration. The final concentration of DMSO in solution did not exceed 0.1%. Concentrations of DP and CB used in the initial screening experiment were 1, 10, 100 $\mu\text{g/mL}$ and 0.75 and 7.5 $\mu\text{g/mL}$, respectively. These concentrations were used previously in this laboratory in experiments involving treatment of HUVEC with DP following 24 hr of tube formation on Matrigel. Concentrations of DPE used were 1, 3, 10, and 20 $\mu\text{g/mL}$. DPE concentrations were based on an *in vitro* LC_{50} value of 17 $\mu\text{g/mL}$ determined in rat heart microvessel endothelial cells (Hirano, et al., 2003). The cells were exposed to the treatments for 4 hr. The results of this initial screen prompted further investigation of the effects of the DPE at 25, 50, 100, and 250 $\mu\text{g/mL}$. The exposure time for this and all subsequent *in vitro* tube formation experiments was reduced to 3 hr. A third experiment exposed HUVECs to a range of DPE from 10 to 100 $\mu\text{g/mL}$ (in increments of 10 $\mu\text{g/mL}$) in order to define a dose response.

Treatment - equivalent fraction

HUVECs were treated with DP or WDP suspended in a vehicle of 0.05% Tween-80 in PBS or DPE dissolved in DMSO. Each treatment was further diluted in EGM-2 media to the final concentration. The final concentration of DMSO in solution did not exceed 0.1%. In the screening study to determine effects on capillary tube formation, HUVECs were treated with DPE at concentrations ranging from

10 - 100 $\mu\text{g/mL}$ in the culture medium. At exposures $\geq 40 \mu\text{g/mL}$, tube formation was completely inhibited following 3 hours of treatment. At 20 and 30 $\mu\text{g/mL}$, tube formation was inhibited in a concentration-dependent manner. At 10 $\mu\text{g/mL}$, tube formation was equivalent to controls. For the current studies, a high dose of 40 $\mu\text{g/mL}$ DPE was selected. Based on the findings from the screening studies, 40 $\mu\text{g/mL}$ was expected to result in complete inhibition of tube formation. Additional doses of 20 and 10 $\mu\text{g/mL}$ DPE were selected to evaluate dose-related effects. Control treatments consisted of 0.1% DMSO in EGM-2 media. DP and WDP concentrations were selected to relate with the DPE doses and the results of the organic extraction from DP. Dry residue resulting from the extraction process was approximately 40% by weight of the whole particle. Based on this information, DPE doses of 40, 20, and 10 $\mu\text{g/mL}$ correlate to DP doses of 100, 50, and 25 $\mu\text{g/mL}$ and WDP doses of 60, 30, and 15 $\mu\text{g/mL}$, respectively.

Capillary tube formation assay

Matrigel-coated 24-well plates were thawed overnight at 4°C. Immediately prior to performing the assay, the Matrigel was allowed to solidify at 37°C for 1 hour. HUVECs in T-75 flasks were trypsinized and 2.5×10^4 cells were added per well in 1 mL of medium. The cells were maintained at 37°C in a humidified 5% CO₂ atmosphere for approximately 30 minutes to allow for attachment to the Matrigel. Following attachment, the medium was gently removed from each well and the cells were treated with DP, WDP, CB, or DPE at the concentrations tested in 1 mL of medium per well. The cells were maintained at 37°C in a humidified 5% CO₂ atmosphere throughout the treatment period. Tube formation was observed periodically over time under a phase contrast

microscope and representative pictures were taken at 3 or 4 hours as described in the treatment sections above.

Recovery assay

HUVECs were treated as described for the tube formation assay. Following 3 hours of treatment, the media was gently removed. Each well of the 24-well plate was gently washed 2 times with 1 mL HBSS warmed to 37°C and 1mL of EGM-2 treatment-free media was added to each well. The cells were maintained at 37°C in a humidified 5% CO₂ atmosphere and representative photographs were taken at approximately 18 hours.

ECM cell adhesion assay

Adhesion of integrins to various ECM components was evaluated using the ECM cell adhesion assay. InnoCyte ECM Cell Adhesion Assay kits coated with collagen type IV, fibronectin, vitronectin, laminin or Matrigel were purchased from Calbiochem. The plates were prepared following the manufacturer's instructions. HUVECs were seeded in the 96-well plates (2.5×10^4 cells/well) then incubated at 37°C for 1 hr with and without treatment. Following the 1 hr incubation, the media was removed from each well and discarded. Each well was gently washed twice, each time adding 200 μ L of 37°C PBS. Following the wash steps, 100 μ L of fresh EGM-2 media containing 10% Neutral Red Solution was added to each well. The culture plates were returned to the 37°C incubator for 2 hrs. During this incubation, viable cells take up the dye by active transport. A change in the number of cells attached to the plate will result in a

concomitant change in the amount of dye incorporated by the cells. At the end of the incubation period, the medium was removed and the cells were quickly rinsed with 37°C PBS. The PBS was removed and the incorporated dye was solubilized in 100 µL of Neutral Red Assay Solubilization Solution for 10 min at room temperature while gently stirring on a gyratory plate shaker. The amount of solubilized neutral red was determined by measuring the absorbance at 490 nm using a 96-well plate reader.

Caspase-9 and caspase-3 activity assays

Caspase activity was measured using the Caspase-3 and Caspase-9 Colorimetric Assay Kits (R&D Systems, Inc.) following the manufacturer's instructions. HUVECs were seeded in 100 mm cell culture plates (5×10^6 cells/plate) coated with Matrigel then incubated for 3 hours with and without treatment. Cisplatin (25 µM) served as a positive control. Caspase activity was determined by measuring the absorbance at 405 nm using a 96-well plate reader.

Lactate dehydrogenase (LDH) cytotoxicity assay

LDH activity was measured in the supernatant culture media using the LDH Cytotoxicity Assay Kit (Cayman) following the manufacturer's instructions. HUVECs (5×10^6 cells/plate) were incubated at 37°C in a humidified 5% CO₂ atmosphere for 3 hours with and without treatment in 100 mm cell culture plates coated with Matrigel. Cisplatin (25 µM) served as a positive control. The LDH activity was determined by measuring the absorbance at 490 nm using a 96-well plate reader.

Annexin V and propidium iodide staining

Annexin V and PI staining was performed using the TACS Annexin V Kit (Trevigen) following the manufacturer's instructions. HUVECs (2.5×10^5) were incubated at 37°C in a humidified 5% CO₂ atmosphere with and without treatment in 4-chamber glass cell culture slides (100 µL Matrigel/chamber) for 3 hours. Cisplatin (25 µM) served as a positive control. After 3 hours, unfixed cells were stained with annexin V-fluorescein and propidium iodide to differentiate apoptotic from necrotic cells. Representative pictures were taken following staining.

Hoechst staining

Hoechst staining was performed using TACS Hoechst Cell Proliferation Assay (Trevigen) following the manufacturers instructions for unfixed adherent cells. HUVECs (2.5×10^5) were incubated at 37°C in a humidified 5% CO₂ atmosphere with and without treatment in 4-chamber glass cell culture slides (100 µL Matrigel/chamber) for 3 hours. Cisplatin (25 µM) served as a positive control. After 3 hours, unfixed cells were stained with Hoechst 33342. Representative pictures were taken following staining.

DNA fragmentation assay

DNA fragmentation was determined using the Cell Death Detection ELISA^{Plus} kit (Roche) following the manufacturer's instructions. HUVECs (5×10^6 cells/plate) were incubated at 37°C in a humidified 5% CO₂ atmosphere for 3 hours with and without treatment in 100 mm plates coated with Matrigel. Cisplatin (25 µM) served as a positive

control. Fragmented DNA was determined by measuring the absorbance at 405 nm using a 96-well plate reader.

Actin cytoskeleton staining

Actin cytoskeleton staining was performed using TRITC-conjugated Phalloidin (Chemicon). HUVECs (2.5×10^5) were incubated at 37°C in a humidified 5% CO₂ atmosphere with and without treatment in 4-chamber glass cell culture slides (100 µL Matrigel/chamber) for 3 hours. After 3 hours, cells were fixed with 4% paraformaldehyde in PBS for 15 minutes at room temperature. Each chamber was washed twice with wash buffer (PBS containing 0.05% Tween-20). Cells were permeabilized with 0.1% Triton X-100 then washed twice again with wash buffer. A blocking solution consisting of 1% BSA in PBS was then applied to the cells for 30 minutes at room temperature. Following the blocking step each chamber was washed three times with wash buffer at room temperature for 10 minutes each wash. TRITC-conjugated Phalloidin diluted 1:500 was then applied and the slides were incubated at 37°C for 30 minutes. Following incubation, the chambers were again washed three times with wash buffer at room temperature for 10 minutes each wash. Representative pictures were taken following staining.

RhoA, Rac1, and Cdc42 activation

Levels of active RhoA, Rac1, and Cdc42 were measured using G-LISA Activation Assay Biochem Kits for the respective proteins (Cytoskeleton) following the manufacturer's instructions. HUVECs were seeded in 100 mm cell culture plates

(5×10^6 cells/plate) coated with Growth-Factor Reduced Matrigel then incubated for 3 hours with and without treatment. Cisplatin (25 μ M) served as a positive control. Protein activity was determined by measuring the absorbance at 490 nm using a 96-well plate reader.

Statistics

For statistical analysis, each experiment was performed at least 2 times. The results were expressed as means \pm SEM and analyzed by using Dunnett's tests. A value of $P < 0.05$ was considered statistically significant.

RESULTS

Capillary tube formation assay

HUVECs grown on Matrigel rapidly elaborate cytoplasmic processes which form capillary-like tubes. The formation of tube-like vessels under these conditions can be used to assess compounds that either inhibit or stimulate angiogenesis.

In the initial screening study, HUVEC tube formation was assessed following a 4-hour treatment with DP, CB, or DPE. After 4 hours, controls showed a full network of tube development. At 1 $\mu\text{g/mL}$ DP, 0.75 and 7.5 $\mu\text{g/mL}$ CB, and 1, 3, 10, and 20 $\mu\text{g/mL}$ DPE, tube development was equivalent to controls. There was a dose-dependent reduction in tube formation at 10 and 100 $\mu\text{g/mL}$ DP with complete inhibition of tube formation at 100 $\mu\text{g/mL}$ (Table 1, Figure 9).

In the subsequent two screening studies, exposure time was reduced to 3 hours. Results of these studies showed a full network of tubes in controls. In the second screening study, at 25 $\mu\text{g/mL}$ DPE, tube formation was significantly decreased compared to controls. At ≥ 50 $\mu\text{g/mL}$ DPE, tube formation was completely inhibited (Table 2, Figure 10). In the final screening study, concentrations of DPE were tested at a range of 10 to 100 $\mu\text{g/mL}$ in 10 $\mu\text{g/mL}$ increments. DPE concentrations ≤ 40 $\mu\text{g/mL}$ inhibited capillary tube formation in a concentration-dependent manner with complete inhibition at 40 $\mu\text{g/mL}$ and a NOAEL of 10 $\mu\text{g/mL}$. At 20 $\mu\text{g/mL}$ DPE, individual cells began to be observed that were not involved in tube formation. At 40 $\mu\text{g/mL}$ DPE, cells were still flattened to the Matrigel matrix; however, tube formation was completely inhibited. At ≥ 50 $\mu\text{g/mL}$ DPE, tube formation was completely inhibited and all cells appeared ball-shaped and not flattened to the matrix (Table 3, Figure 11).

In the equivalent fraction study, capillary tube formation at 10 $\mu\text{g/mL}$ DPE was equivalent to control. At 25 $\mu\text{g/mL}$ DP, tube formation was decreased as compared to control. At 50 and 100 $\mu\text{g/mL}$ DP, capillary tube formation was completely inhibited. However, cells at 50 $\mu\text{g/mL}$ DP were flattened to the matrix, while the cells treated with 100 $\mu\text{g/mL}$ DP appeared ball shaped. At 20 and 40 $\mu\text{g/mL}$ DPE, tube formation was inhibited in a concentration-dependent manner with complete inhibition observed at 40 $\mu\text{g/mL}$. WDP did not inhibit tube formation at any concentration tested (Table 4, Figure 12).

Recovery assay

The reversibility of the observed effects of DP and DPE on HUVEC tube formation was tested by allowing the treated cells to grow for approximately 18 hr following replacement of the treatment media with fresh, treatment-free growth media. The ability of the cells to form tubes was restored in all treatment groups with the exception of exposure to whole DP at 100 $\mu\text{g/mL}$. Cells treated with 100 $\mu\text{g/mL}$ DP remained attached to the Matrigel matrix and still appeared ball shaped following the 18-hr recovery period (Table 5, Figure 13).

ECM cell adhesion assay

The ECM cell attachment assay was used to determine the relative attachment of adherent cell lines to ECM proteins. Integrins interact in a specific manner with different ECM proteins. Binding of HUVEC treated with DPE to the ECM proteins collagen IV,

fibronectin, vitronectin, laminin I, or Matrigel (ECM) was not significantly different from control with any treatment (Table 6, Figure 14).

Caspase-9 and Caspase-3 activity assays

In order to determine if exposure of HUVEC to DPE induces apoptosis, enzyme activity assays were used to determine levels of active caspase-9 and caspase-3. Caspase-9 and caspase-3 are intracellular proenzymes that are activated early during the cascade of events associated with apoptosis. Caspase-9 is an upstream proenzyme in the cascade of enzymatic reactions required to induce cellular apoptosis. Caspase-3 is an intracellular cysteine protease that exists as a proenzyme. Active caspase-9 activates pro-caspase-3 during the cascade of events associated with apoptosis. Activated caspase-3 is a key enzyme required for the execution of apoptosis. Caspase-9 or caspase-3 activity was not significantly different from control with any treatment (Table 7, Figure 15).

Lactate dehydrogenase assay

In order to determine if exposure to DPE causes cell death, a lactate dehydrogenase (LDH) assay was used to determine levels of LDH released into the culture medium. LDH is a soluble, cytosolic enzyme released into the culture medium upon cell damage or lysis; therefore, LDH activity in the culture medium can be used as an indicator of cell membrane integrity. LDH activity was not significantly different from control with any treatment (Table 7, Figure 16).

Annexin V and propidium iodide staining

Early in the apoptotic process phosphatidylserine (PS) becomes exposed on the cell surface by flipping from the inner to the outer surface of the cytoplasmic membrane. Annexin V binds to PS and can be used to identify these membrane changes associated with apoptosis. Propidium iodide is used to identify cells that have lost membrane integrity. Representative images of the annexin-V and propidium iodide staining results are shown in Figure 17. HUVECs, treated or untreated, did not stain with either annexin-V or propidium iodide (Table 6, Figure 17).

Hoechst staining

Hoechst (H33342) penetrates the plasma membrane and stains DNA in cells without permeabilization. The nuclei of apoptotic cells have highly condensed chromatin that is uniformly stained by H33342. These morphological changes in the nuclei can be visualized by fluorescence microscopy. Representative images of the Hoechst staining results are shown in Figure 18. The nuclear morphology of treated HUVECs was not significantly different from that of the untreated cells (Table 6, Figure 18).

DNA fragmentation assay

Late in the apoptotic process, endonucleases cleave nuclear DNA between nucleosomes producing a mix of DNA fragments that vary in length from 180 - 200 base pairs. This degradation of the DNA occurs several hours prior to plasma membrane breakdown. The cell death detection assay measures the amount of histone-associated

DNA fragments after induced apoptosis. DNA fragmentation was not significantly different from control with any treatment (Table 6, Figure 19).

Actin cytoskeleton staining

The cytoskeleton is a dynamic network composed mainly of actin polymers and associated proteins. Disruption of the normal regulation of the organization of the actin cytoskeleton may lead to an interruption of cellular processes including cell motility and vascular tube formation. In order to determine the effects of DPE on cytoskeletal organization, HUVEC treated with various concentrations of DPE were stained with TRITC-conjugated Phalloidin. Results of our staining of the actin cytoskeleton show a disruption in the organization of actin into filaments in conjunction with the inhibition of tube formation observed with exposure to DPE (Figure 20).

RhoA, Rac1, and Cdc42 activation

Cytoskeletal reorganization of actin microfilaments is regulated by the Rho family of GTPases. Proteins such as RhoA, Rac1, and Cdc42 are key contributors to this process. Our data show a statistically significant decrease in activation of Cdc42 and Rac proteins including Rac1, but no change in activated RhoA when compared to control in HUVEC treated with DPE levels sufficient to inhibit HUVEC tube formation (Figure 21).

Summary of the Data

The formation of capillary-like structures by HUVEC grown on Matrigel was inhibited in a dose-dependent manner following treatment with DP (Figure 9). After 4 hours, controls showed a full network of tube development. At 1 $\mu\text{g/mL}$ DP, 0.75 and 7.5 $\mu\text{g/mL}$ CB, and 1, 3, 10, and 20 $\mu\text{g/mL}$ DPE, tube development was equivalent to controls. There was a dose-dependent reduction in tube formation at 10 and 100 $\mu\text{g/mL}$ DP with complete inhibition of tube formation at 100 $\mu\text{g/mL}$.

Concentrations of DPE at a range of 10 to 100 $\mu\text{g/mL}$ in 10 $\mu\text{g/mL}$ increments were tested for the ability to inhibit the formation of capillary-like structures by HUVEC grown on Matrigel. DPE concentrations ≤ 40 $\mu\text{g/mL}$, inhibited capillary tube formation in a concentration-dependent manner with complete inhibition at 40 $\mu\text{g/mL}$ and a NOAEL of 10 $\mu\text{g/mL}$. At 20 $\mu\text{g/mL}$ DPE, individual cells began to be observed that were not involved in tube formation. At 40 $\mu\text{g/mL}$ DPE, cells were still flattened to the Matrigel matrix; however, tube formation was completely inhibited. At ≥ 50 $\mu\text{g/mL}$ DPE, tube formation was completely inhibited and all cells appeared ball-shaped and not flattened to the matrix (Figures 10 and 11).

Capillary tube formation in HUVEC grown on Matrigel and treated with 25 $\mu\text{g/mL}$ DP and 10 $\mu\text{g/mL}$ DPE was equivalent to control. At concentrations of 50 and 100 $\mu\text{g/mL}$ DP, capillary tube formation was completely inhibited. However, cells at 50 $\mu\text{g/mL}$ DP were flattened to the matrix (arrows), while the cells treated with 100 $\mu\text{g/mL}$ DP appeared ball shaped. At 20 and 40 $\mu\text{g/mL}$ DPE, tube formation was inhibited in a concentration-dependent manner. WDP did not inhibit tube formation at any concentration tested (Figure 12). The ability of HUVEC to form tubes was

restored in all treatment groups with the exception of exposure to whole DP at 100 $\mu\text{g/mL}$. Cells treated with 100 $\mu\text{g/mL}$ DP remained attached to the Matrigel matrix and still appeared ball shaped following the 18-hr recovery period (Figure 13).

Binding of HUVEC treated with DPE to components of the ECM was not significantly different from control with any treatment (Figure 14). Inhibition of vascular tube formation in HUVEC grown on Matrigel following treatment with DPE is not due to apoptosis or cell death (Figures 15 - 19). However, exposure of HUVEC to DPE was shown to disrupt the organization of the actin cytoskeleton in cells grown on Matrigel (Figure 20) and did result in decreases in the activation of the Rho GTPases Rac and Cdc42 (Figure 21). This biochemical pathway is critical for the vascular endothelial cells to form normal cytoskeleton, and can be used to explain the morphological observations and the ability of the cells to recover. The DPE caused the majority of the effects from the DP, but there does appear to be an enhanced toxicity when the whole DP is tested. Studies need to be conducted to determine if chronic exposure to DP entering into the lung and the systemic circulation could result in decreased angiogenesis and contribute to the health effects observed during high particulate events.

FIGURES AND TABLES

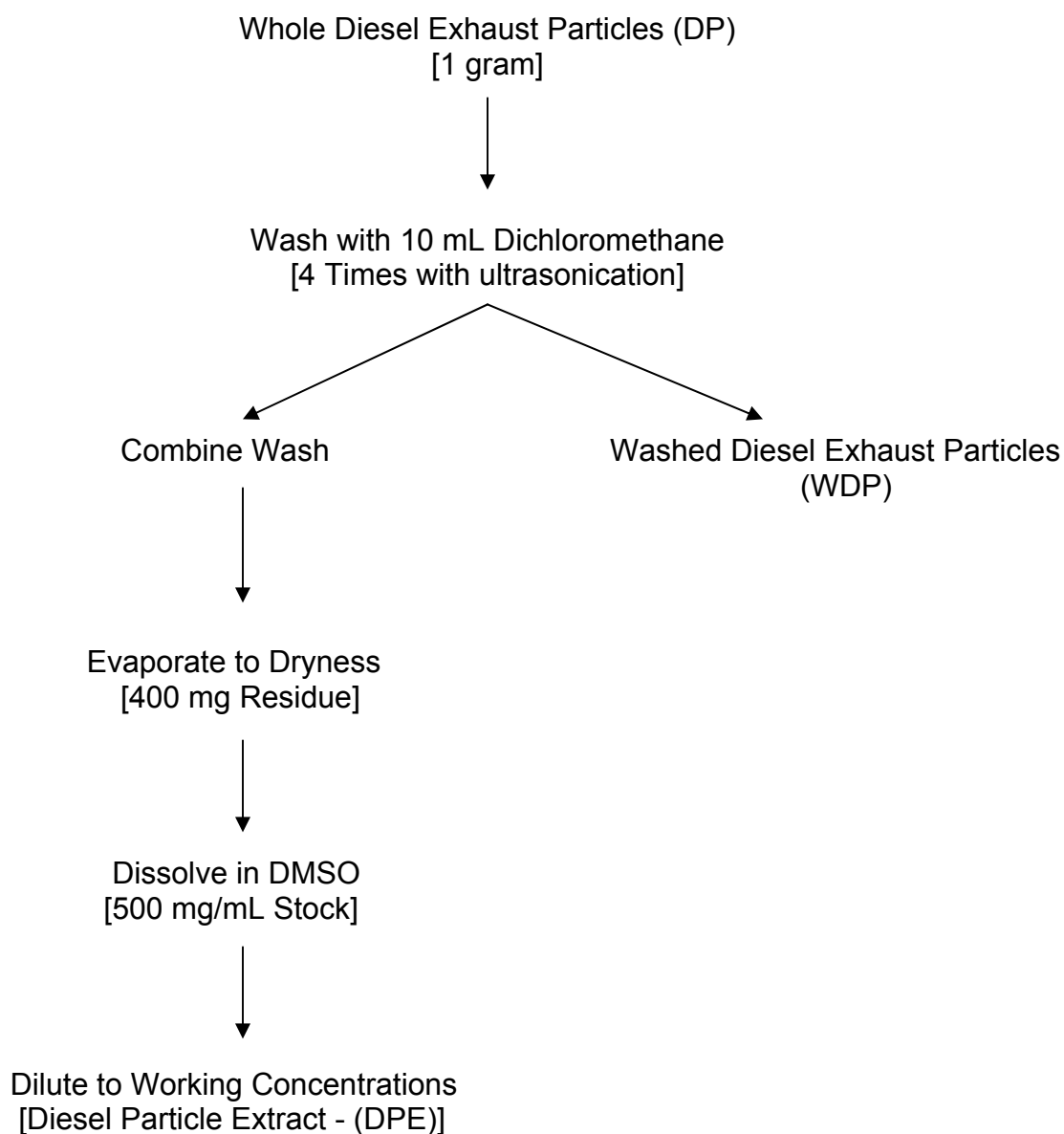
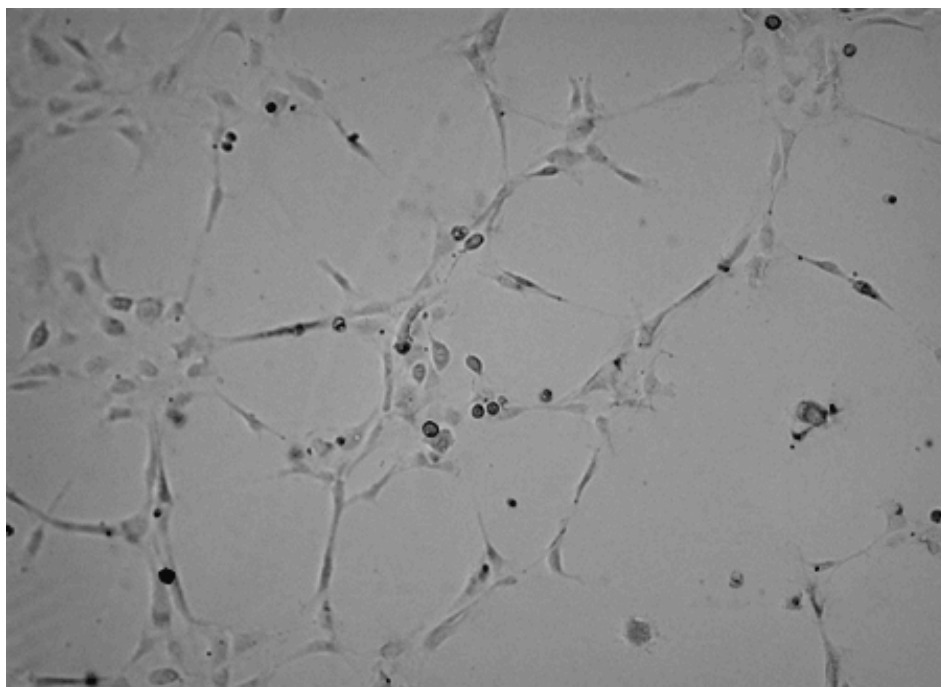


Figure 8. Preparation of an organic extract from diesel particles (DPE) and washed diesel particles (WDP): One gram of whole diesel particles (DP) was washed 4 times with dichloromethane to create an organic extract from the particles and washed diesel particles.

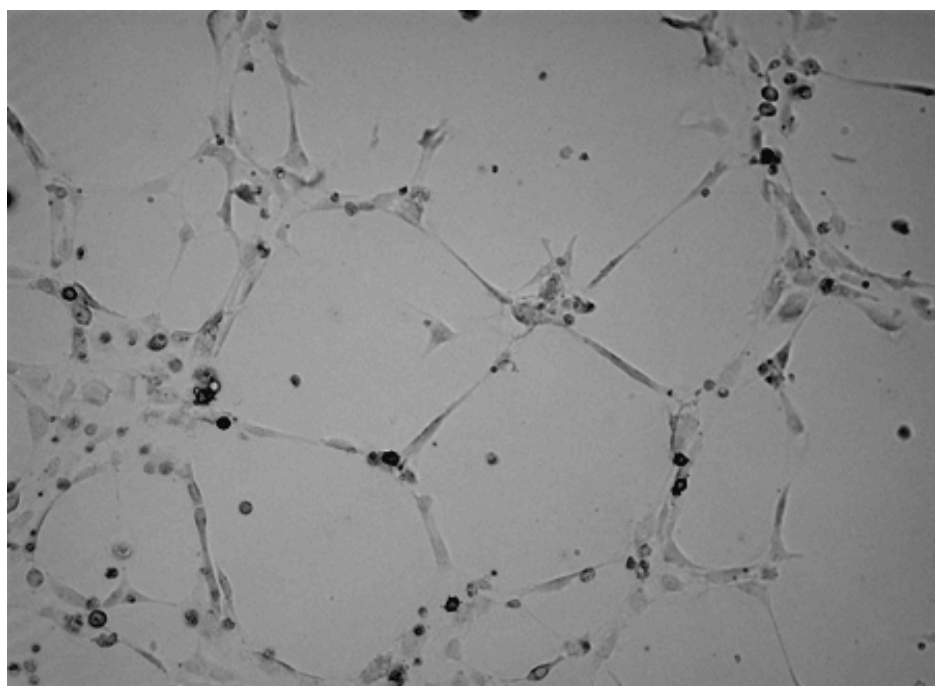
Initial Screen for Effects on <i>in vitro</i> Vascular Formation - 4 hours	
Treatment	Branching
Control (No Treatment)	+++
DMSO (0.1% in Media)	+++
Carbon Black (0.75 µg/mL)	+++
Carbon Black (7.5 µg/mL)	+++
Diesel Particle (1 µg/mL)	+++
Diesel Particle (10 µg/mL)	+++
Diesel Particle (100 µg/mL)	–
Diesel Particle Extract (1 µg/mL)	+++
Diesel Particle Extract (3 µg/mL)	+++
Diesel Particle Extract (10 µg/mL)	+++
Diesel Particle Extract (20 µg/mL)	+++

Table 1: Summary of effects observed in HUVEC at 4 hours following various treatments (+++ = no difference from control; - = no vascular formation). Corresponding data is shown in Figure 9.

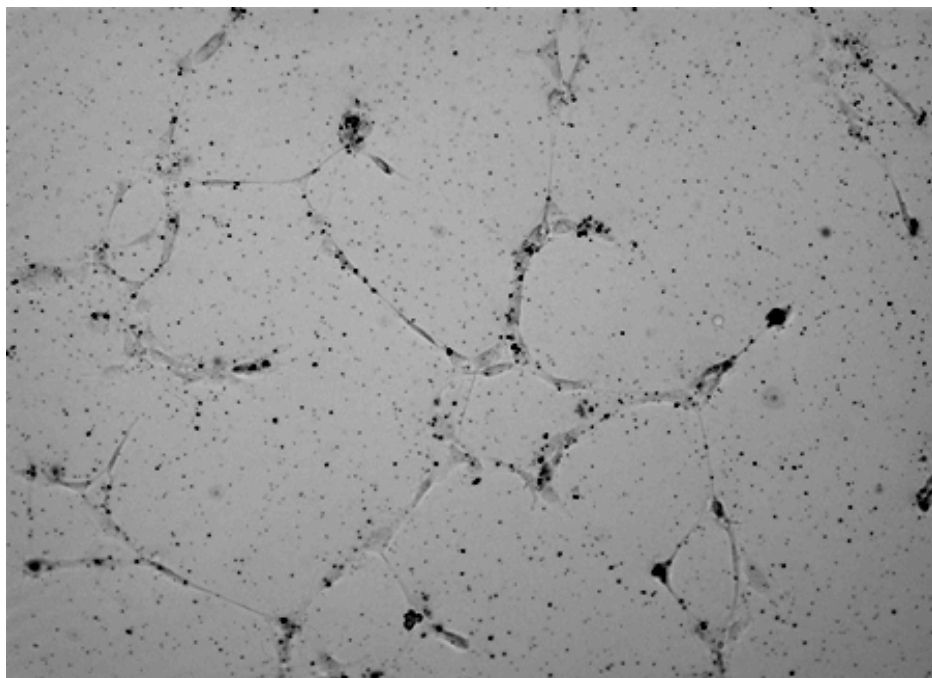
Figure 9. Representative images of *in vitro* HUVEC tube formation following 4 hour exposure to 1, 10, or 100 $\mu\text{g/mL}$ diesel particles, 0.75 or 7.5 $\mu\text{g/mL}$ carbon black, or 1, 3, 10, or 20 $\mu\text{g/mL}$ diesel particle extract: Representative photographs (200X) of (A) untreated HUVEC seeded on Matrigel after 4 hours and following treatment with (B) 0.1% DMSO, (C, D) 0.75 or 7.5 $\mu\text{g/mL}$ carbon black; (E, F, G) 1, 10, or 100 $\mu\text{g/mL}$ diesel particles; or (H, I, J, K) 1, 3, 10, or 20 $\mu\text{g/mL}$ diesel particle extract for 4 hours. Images are of unfixed cells.



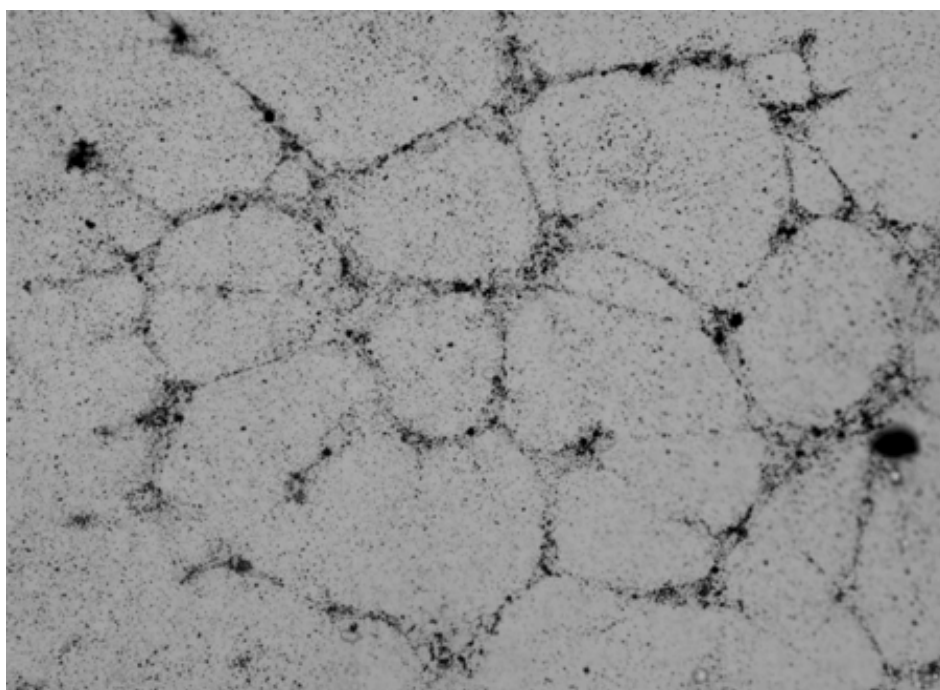
A - Media Control



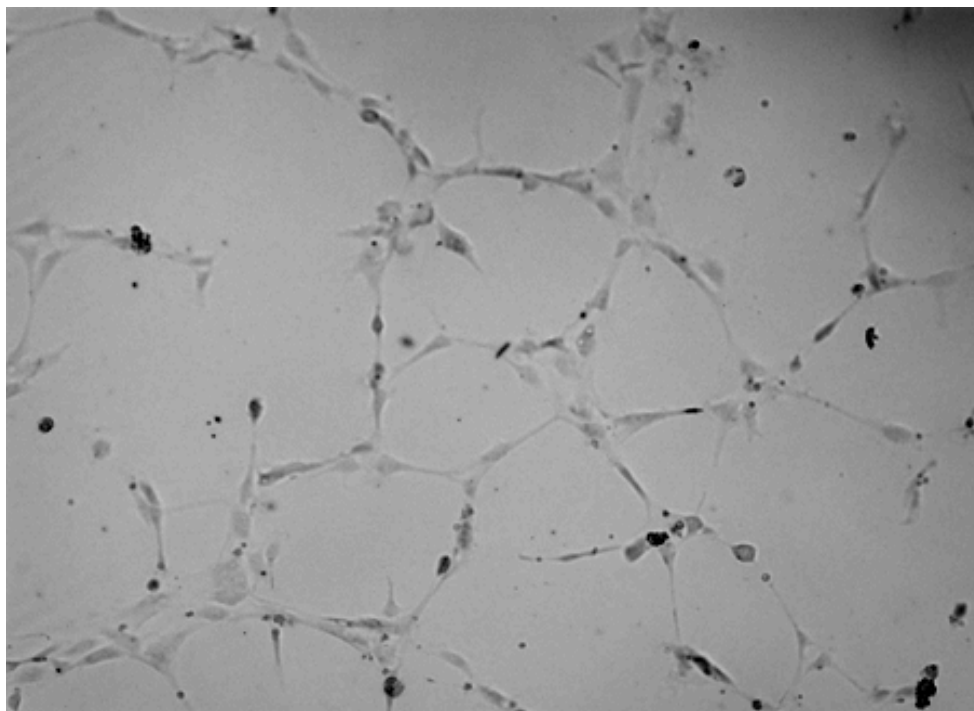
B - 0.1% DMSO



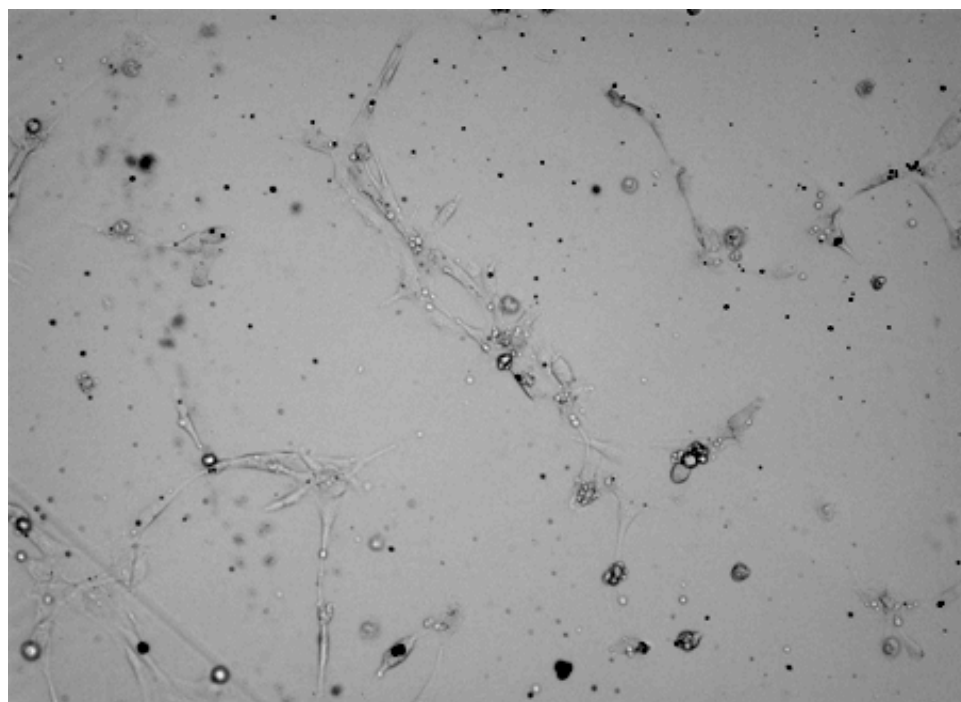
C - 0.75 $\mu\text{g/mL}$ Carbon Black



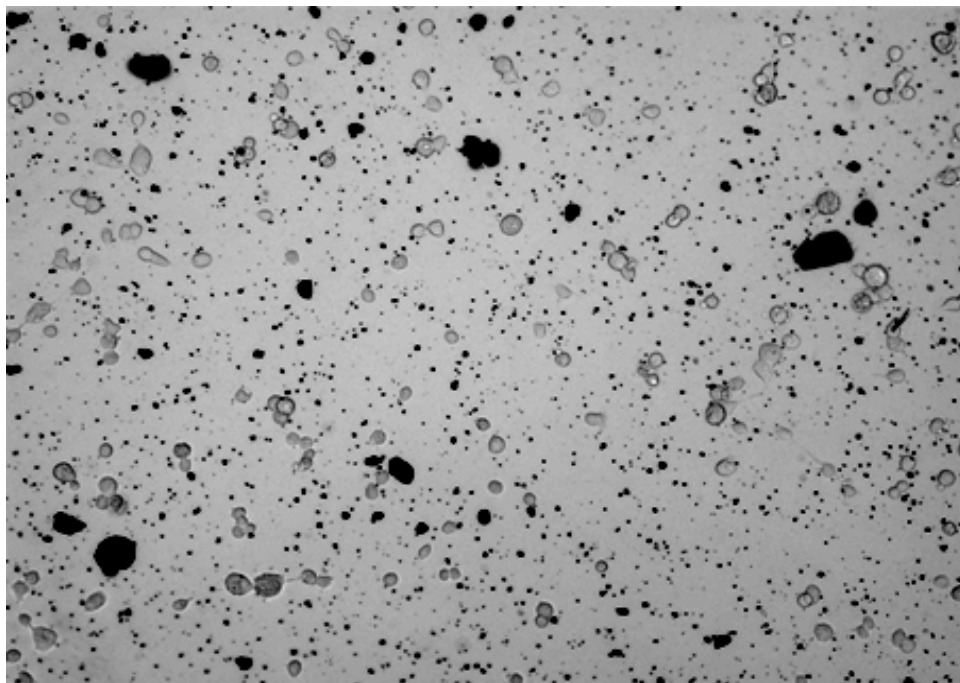
D - 7.5 $\mu\text{g/mL}$ Carbon Black



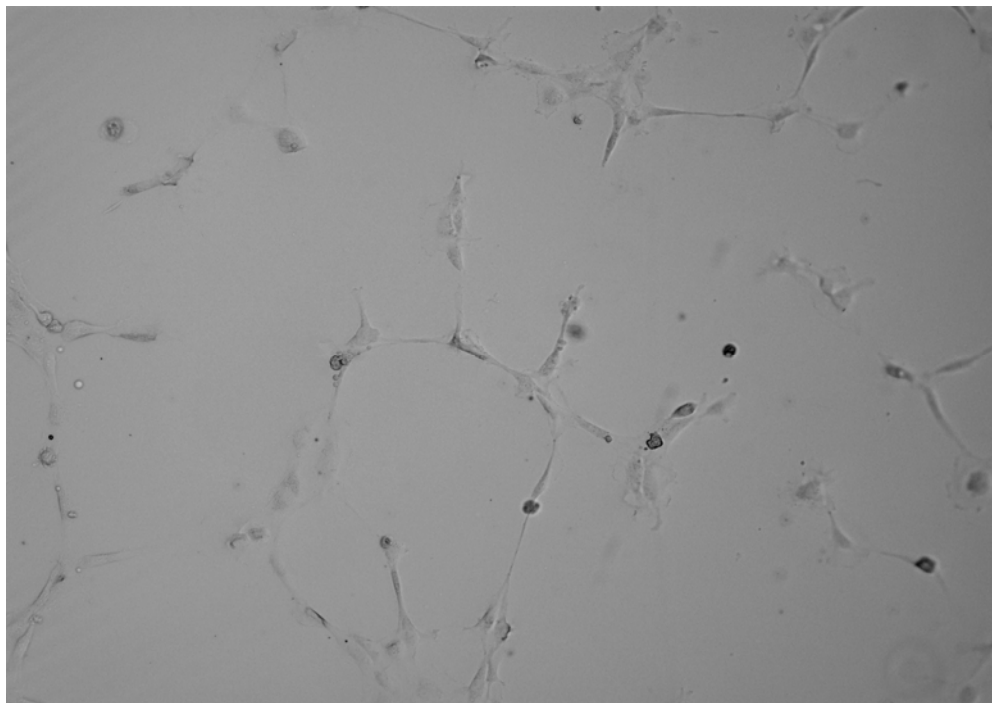
E - 1 $\mu\text{g/mL}$ Diesel Particles



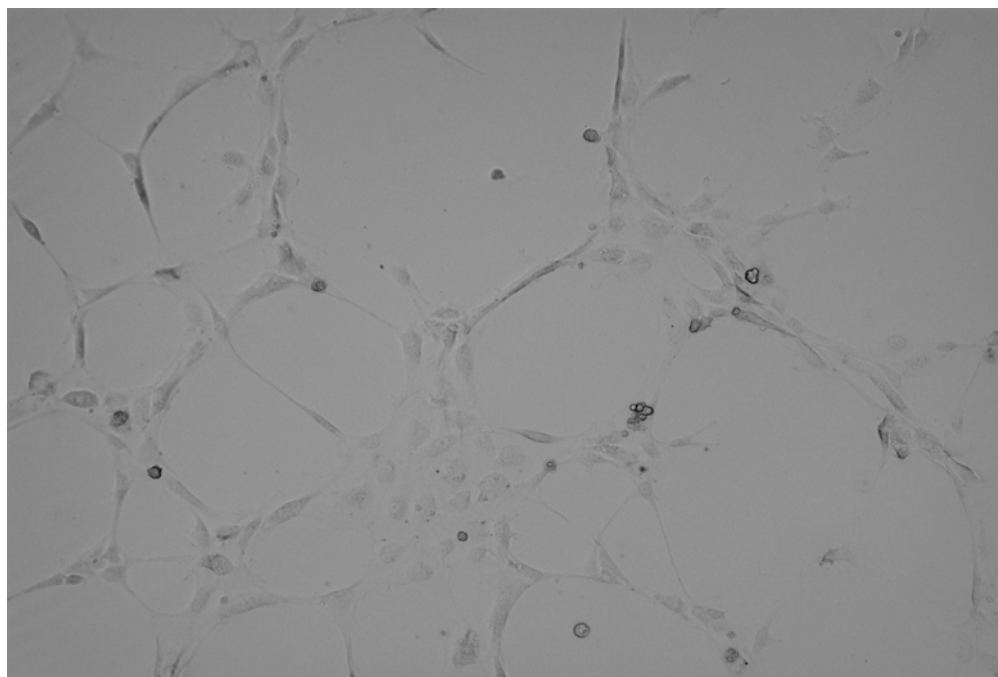
F - 10 $\mu\text{g/mL}$ Diesel Particles



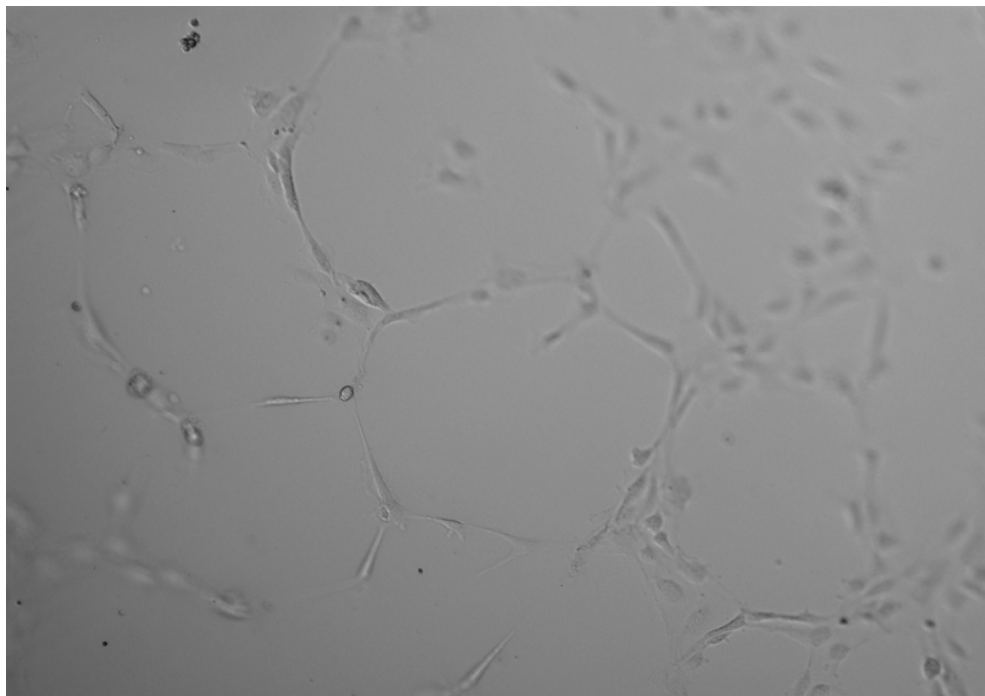
G - 100 $\mu\text{g/mL}$ Diesel Particles



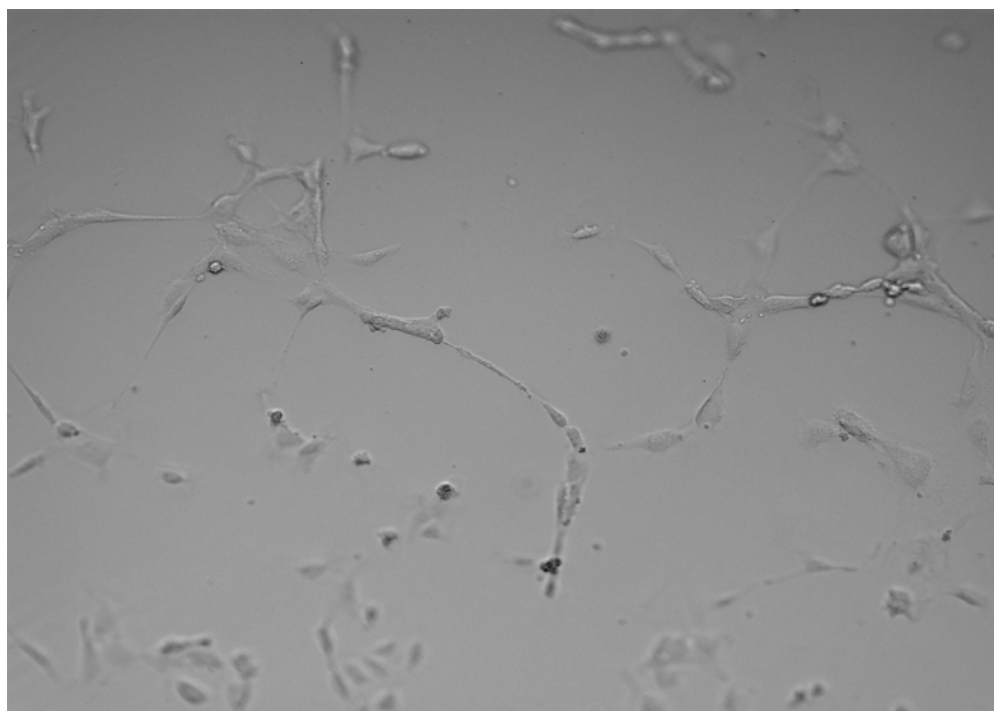
H - 1 $\mu\text{g/mL}$ Diesel Particle Extract



I - 3 $\mu\text{g/mL}$ Diesel Particle Extract



J - 10 $\mu\text{g/mL}$ Diesel Particle Extract

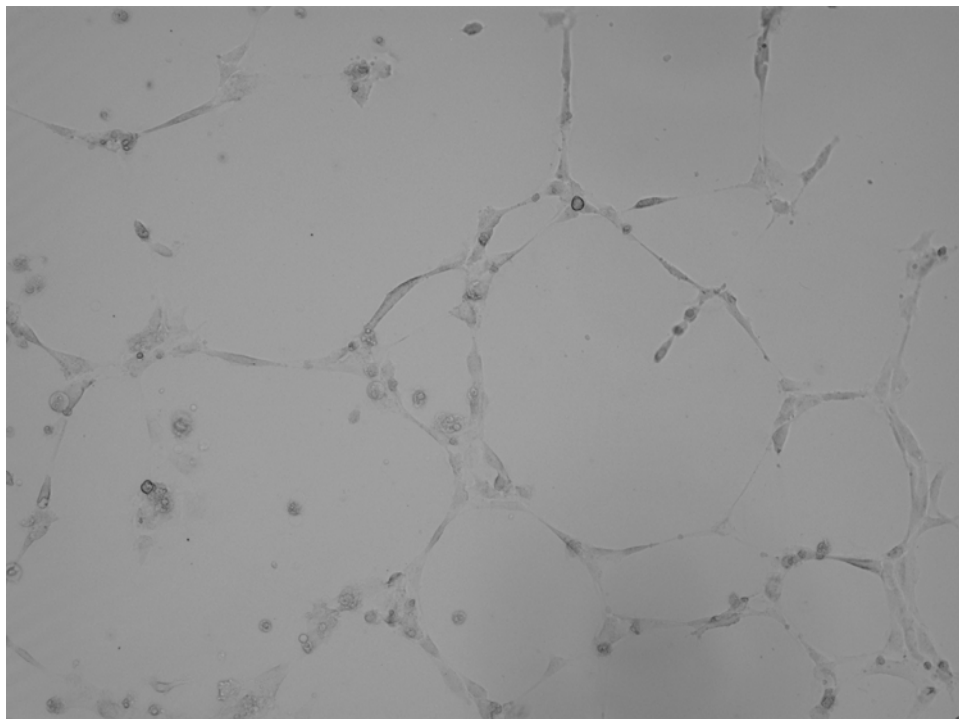


K - 20 $\mu\text{g/mL}$ Diesel Particle Extract

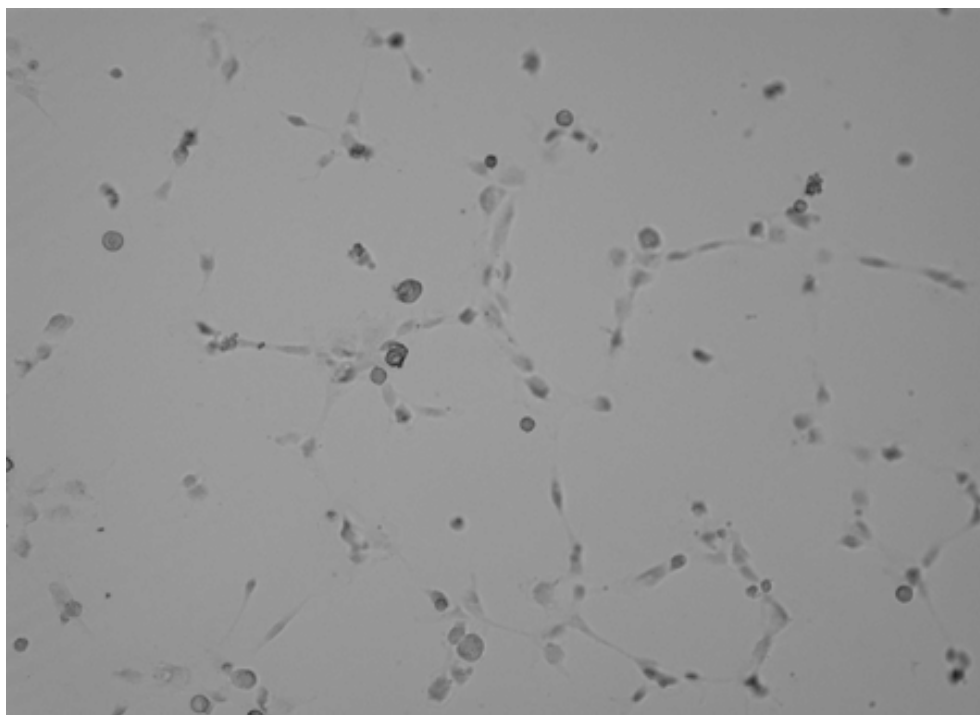
Screen for Effects of DPE on <i>in vitro</i> Vascular Formation - 3 hours	
Treatment	Branching
DMSO (0.1% in Media)	+++
Diesel Particle Extract (25 µg/mL)	++
Diesel Particle Extract (50 µg/mL)	—
Diesel Particle Extract (100 µg/mL)	—
Diesel Particle Extract (200 µg/mL)	—

Table 2: Summary of effects observed in HUVEC at 3 hours following treatment with diesel particle extract (+++ = no difference from control; ++ = decreased as compared to control; - = no vascular formation). Corresponding data is shown in Figure 10.

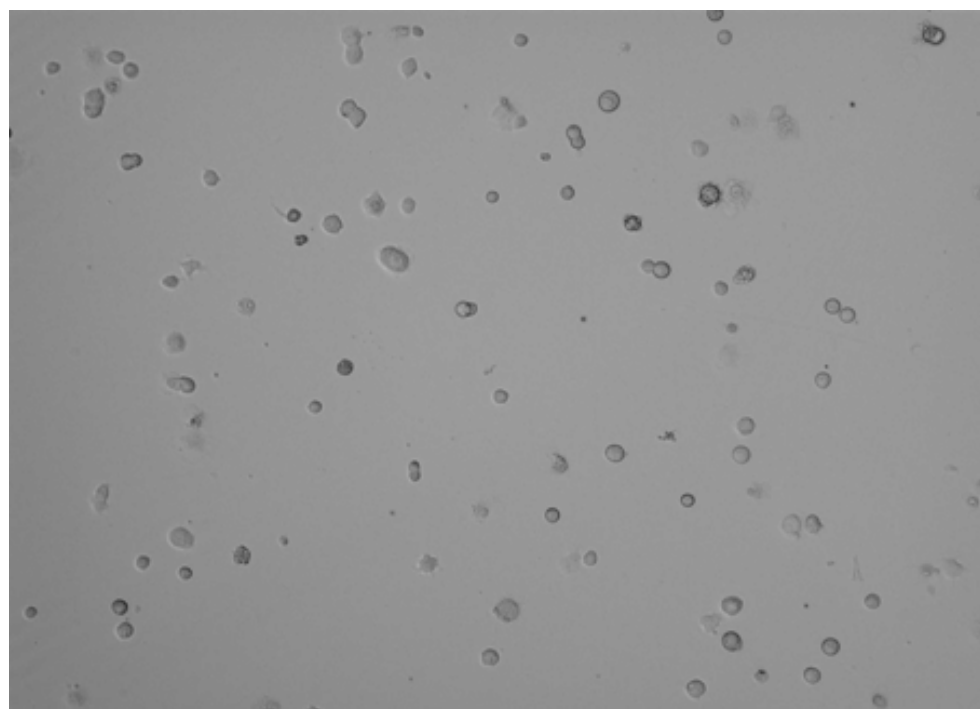
Figure 10. Representative images of *in vitro* HUVEC tube formation following 3 hour exposure to 25, 50, 100, or 200 µg/mL diesel particle extract: Representative photographs (200X) of HUVEC seeded on Matrigel and treated for 3 hours with (A) 0.1% DMSO, (B) 25 µg/mL diesel particle extract; (C) 50 µg/mL diesel particle extract; (D) 100 µg/mL diesel particle extract; or (E) 200 µg/mL diesel particle extract. Images are of unfixed cells.



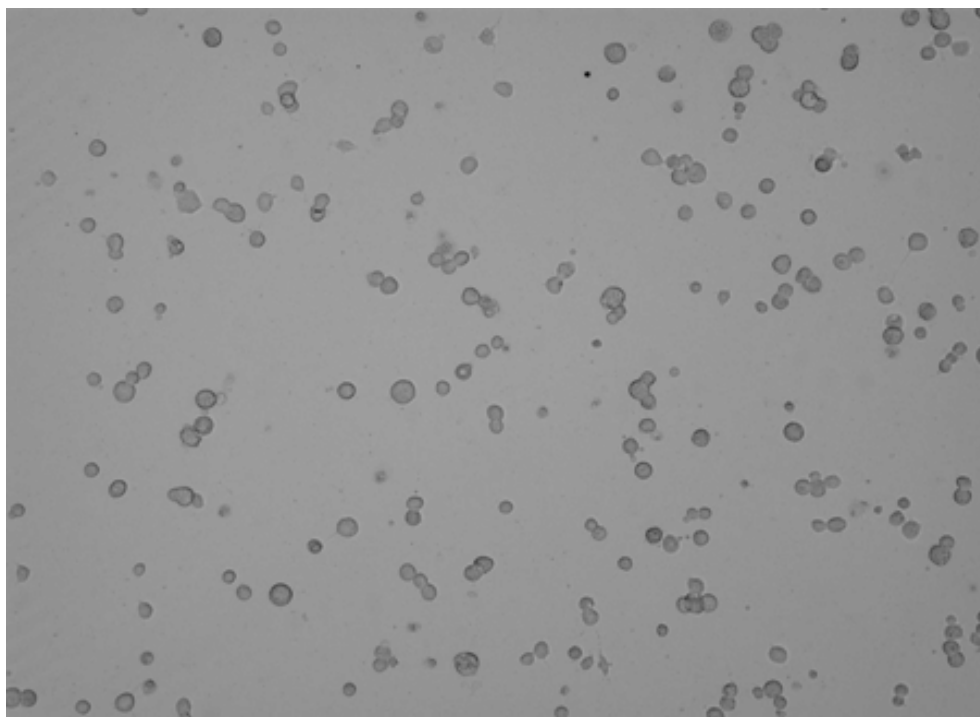
A - 0.1% DMSO Control



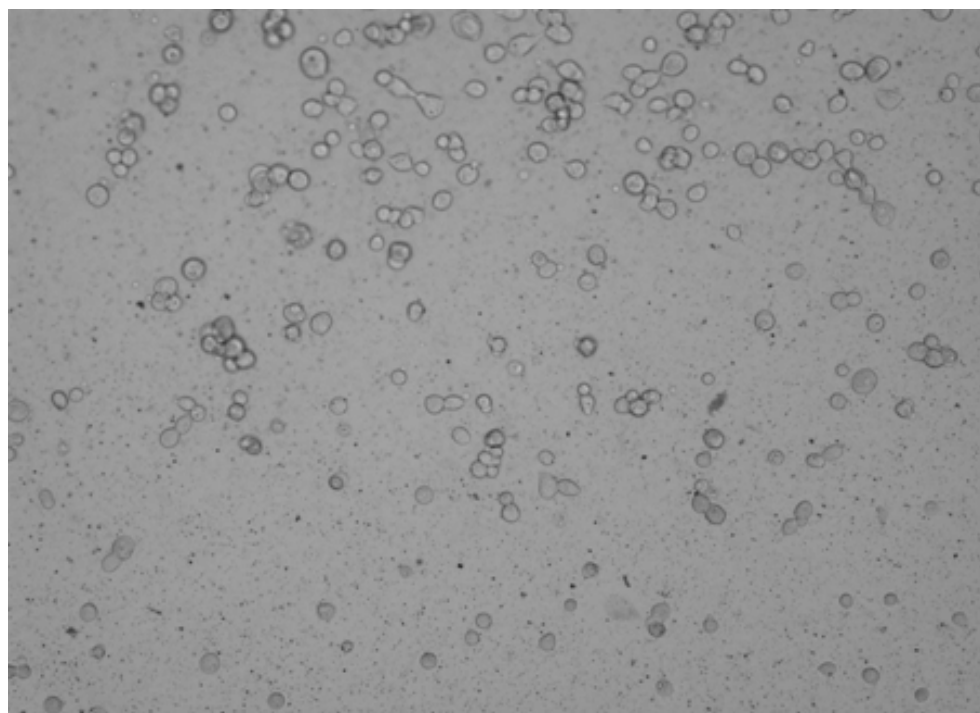
B - 25 µg/mL Diesel Particle Extract



C - 50 µg/mL Diesel Particle Extract



D - 100 $\mu\text{g/mL}$ Diesel Particle Extract



E - 200 $\mu\text{g/mL}$ Diesel Particle Extract

DPE Range-Finding - 3 hours	
Treatment	Tube Formation
DMSO (0.1% in Media)	+++
Diesel Particle Extract (10 µg/mL)	+++
Diesel Particle Extract (20 µg/mL)	++*
Diesel Particle Extract (30 µg/mL)	+
Diesel Particle Extract (40 µg/mL)	—**
Diesel Particle Extract (50 µg/mL and higher)	—***

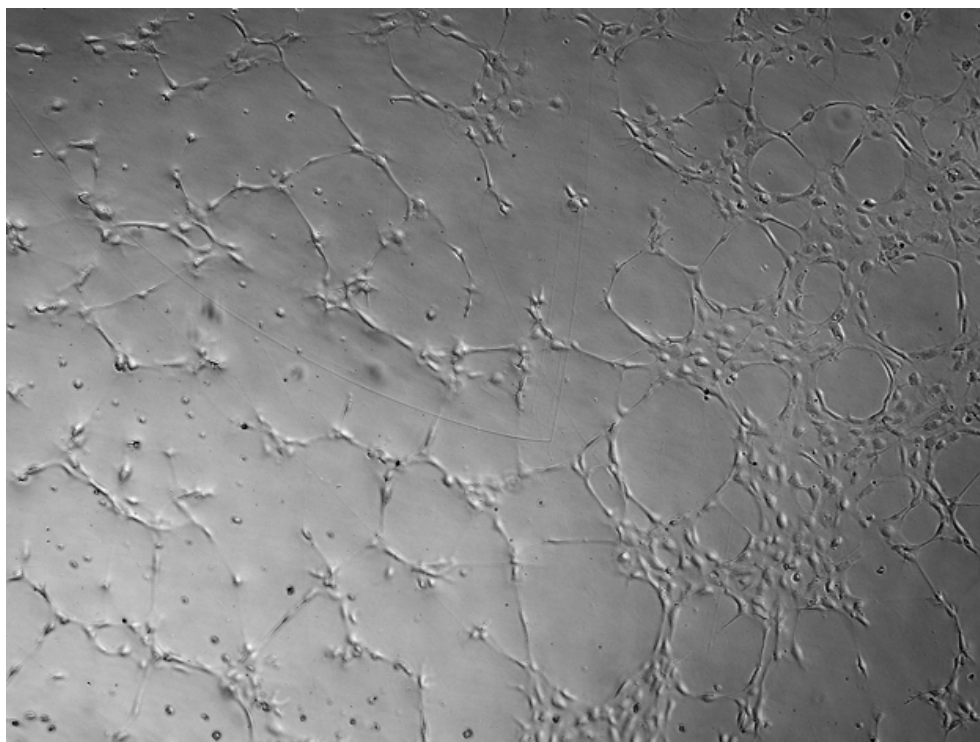
Table 3: Summary of effects observed in HUVEC at 3 hours following treatment with diesel particle extract (+++ = no difference from control; ++ = slight difference from control; + = marked difference from control; - = no vascular formation). Corresponding effects are shown in Figure 11.

* - Begin to see cells not involved in tube formation.

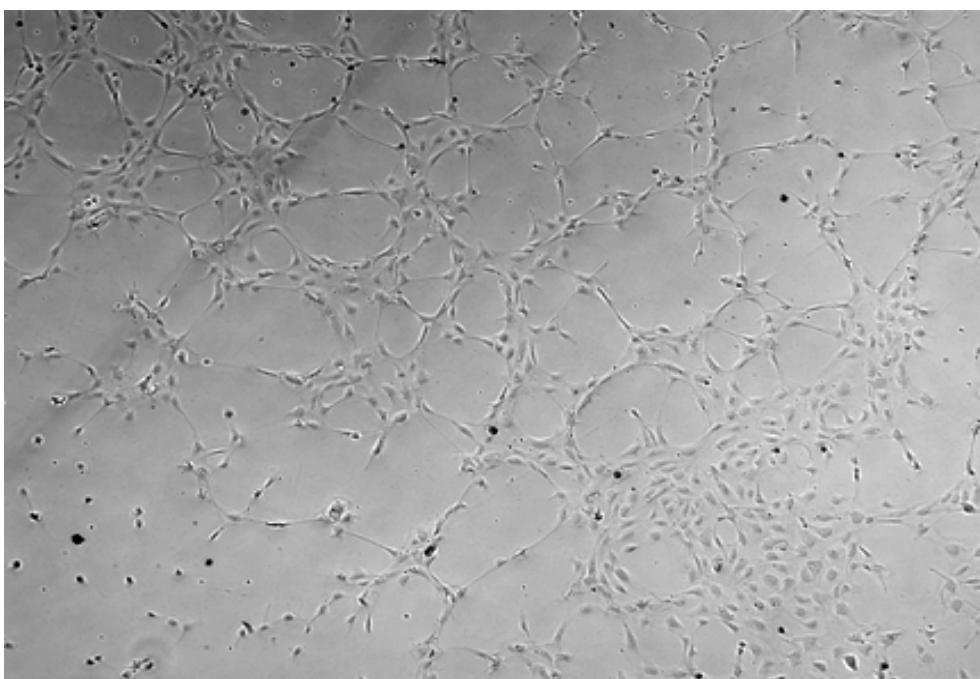
** - HUVEC flattened to the Matrigel matrix, but no tube formation observed.

*** - All cells have ball-shaped appearance.

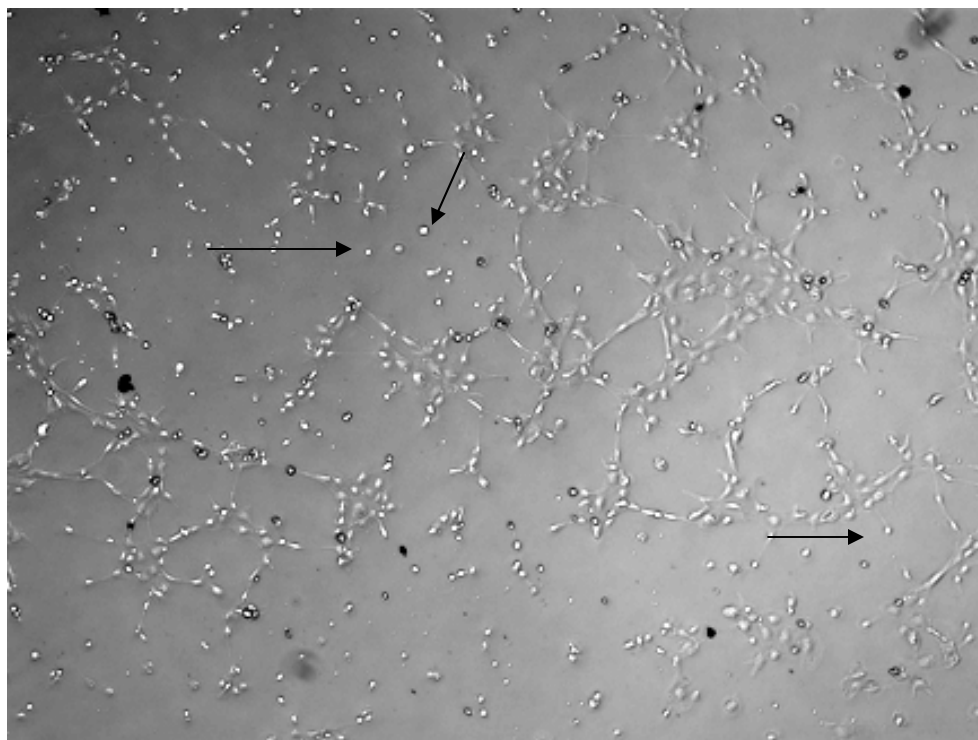
Figure 11. Representative images of *in vitro* HUVEC tube formation following 3 hour exposure to 10 - 100 $\mu\text{g/mL}$ diesel particle extract: Representative photographs (100X) of HUVEC seeded on Matrigel and treated for 3 hours with (A) 0.1% DMSO, (B) 10 $\mu\text{g/mL}$ diesel particle extract; (C) 20 $\mu\text{g/mL}$ diesel particle extract (arrows indicate individual cells not involved in tube formation); (D) 30 $\mu\text{g/mL}$ diesel particle extract; (E) 40 $\mu\text{g/mL}$ diesel particle extract, or (F) 50 $\mu\text{g/mL}$ diesel particle extract. At > 50 $\mu\text{g/mL}$ diesel particle extract, tube formation was completely inhibited and all cells appeared ball-shaped and not flattened to the matrix (images not shown). Images are of unfixed cells.



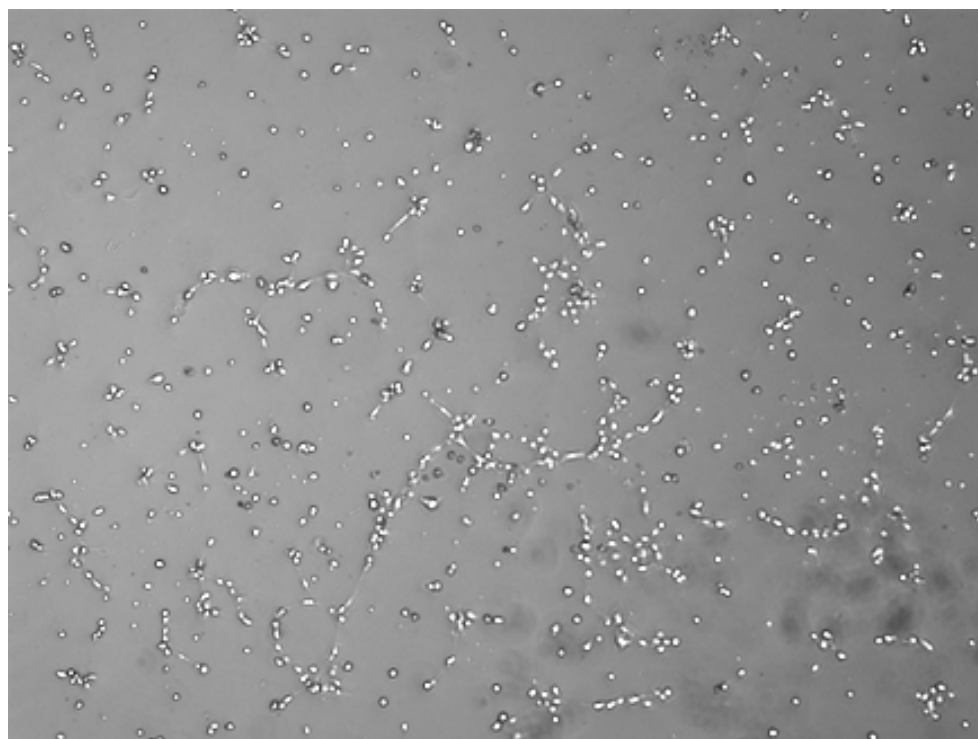
A - 0.1% DMSO Control



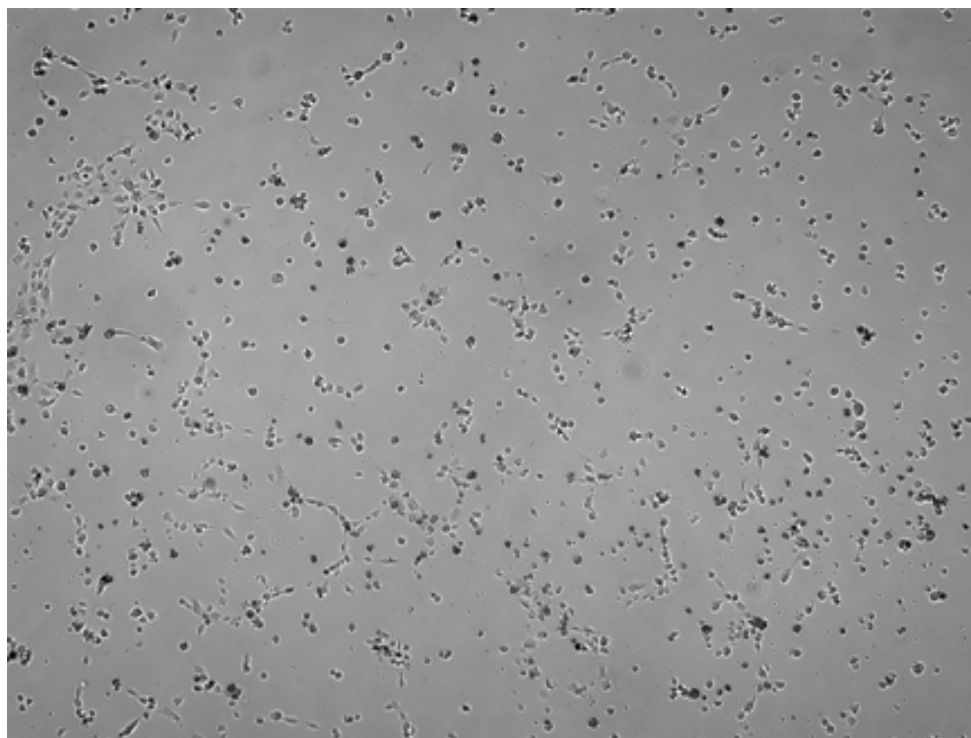
B- 10 $\mu\text{g/mL}$ Diesel Particle Extract



C - 20 µg/mL Diesel Particle Extract



D - 30 µg/mL Diesel Particle Extract



E - 40 µg/mL Diesel Particle Extract

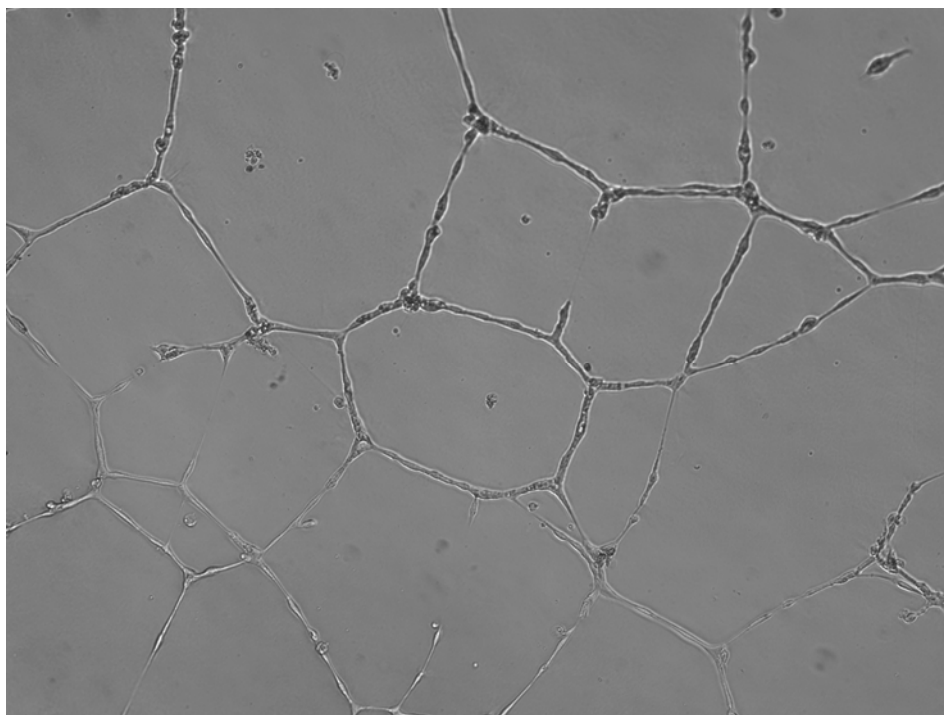


F - 50 µg/mL Diesel Particle Extract

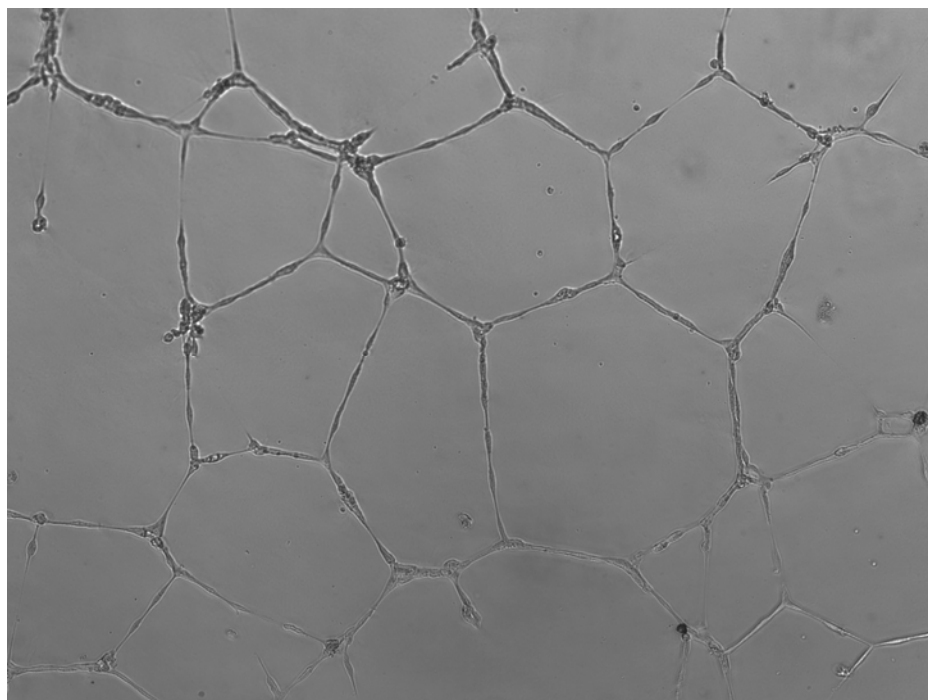
Exposure to DP, DPE, or WDP - 3 hours		
Diesel Particles (100 µg/mL)	Diesel Particle Extract (40 µg/mL)	Washed Particles (60 µg/mL)
—	—	+++
Diesel Particles (50 µg/mL)	Diesel Particle Extract (20 µg/mL)	Washed Particles (30 µg/mL)
—	++	+++
Diesel Particles (25 µg/mL)	Diesel Particle Extract (10 µg/mL)	Washed Particles (15 µg/mL)
+	+++	+++

Table 4: Summary of effects observed in HUVEC at 3 hours following various treatments (+++ = no difference from control; ++ = slight difference from control; + = marked difference from control; - = no vascular formation). 0.1% DMSO showed no difference from control. Corresponding effects are shown in Figure 12.

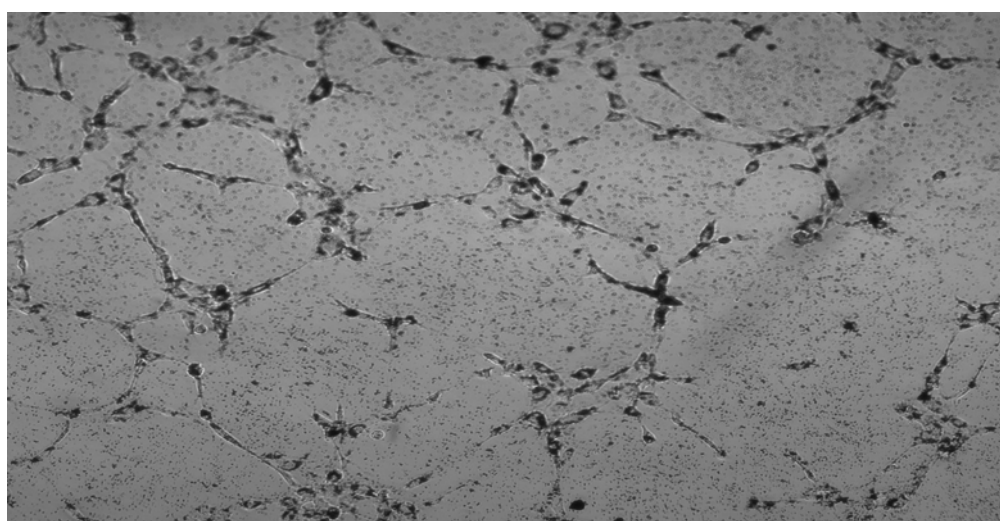
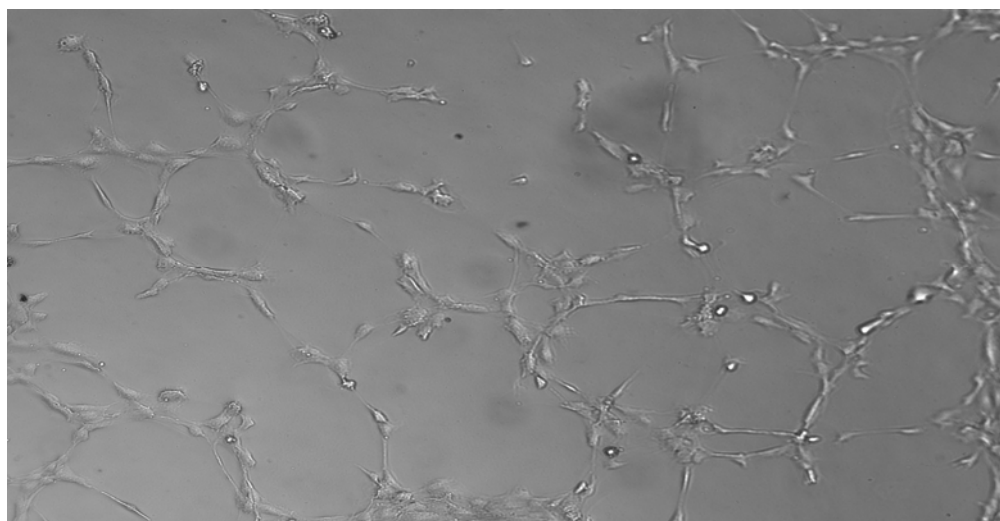
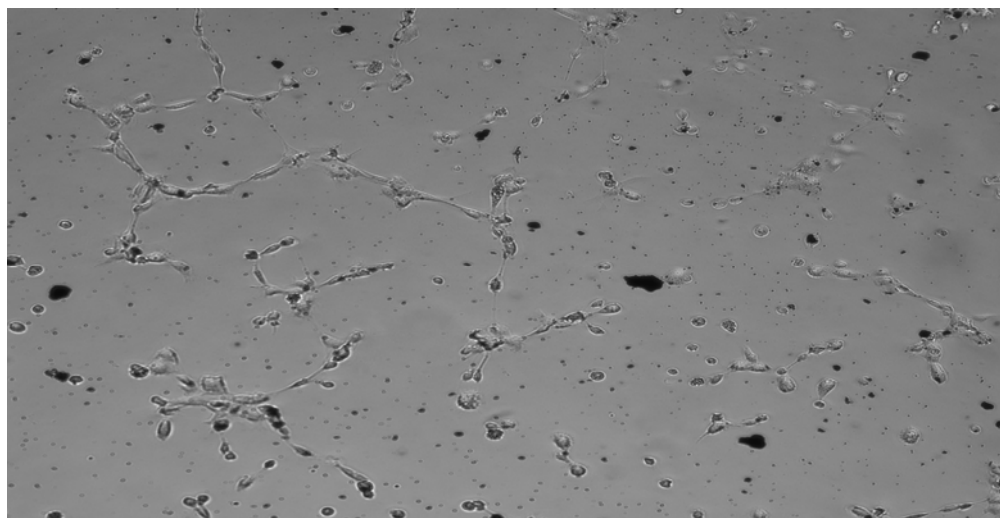
Figure 12. Representative images of *in vitro* HUVEC tube formation following 3 hour exposure to 25, 50, or 100 $\mu\text{g/mL}$ diesel particles, 10, 20, or 40 $\mu\text{g/mL}$ diesel particle extract, or 15, 30, or 60 $\mu\text{g/mL}$ washed diesel particles: Representative photographs (200X) of HUVEC seeded on Matrigel and treated for 3 hours with (A) untreated media (B) 0.1% DMSO, (C) 25 $\mu\text{g/mL}$ DP (top), 10 $\mu\text{g/mL}$ DPE (middle), 15 $\mu\text{g/mL}$ WDP (bottom); (D) 50 $\mu\text{g/mL}$ DP (top - arrows indicate cells flattened to the matrix but not involved in tube formation), 20 $\mu\text{g/mL}$ DPE (middle), 30 $\mu\text{g/mL}$ WDP (bottom); or (E) 100 $\mu\text{g/mL}$ DP (top), 40 $\mu\text{g/mL}$ DPE (middle), 60 $\mu\text{g/mL}$ WDP (bottom).



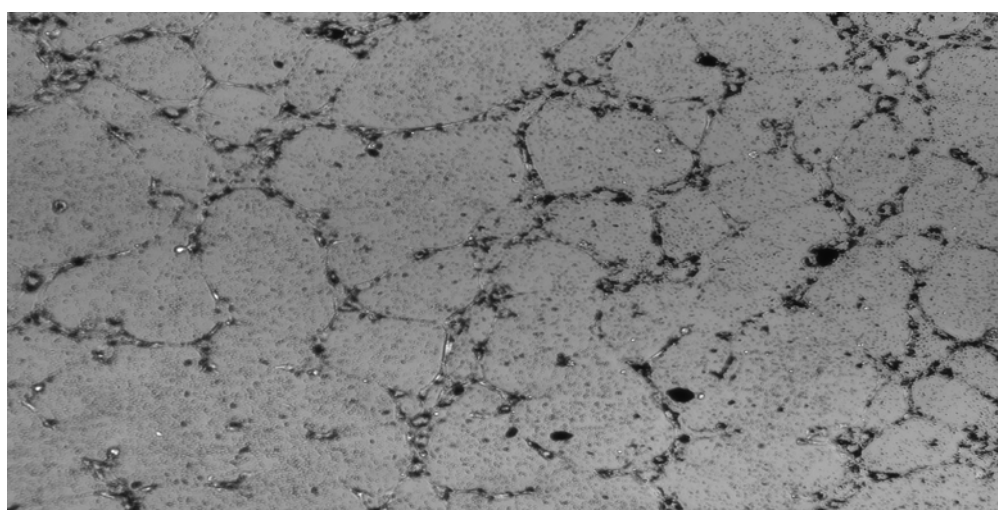
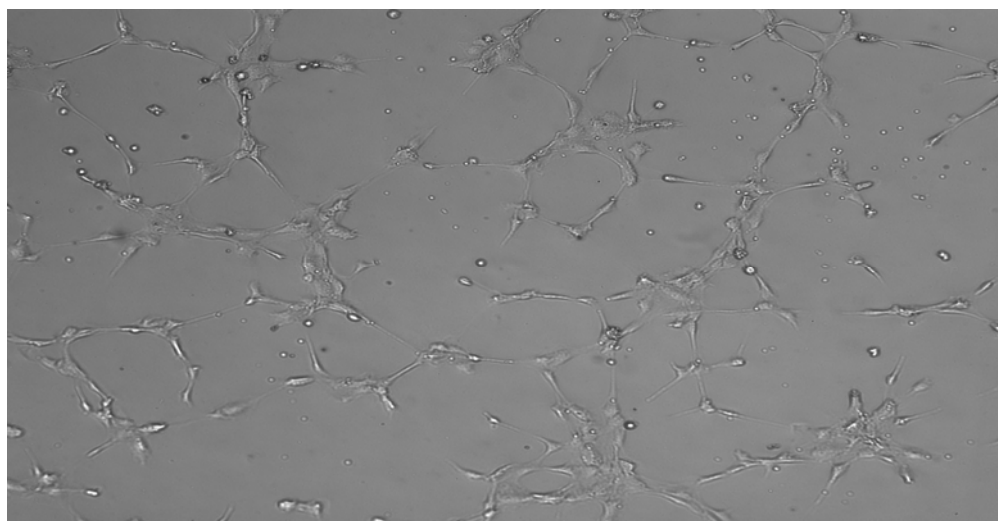
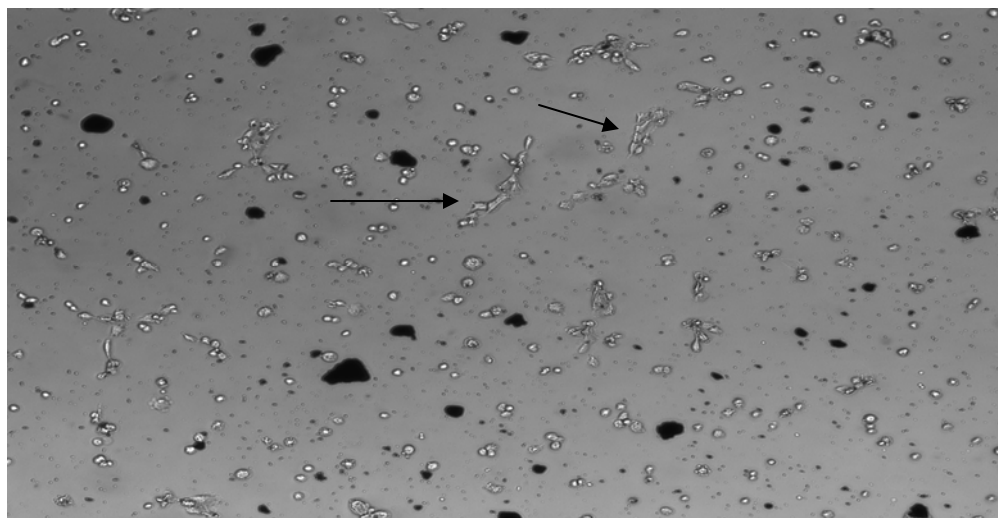
A - Media Control



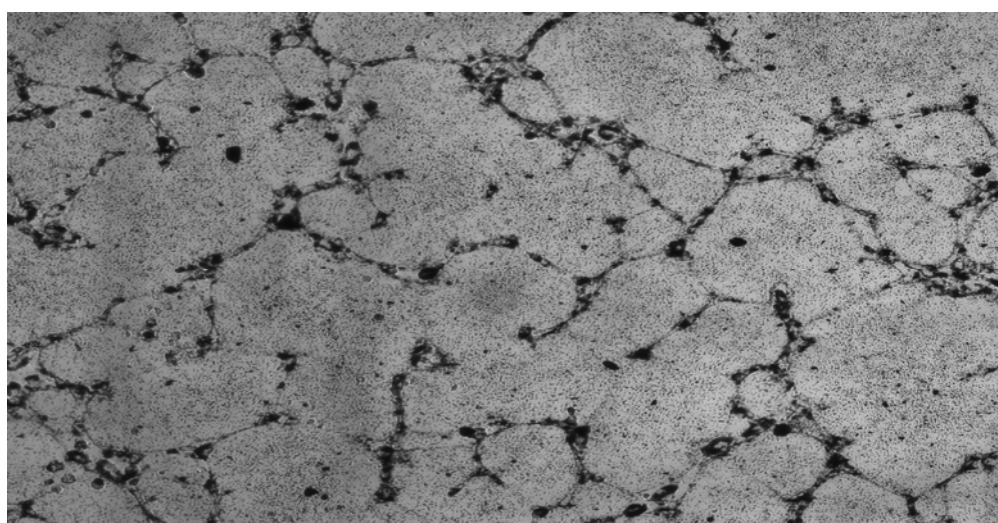
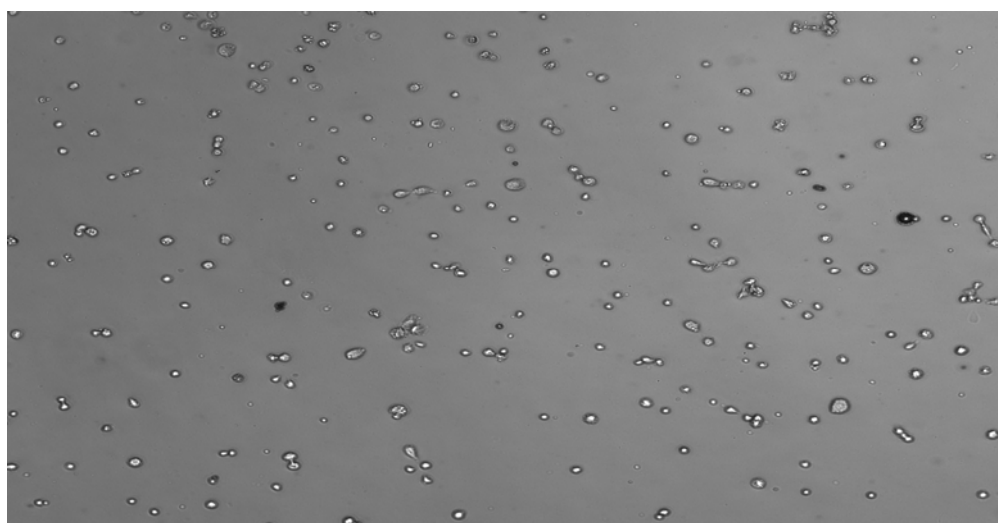
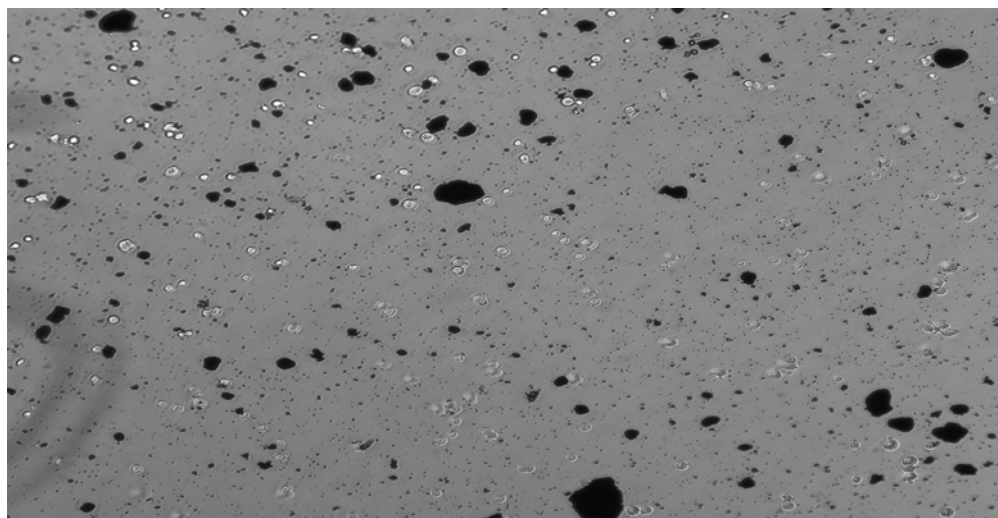
B - 0.1% DMSO



C - 25 $\mu\text{g/mL}$ DP (top), 10 $\mu\text{g/mL}$ DPE (middle), 15 $\mu\text{g/mL}$ WDP (bottom)



D - 50 µg/mL DP (top), 20 µg/mL DPE (middle), 30 µg/mL WDP (bottom)



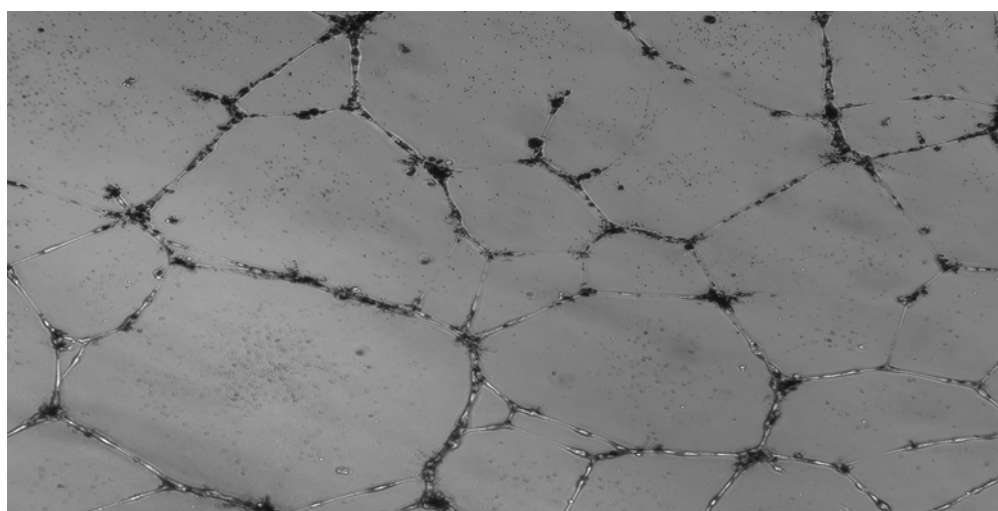
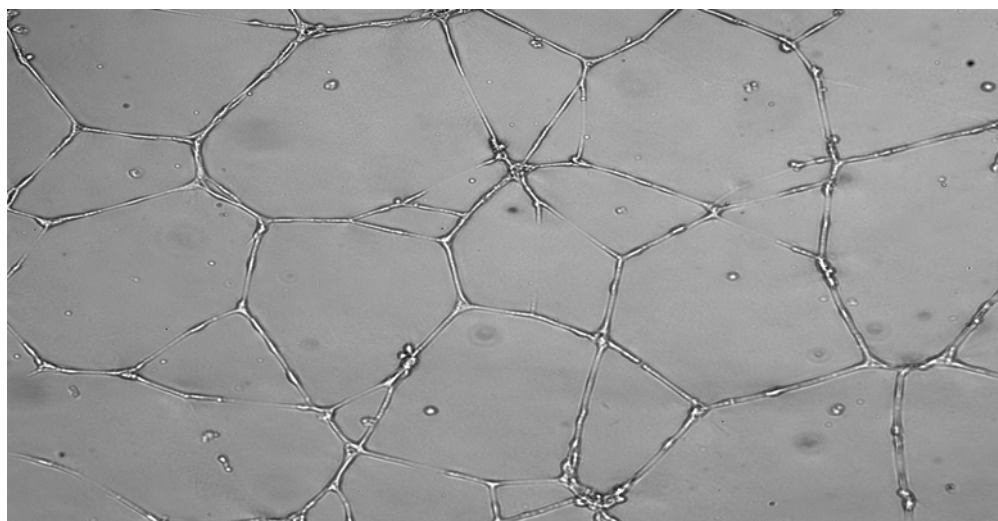
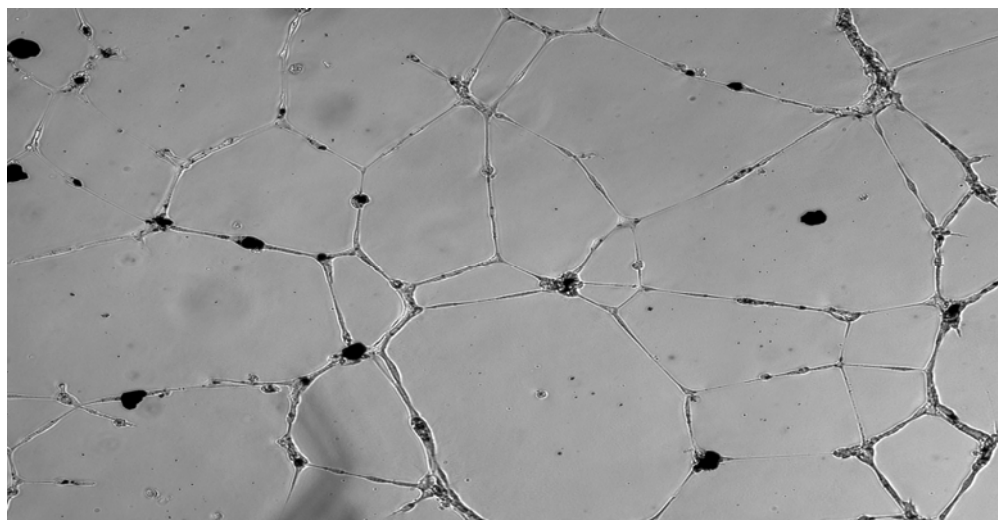
E - 100 µg/mL DP (top), 40 µg/mL DPE (middle), 60 µg/mL WDP (bottom)

Recovery of Tube Formation - 18 hours		
Diesel Particles (100 µg/mL)	Diesel Particle Extract (40 µg/mL)	Washed Particles (60 µg/mL)
—	+++	+++
Diesel Particles (50 µg/mL)	Diesel Particle Extract (20 µg/mL)	Washed Particles (30 µg/mL)
+++	+++	+++
Diesel Particles (25 µg/mL)	Diesel Particle Extract (10 µg/mL)	Washed Particles (15 µg/mL)
+++	+++	+++

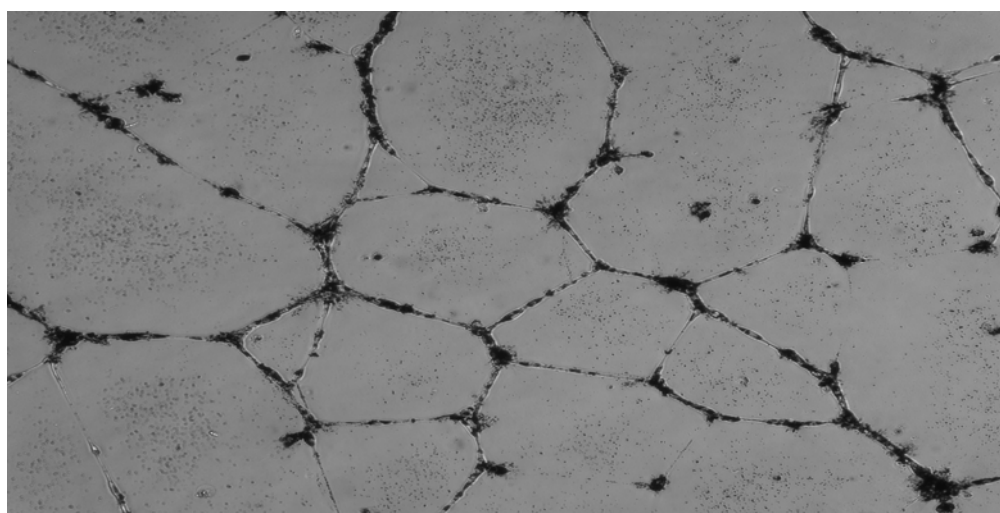
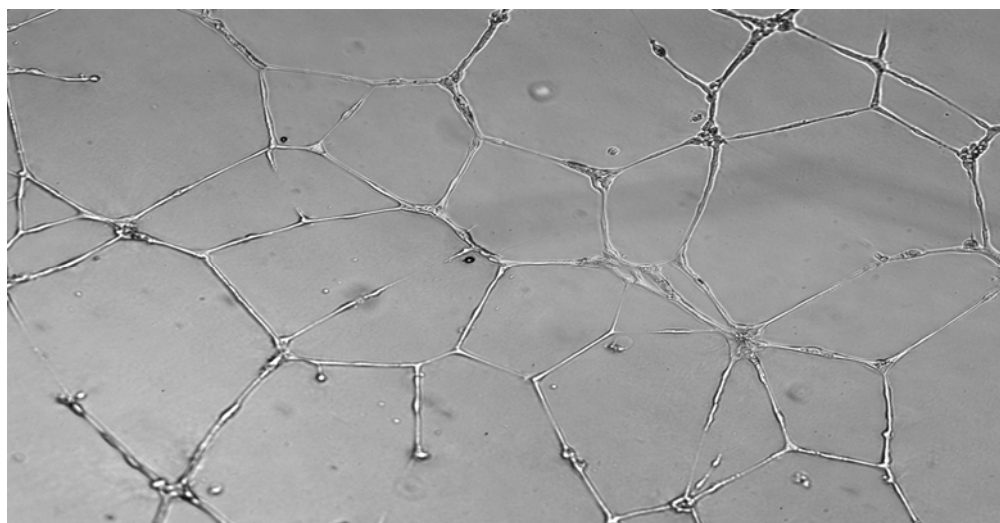
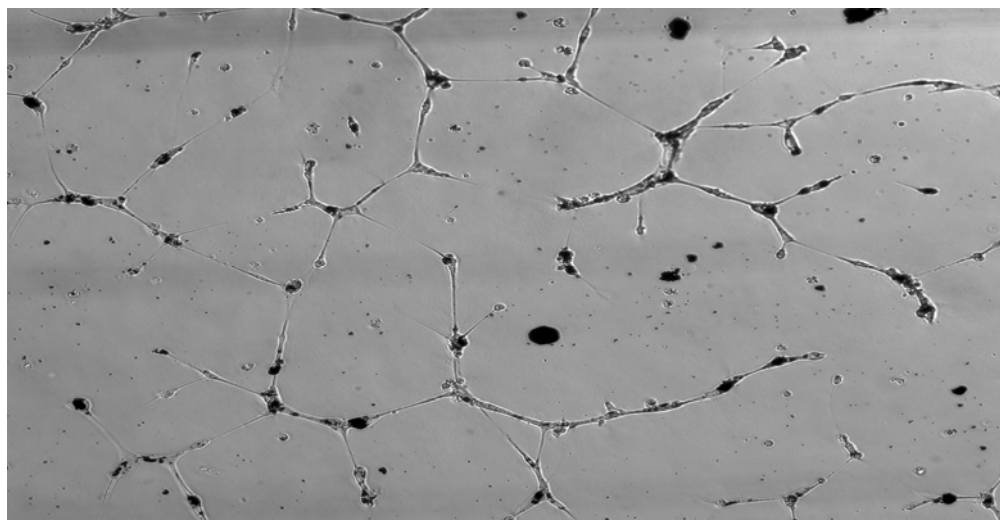
Table 5: Summary of the reversibility of effects observed in HUVEC at 3 hours following various treatments (+++ = no difference from control; - = no vascular formation).

Treatments were washed from the cells following 3 hours of exposure. Cells were then incubated for 18 hours in untreated media. 0.1% DMSO showed no difference from control. Corresponding effects are shown in Figure 13.

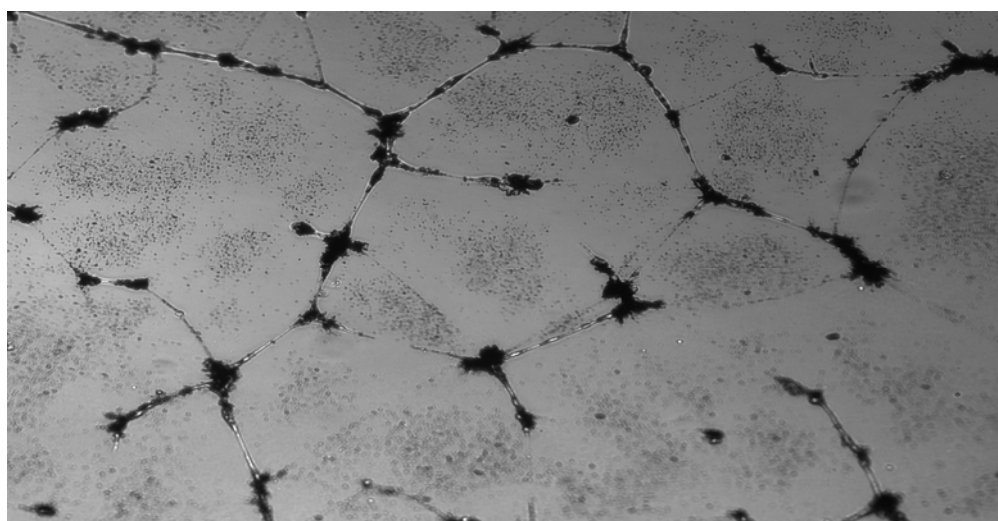
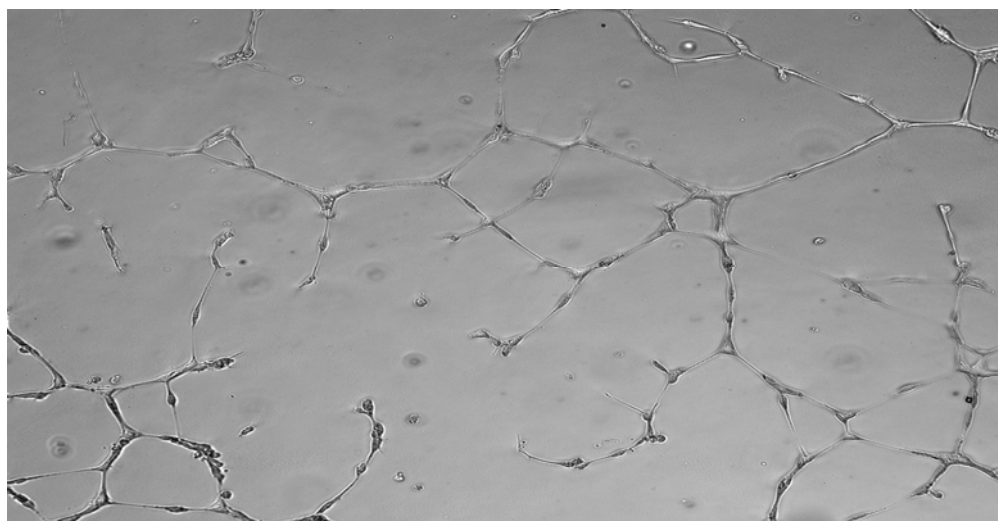
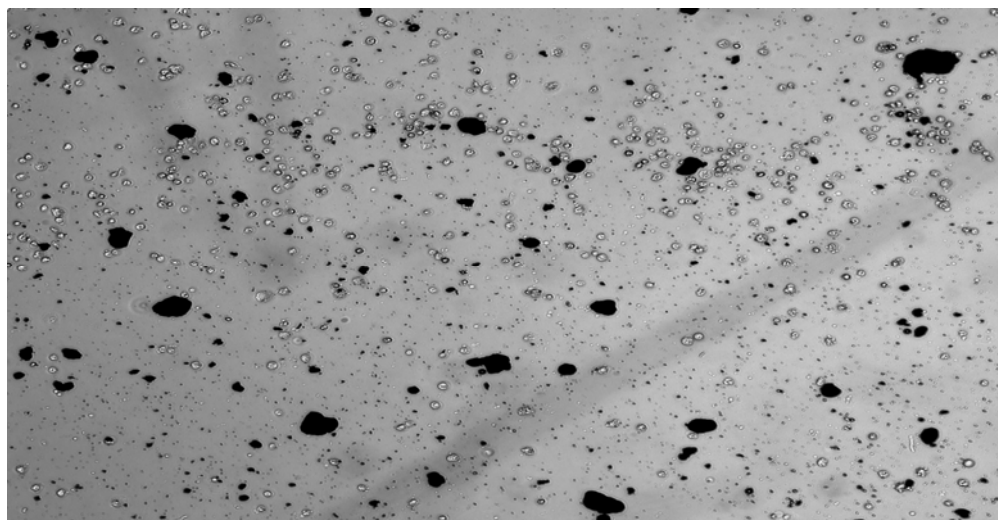
Figure 13. Representative images of *in vitro* HUVEC tube formation following 3 hour exposure to 25, 50, or 100 µg/mL diesel particles, 10, 20, or 40 µg/mL diesel particle extract, or 15, 30, or 60 µg/mL washed diesel particles and subsequent 18-hour incubation with untreated fresh media: Representative photographs (200X) of HUVEC seeded on Matrigel and treated for 3 hours with (A) 25 µg/mL DP (top), 10 µg/mL DPE (middle), 15 µg/mL WDP (bottom) (B) 50 µg/mL DP (top), 20 µg/mL DPE (middle), 30 µg/mL WDP (bottom) (C) 100 µg/mL DP (top), 40 µg/mL DPE (middle), 60 µg/mL WDP (bottom) then washed free of treatment media. Subsequent to washing, cells were incubated for 18 hours with untreated fresh media.



A - 25 $\mu\text{g/mL}$ DP (top), 10 $\mu\text{g/mL}$ DPE (middle), 15 $\mu\text{g/mL}$ WDP (bottom)



B - 50 $\mu\text{g/mL}$ DP (top), 20 $\mu\text{g/mL}$ DPE (middle), 30 $\mu\text{g/mL}$ WDP (bottom)

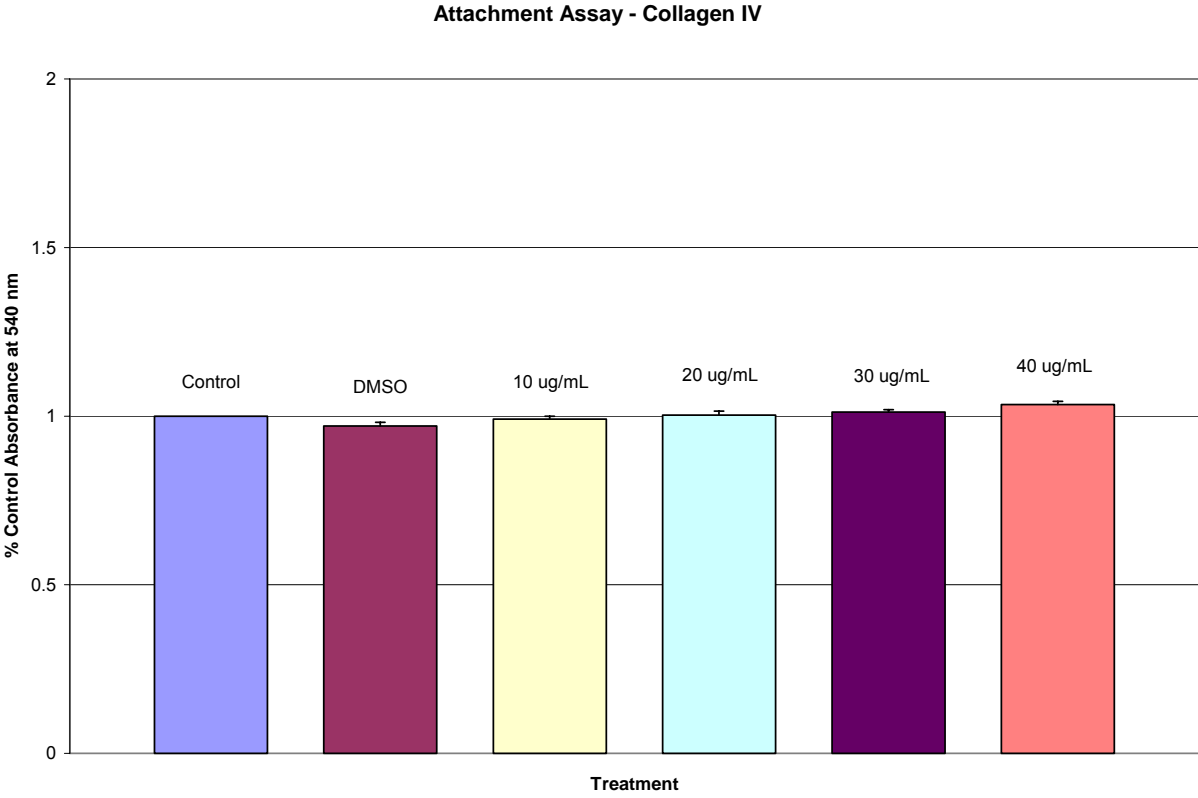


C - 100 $\mu\text{g/mL}$ DP (top), 40 $\mu\text{g/mL}$ DPE (middle), 60 $\mu\text{g/mL}$ WDP (bottom)

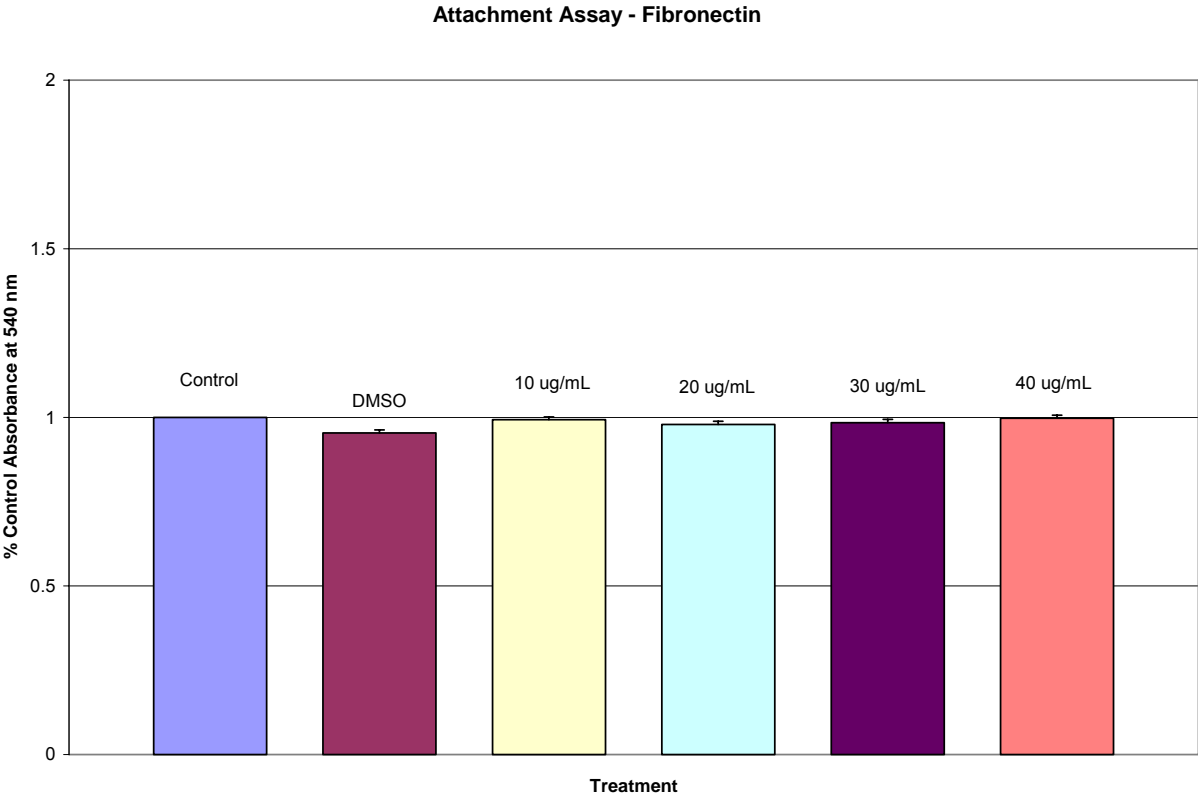
HUVEC Attachment to Components of the ECM					
Treatment	Collagen IV	Fibronectin	Vitronectin	Laminin I	ECM
Control	+++	+++	+++	+++	+++
DMSO	+++	+++	+++	+++	+++
Diesel Particle Extract (10 µg/mL)	+++	+++	+++	+++	+++
Diesel Particle Extract (20 µg/mL)	+++	+++	+++	+++	+++
Diesel Particle Extract (30 µg/mL)	+++	+++	+++	+++	+++
Diesel Particle Extract (40 µg/mL)	+++	+++	+++	+++	+++

Table 6: Evaluation of HUVEC attachment to components of the extracellular matrix following treatment with 10 - 40 µg/mL DPE (+++ = no loss of attachment compared to control). Corresponding data is shown in Figure 14.

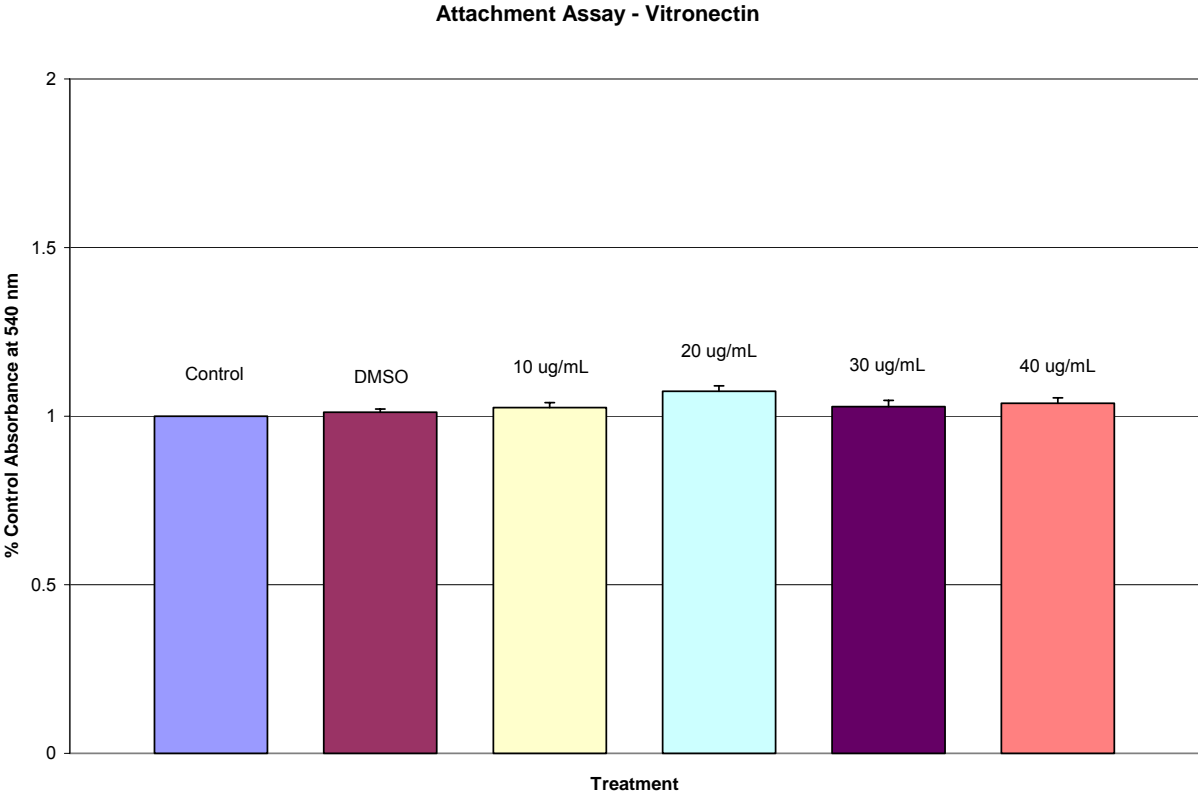
Figure 14. HUVEC adhesion to components of the ECM following 3 hour exposure to 10, 20, 30, or 40 $\mu\text{g/mL}$ DPE: Binding of HUVEC treated with DPE to the ECM proteins (A) collagen IV, (B) fibronectin, (C) vitronectin, (D) laminin I, or (E) Matrigel (ECM) as a percentage of control. Statistical significance from untreated control was determined by Dunnett's Test. Error bars denote standard deviation.



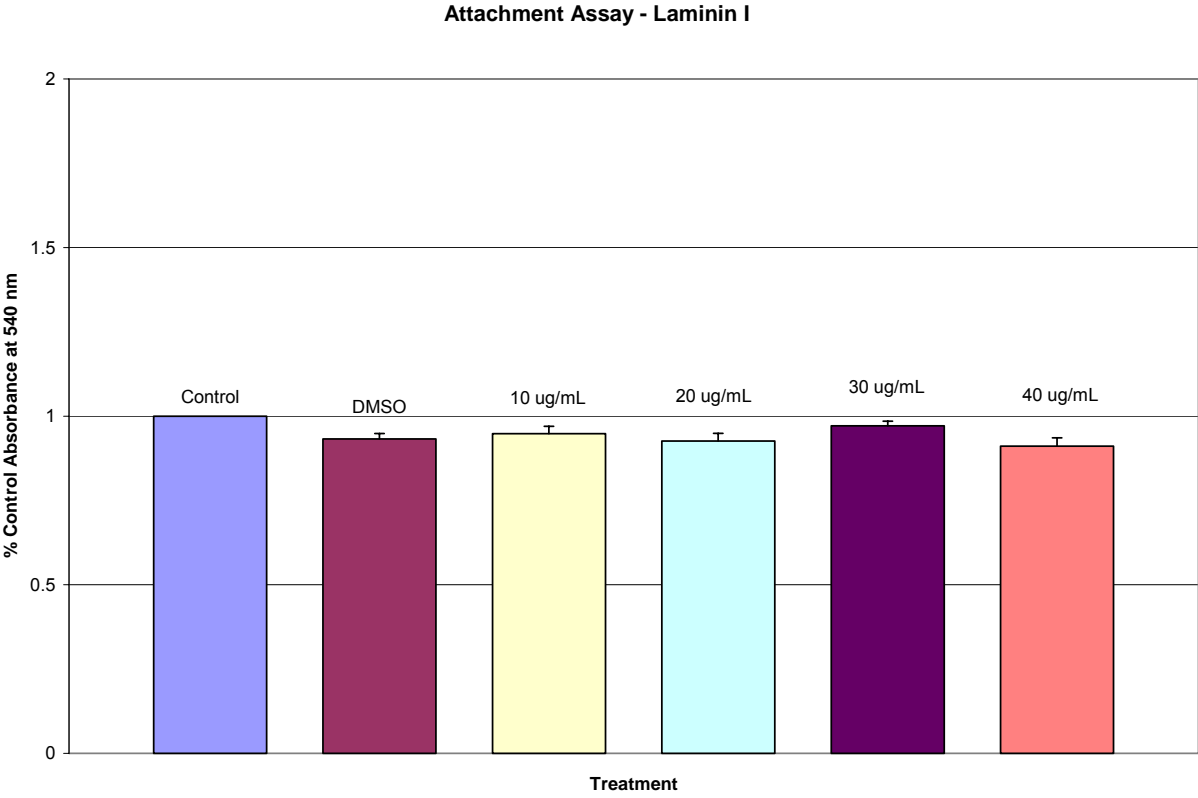
A



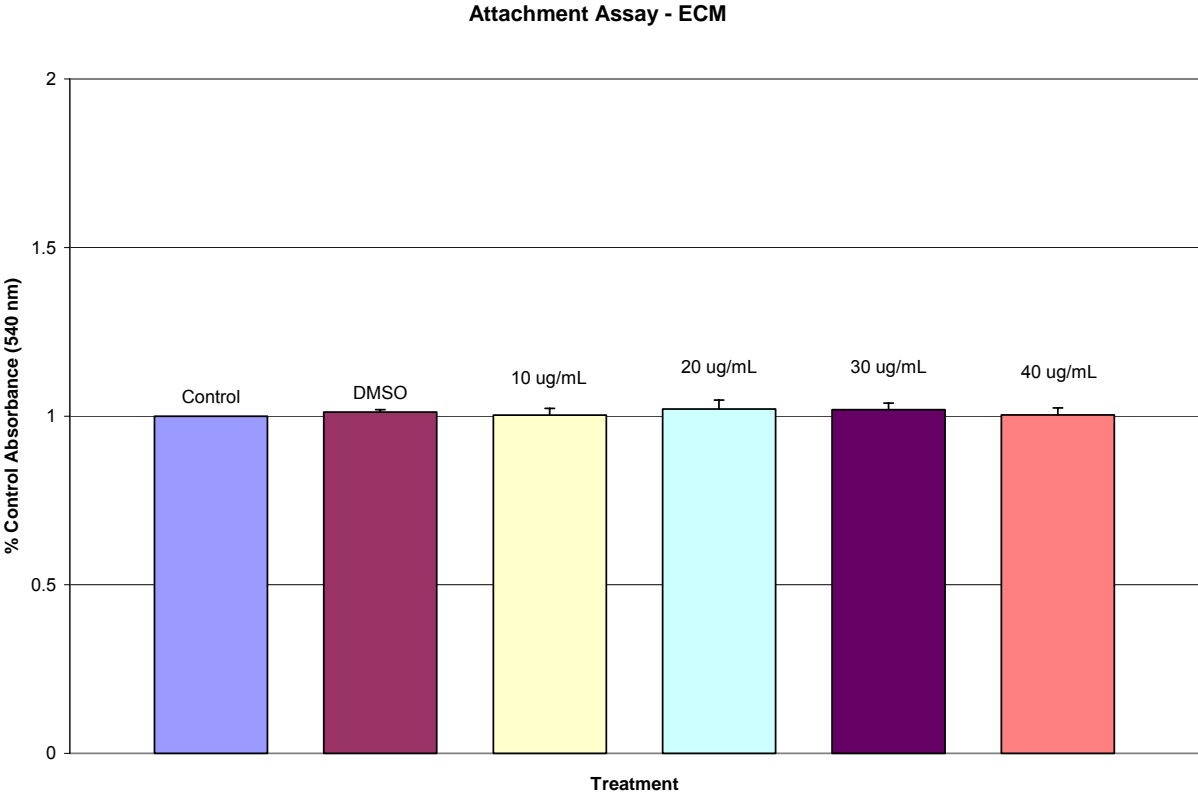
B



C



D

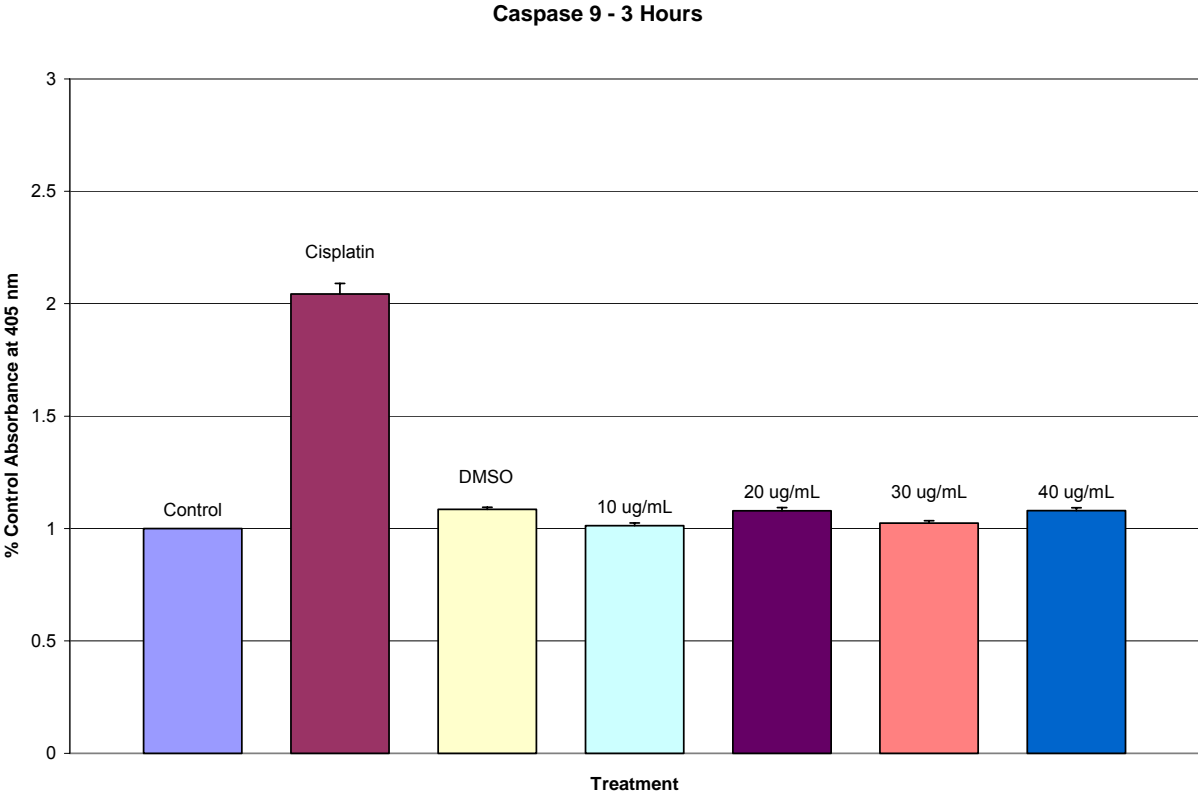


E

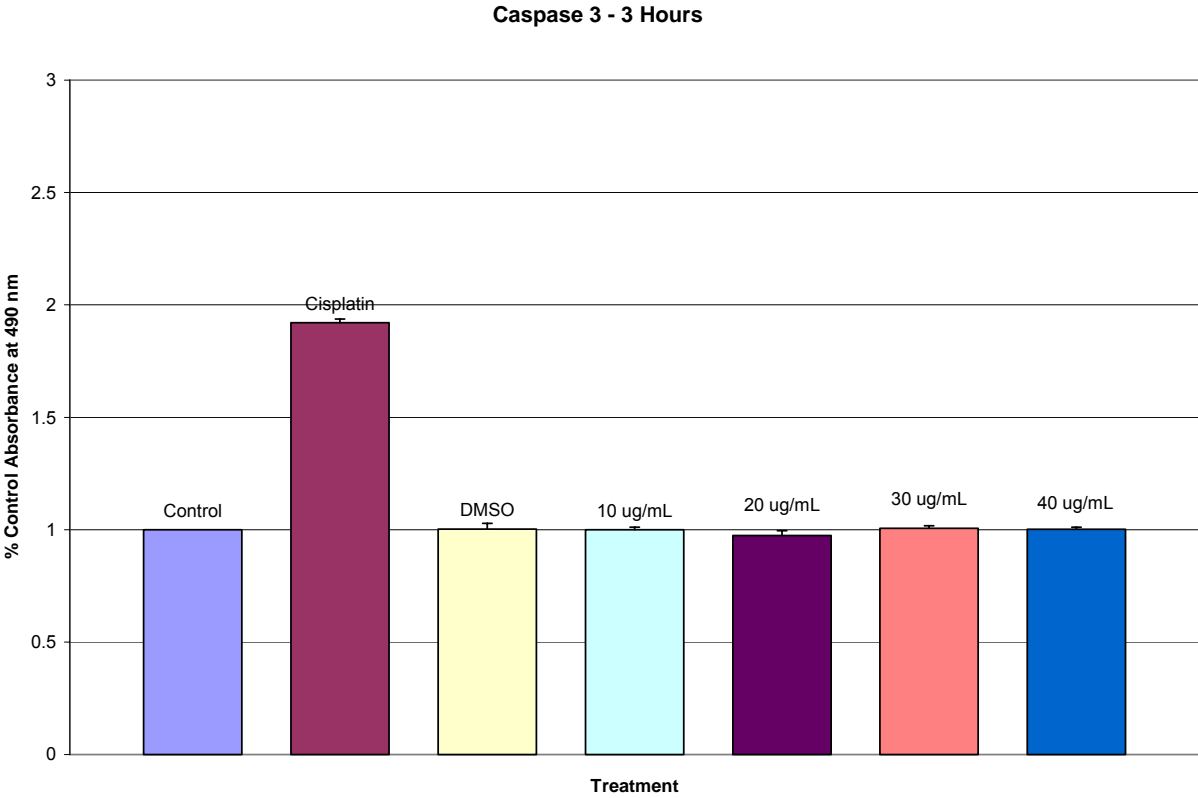
Apoptosis/Cell Death							
	Control	Cisplatin	DMSO	Diesel Particle Extract (10µg/mL)	Diesel Particle Extract (20µg/mL)	Diesel Particle Extract (30µg/mL)	Diesel Particle Extract (40µg/mL)
Caspase 9	–	+++	–	–	–	–	–
Caspase 3	–	+++	–	–	–	–	–
LDH	–	+++	–	–	–	–	–
Annexin V	–	+++	–	–	–	–	–
Propidium Iodide	–	+++	–	–	–	–	–
Hoechst	–	+++	–	–	–	–	–
DNA Fragmentation	–	+++	–	–	–	–	–

Table 7: Summary of effects observed in several indicators of apoptosis in HUVEC at 3 hours following various treatments (+++ = markedly different from control; - = no difference from control). Corresponding data are shown in Figures 15 - 19.

Figure 15. Activation of caspase-9 or caspase-3 following 3 hour exposure of HUVEC to 10, 20, 30, or 40 μ g/mL DPE: Caspase activity for (A) caspase-9 (B) caspase-3 as measured by ELISA. 25 μ M cisplatin served as a positive control. Statistical significance from untreated control was determined by Dunnett's Test. Error bars denote standard deviation.



A



B

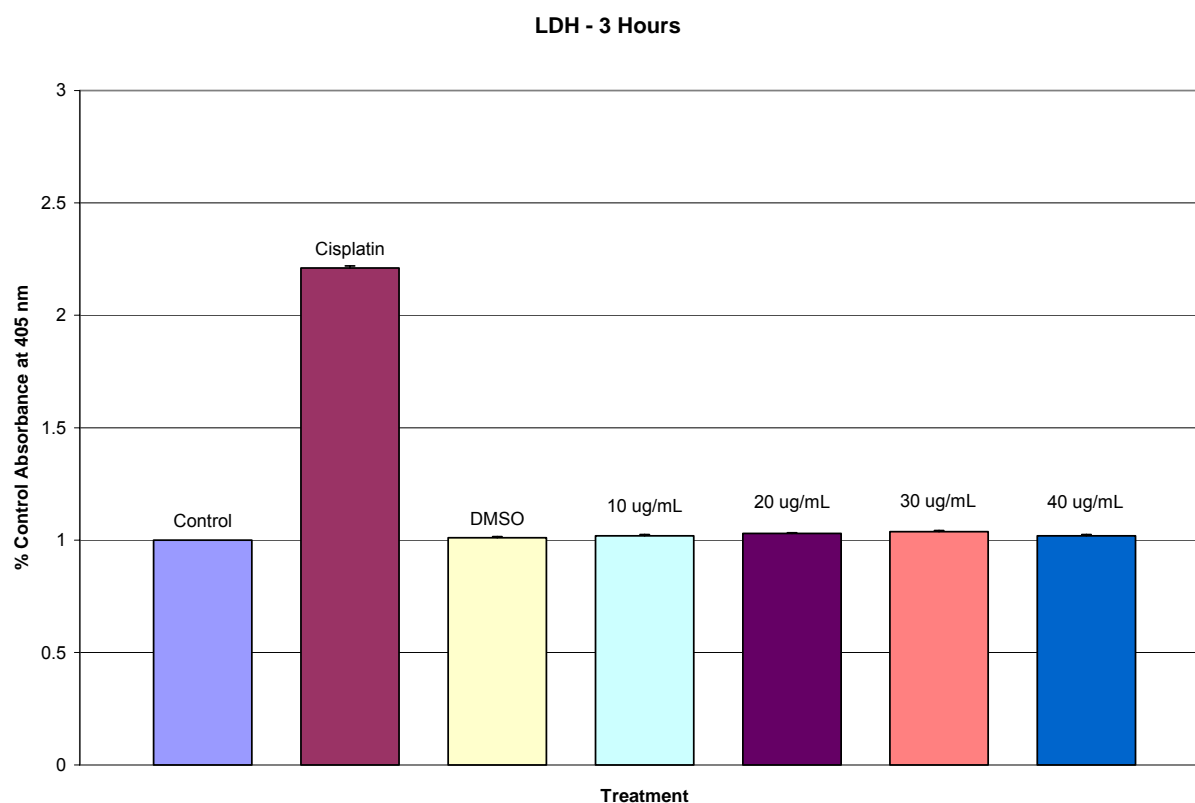
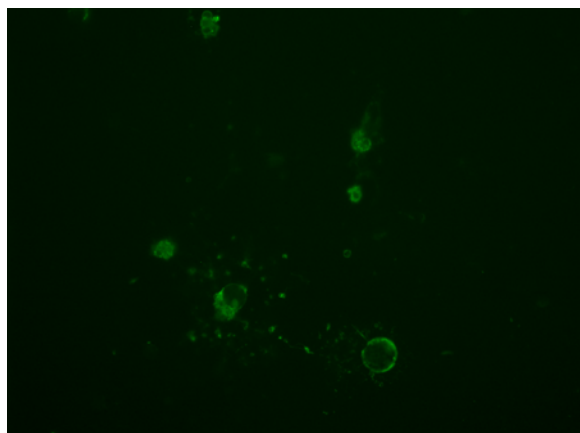
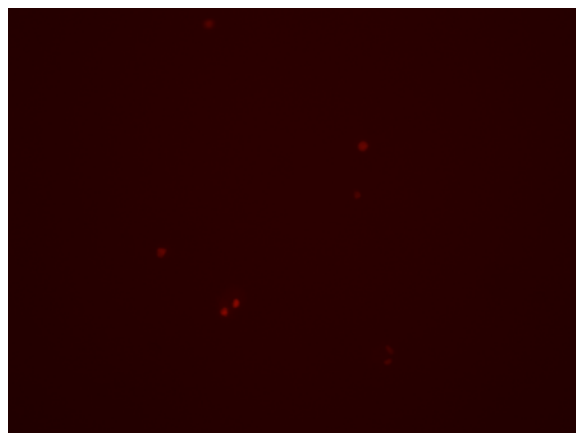


Figure 16. LDH activity following 3 hour exposure of HUVEC to 10, 20, 30, or 40 $\mu\text{g/mL}$ DPE: LDH activity as measured by ELISA. 25 μM cisplatin served as a positive control. Statistical significance from untreated control was determined by Dunnett's Test. Error bars denote standard deviation.

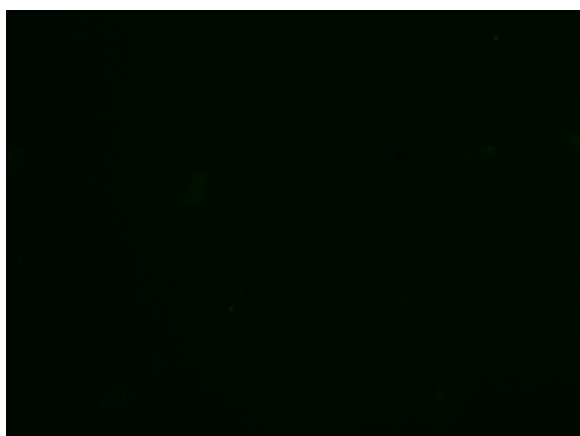
Figure 17. Representative images of HUVEC immunostained for annexin V and propidium iodide following 3 hour exposure to 25, 50, or 100 $\mu\text{g/mL}$ diesel particles, 10, 20, or 40 $\mu\text{g/mL}$ diesel particle extract, or 15, 30, or 60 $\mu\text{g/mL}$ washed diesel particles: Representative annexin V stained (left) and propidium iodide stained (right) photographs (400X) of HUVEC treated with (A) 25 μM cisplatin (+ control) (B) 0.1% DMSO (C, D, E) 25, 50, or 100 $\mu\text{g/mL}$ DP; (F, G, H) 1-, 20, or 40 $\mu\text{g/mL}$ DPE; or (I, J, K) 15, 30, or 60 $\mu\text{g/mL}$ WDP for 3 hours.



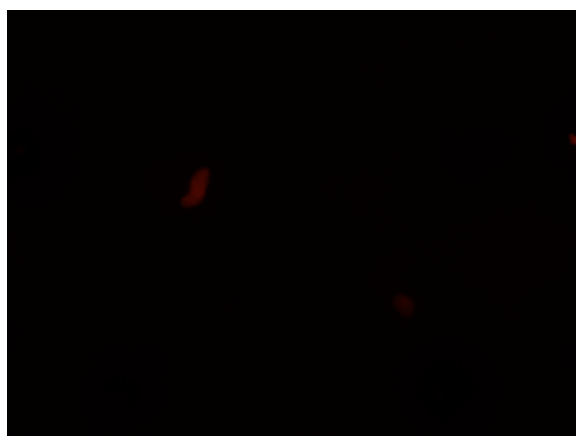
A - Cisplatin (+ control) Annexin V



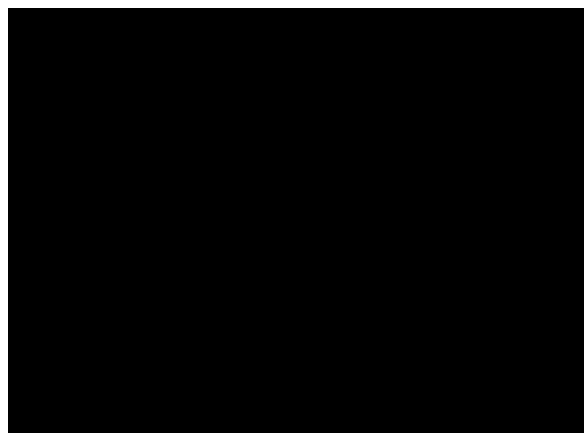
Propidium Iodide



B - 0.1% DMSO Annexin V



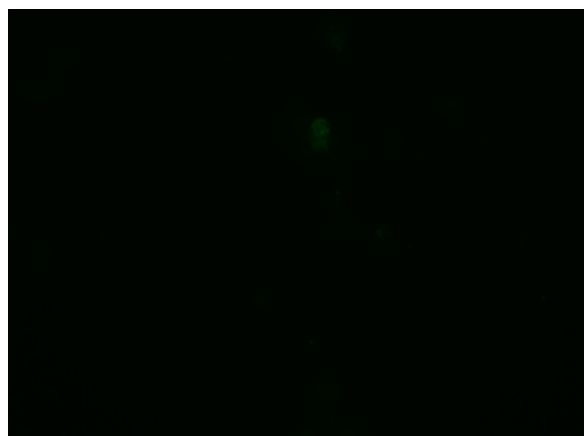
Propidium Iodide



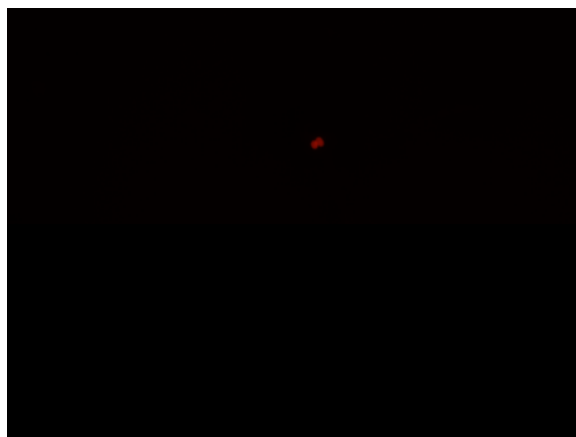
C - 25 µg/mL DP Annexin V



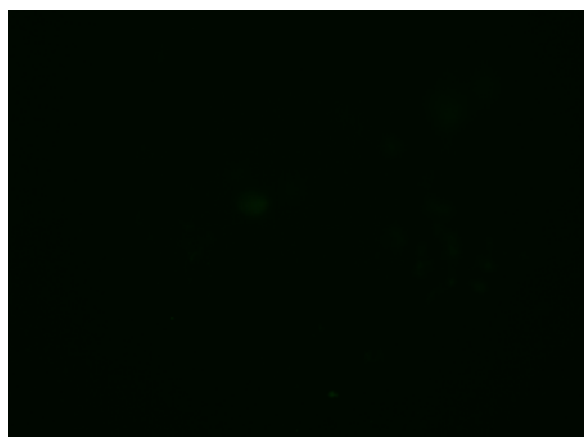
Propidium Iodide



D - 50 µg/mL DP Annexin V



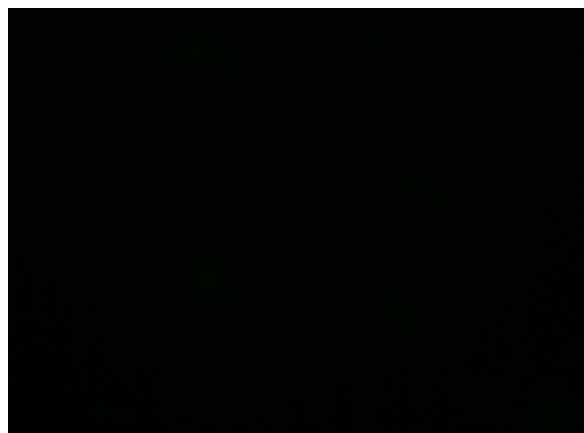
Propidium Iodide



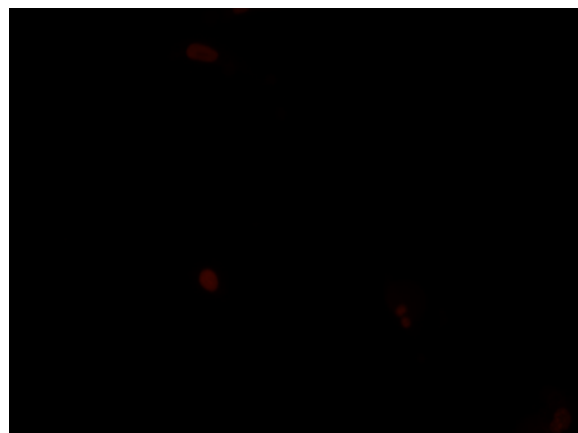
E - 100 µg/mL DP Annexin V



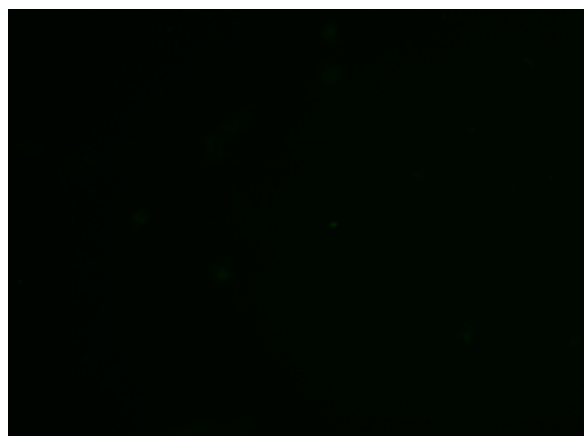
Propidium Iodide



F - 10 µg/mL DPE Annexin V



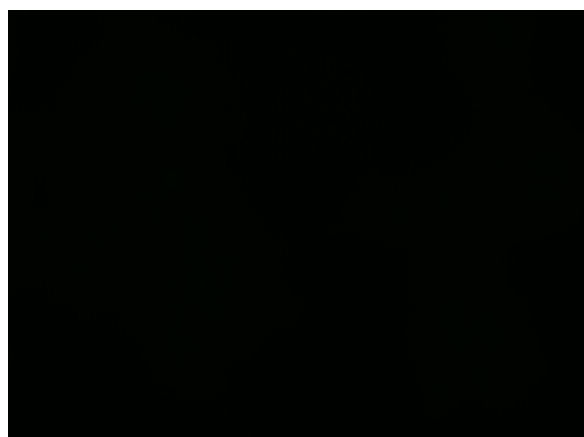
Propidium Iodide



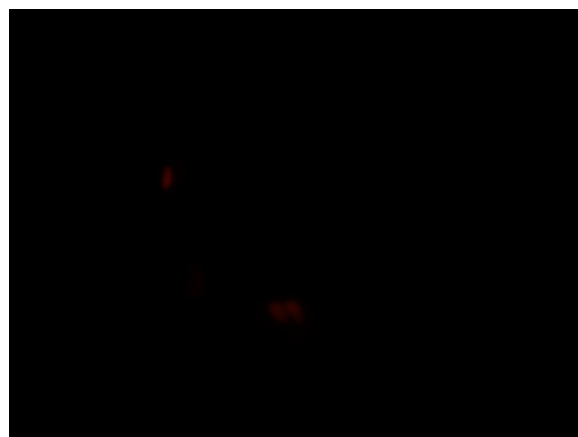
G - 20 µg/mL DPE Annexin V



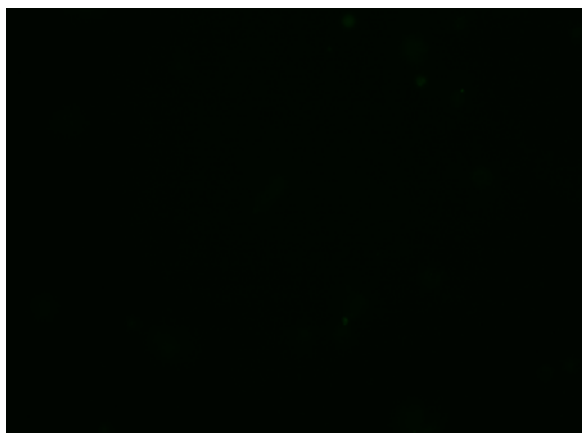
Propidium Iodide



H - 40 µg/mL DPE Annexin V



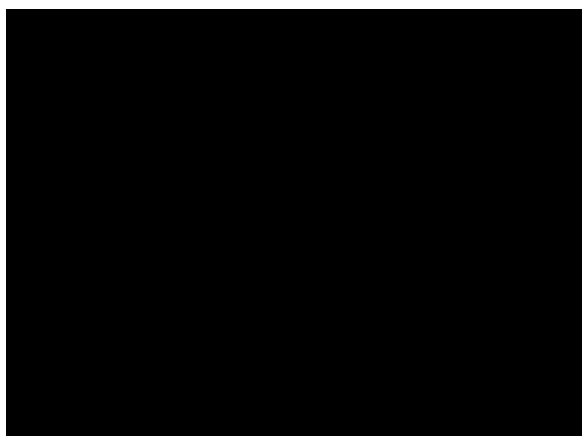
Propidium Iodide



I - 15 µg/mL WDP Annexin V



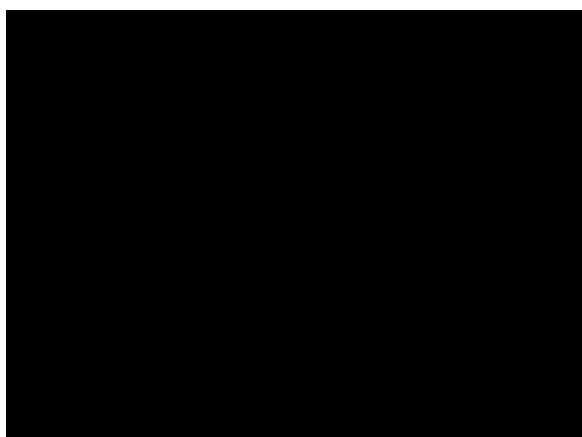
Propidium Iodide



J - 30 µg/mL WDP Annexin V



Propidium Iodide

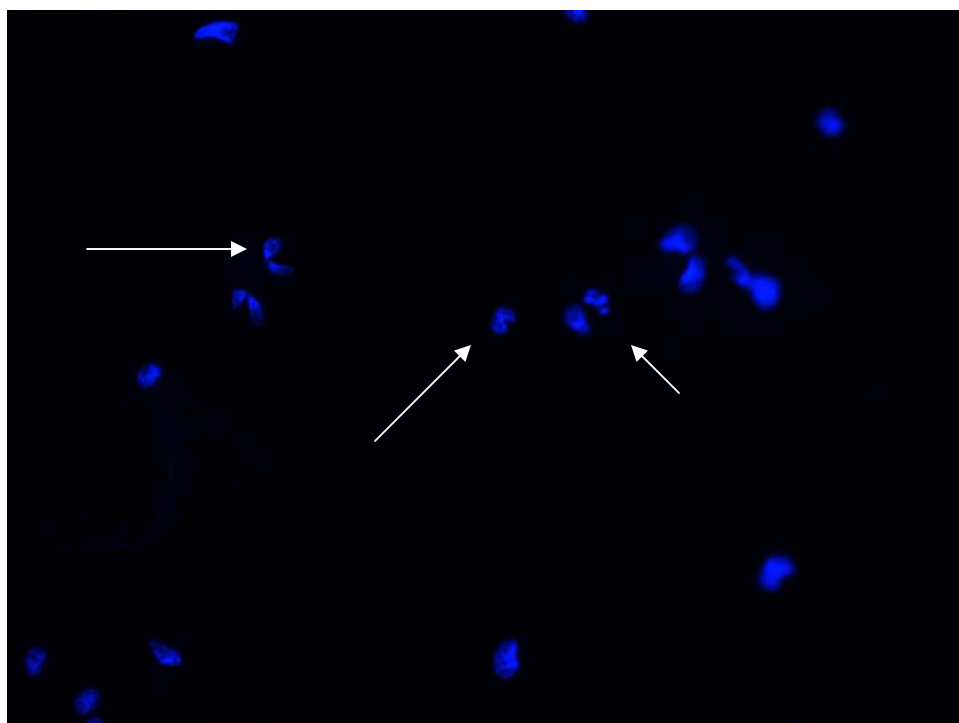


K - 60 µg/mL WDP Annexin V

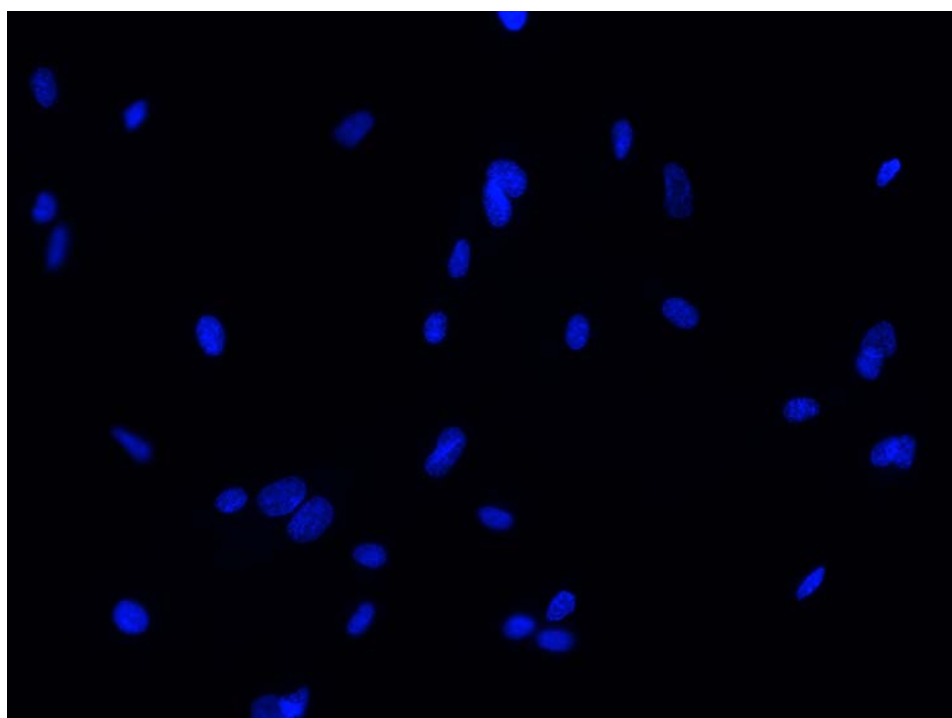


Propidium Iodide

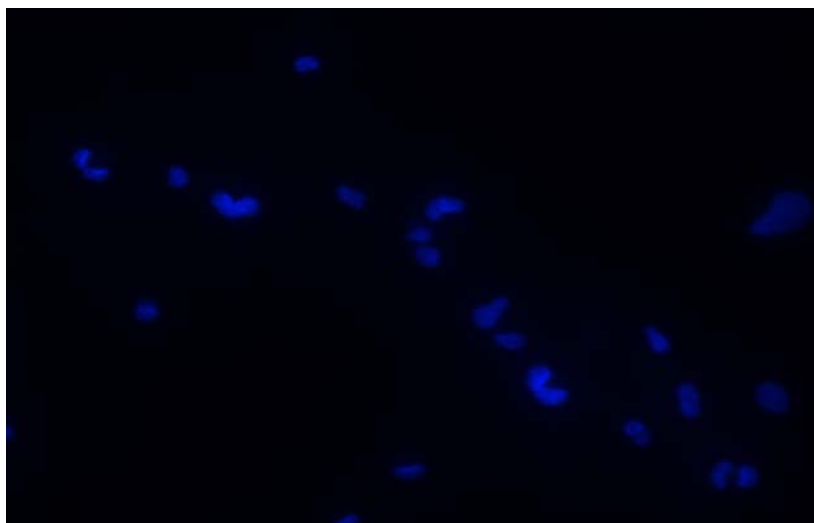
Figure 18. Representative images of HUVEC immunostained with Hoechst (H333342) following 3 hour exposure to 25, 50, or 100 $\mu\text{g/mL}$ diesel particles, 10, 20, or 40 $\mu\text{g/mL}$ diesel particle extract, or 15, 30, or 60 $\mu\text{g/mL}$ washed diesel particles: Representative photographs (400X) of Hoechst-stained HUVEC treated with (A) 25 μM cisplatin (+ control - arrows indicate condensed nuclei) (B) 0.1% DMSO (C, D, E) 25, 50, or 100 $\mu\text{g/mL}$ DP; (F, G, H) 1-, 20, or 40 $\mu\text{g/mL}$ DPE; or (I, J, K) 15, 30, or 60 $\mu\text{g/mL}$ WDP for 3 hours.



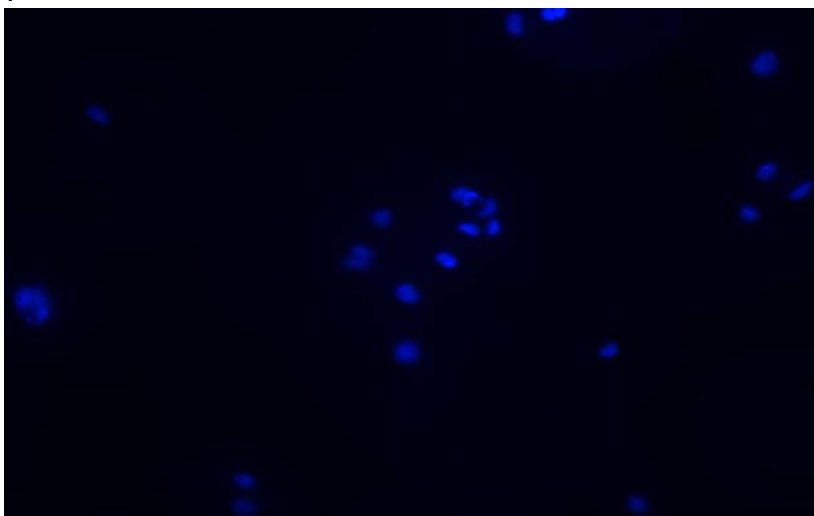
A - Cisplatin (+control)



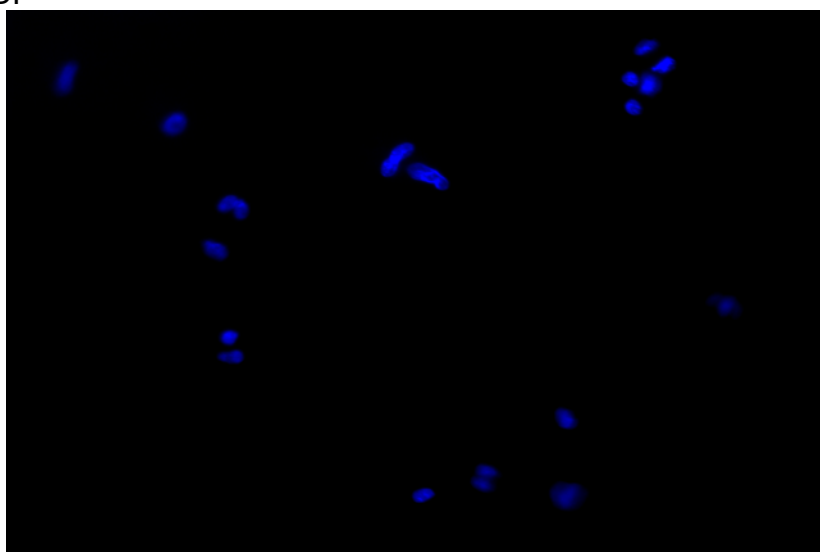
B - 0.1% DMSO



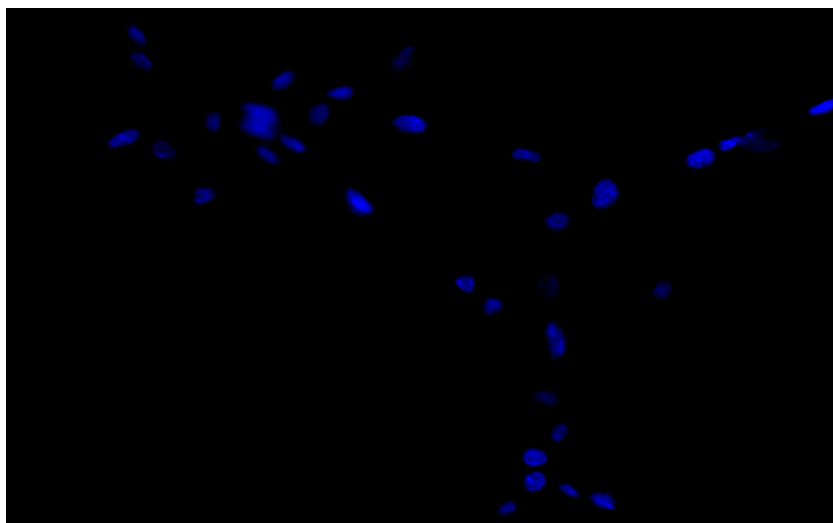
C - 25 µg/mL DP



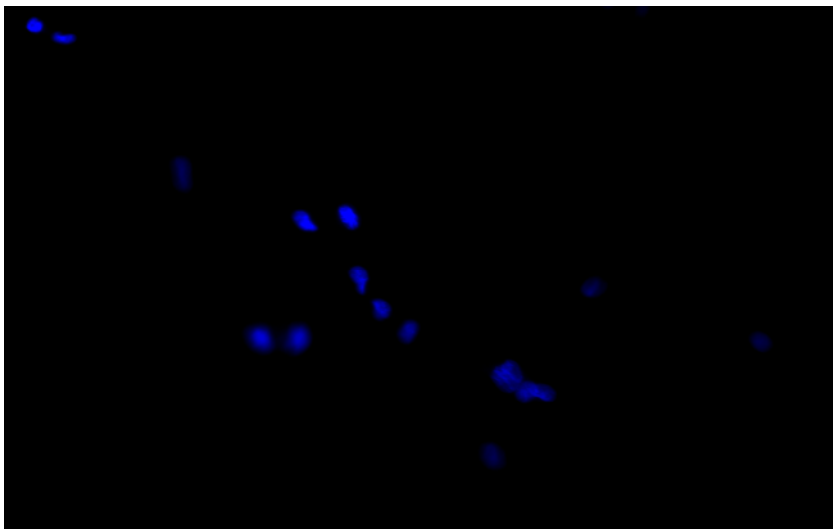
D - 50 µg/mL DP



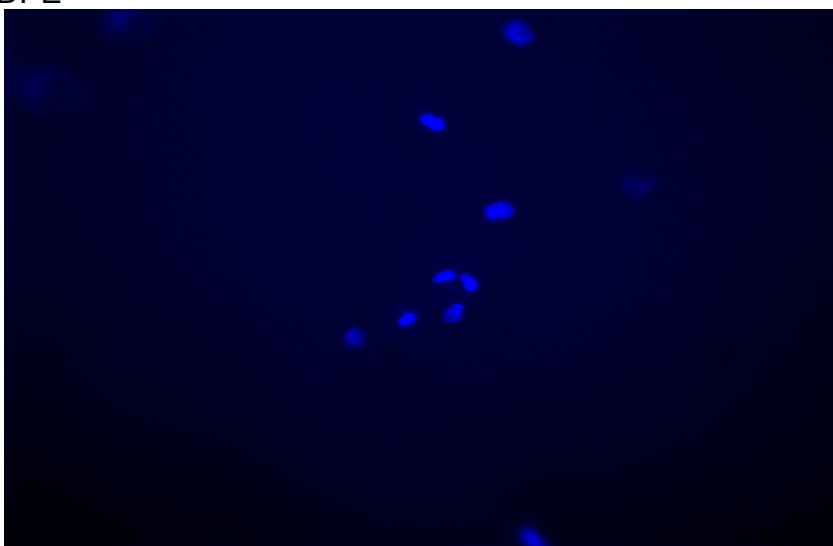
E - 100 µg/mL DP



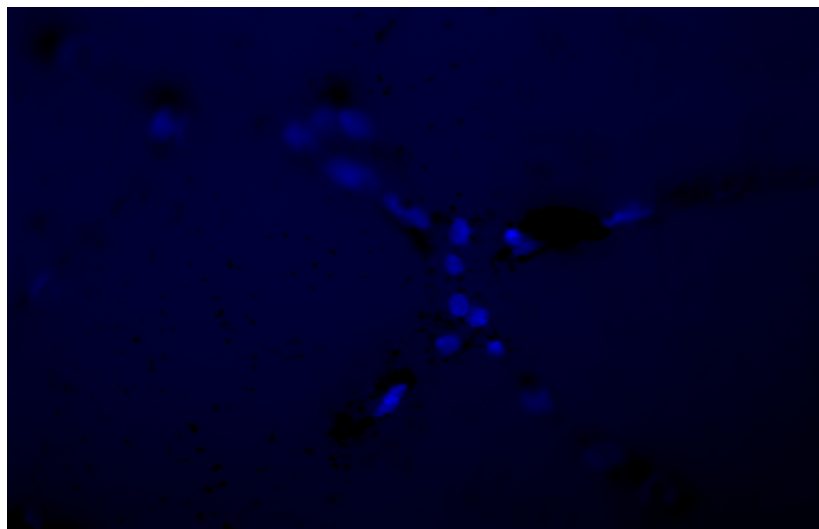
F - 10 $\mu\text{g/mL}$ DPE



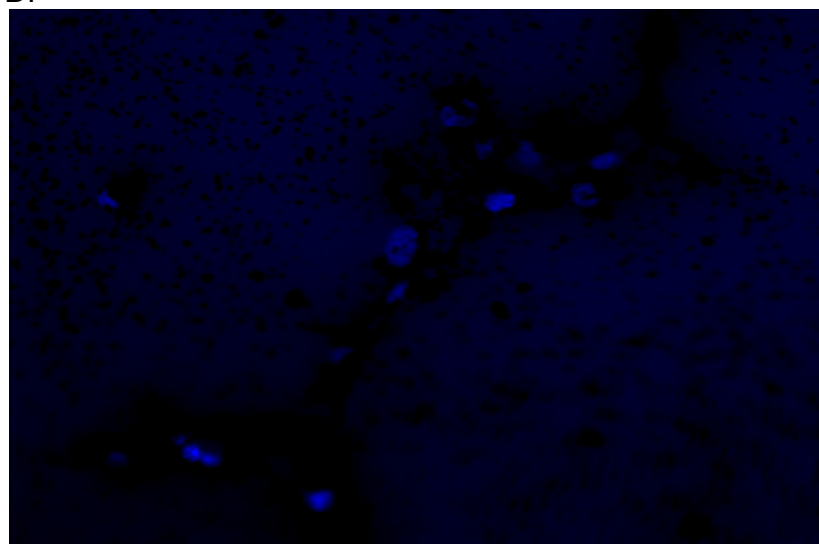
G - 20 $\mu\text{g/mL}$ DPE



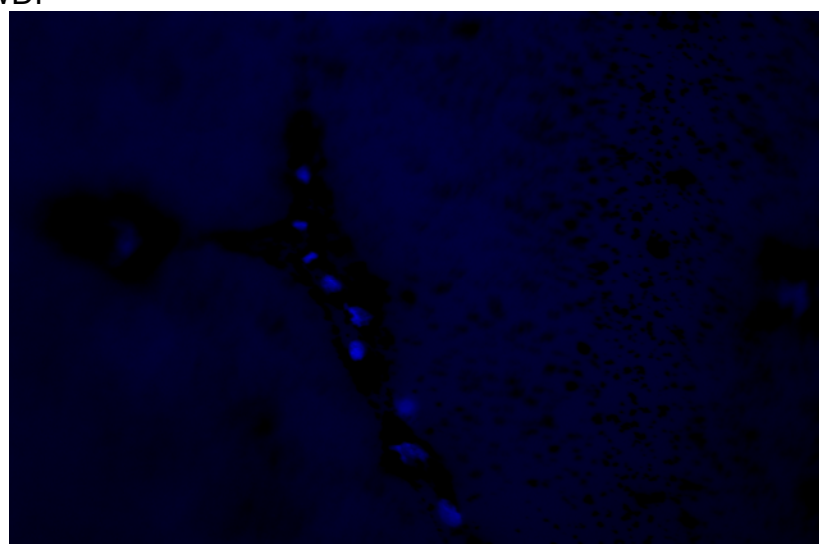
H - 40 $\mu\text{g/mL}$ DPE



I - 15 $\mu\text{g/mL}$ WDP



J - 30 $\mu\text{g/mL}$ WDP



K - 60 $\mu\text{g/mL}$ WDP

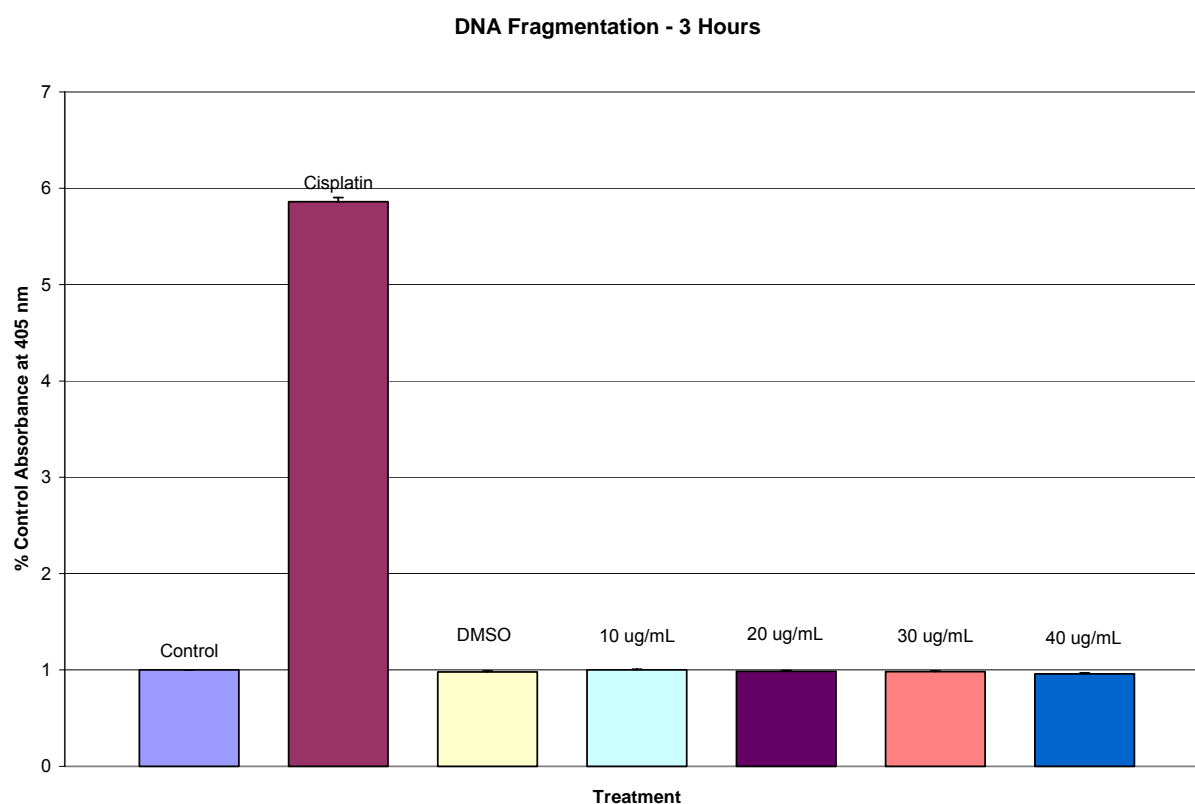
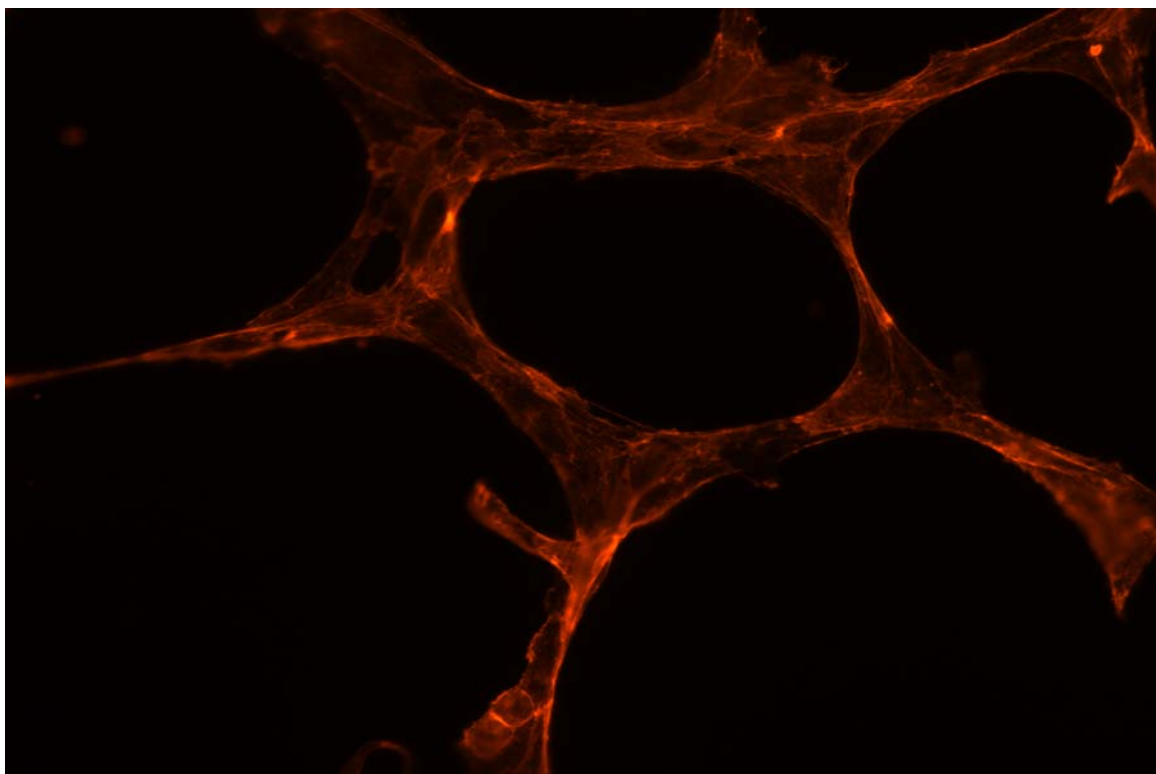
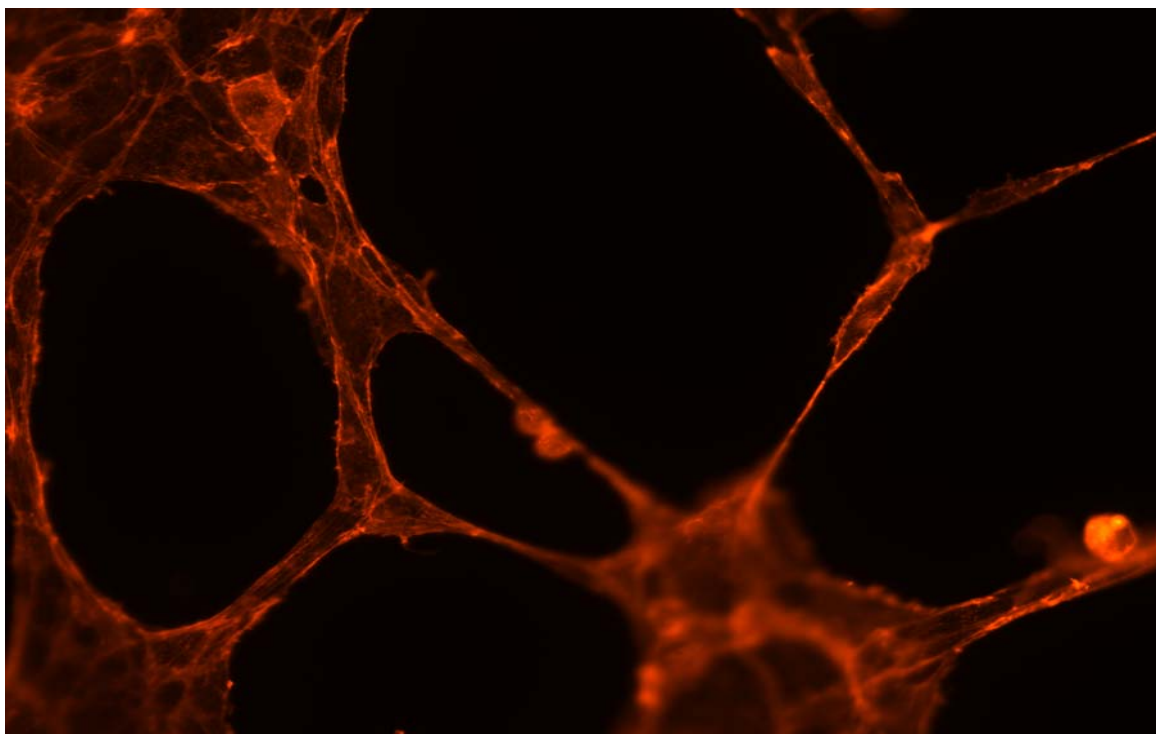


Figure 19. DNA fragmentation following 3 hour exposure of HUVEC to 10, 20, 30, or 40 $\mu\text{g/mL}$ DPE: DNA fragmentation as measured by ELISA. 25 μM cisplatin served as a positive control. Statistical significance from untreated control was determined by Dunnett's Test. Error bars denote standard deviation.

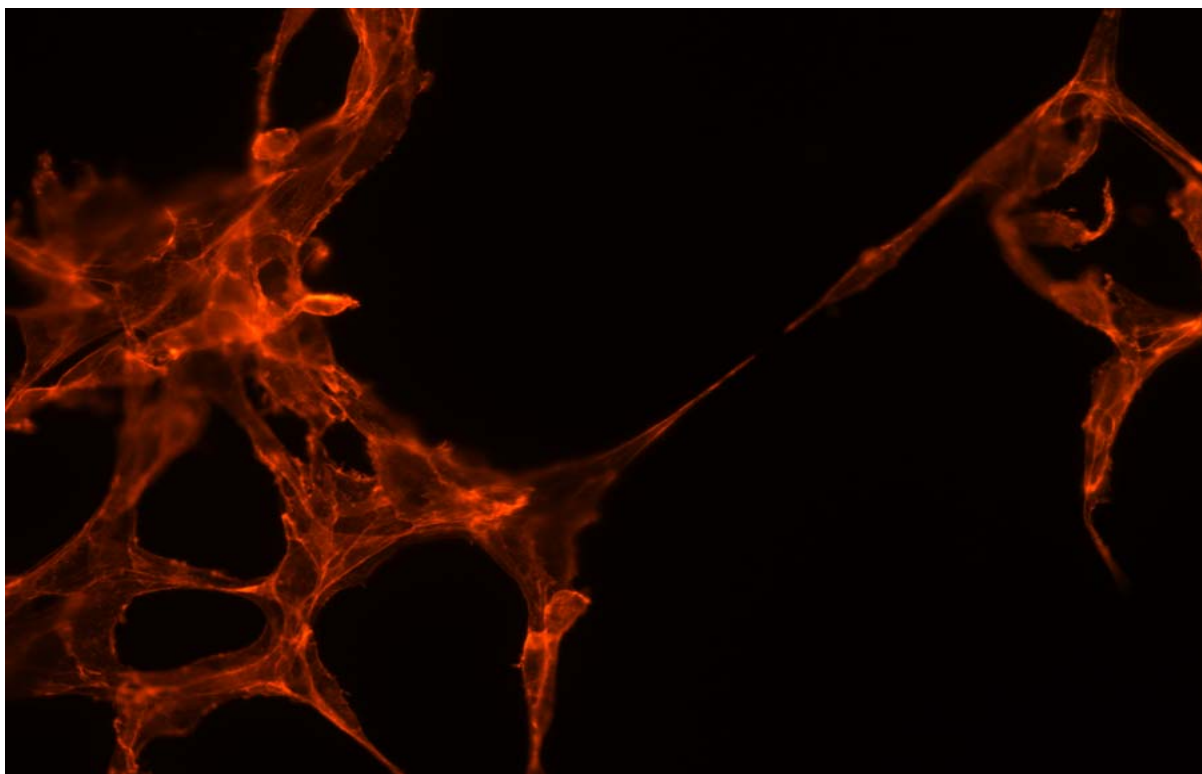
Figure 20. Immunocytochemical staining of the actin cytoskeleton with TRITC-conjugated Phalloidin in HUVEC treated with 10, 20, 30 or 40 $\mu\text{g/mL}$ DPE: Representative photographs (400X) of HUVEC treated with (A) untreated media control (B) 0.1% DMSO (C) 10 $\mu\text{g/mL}$ DPE; (D) 20 $\mu\text{g/mL}$ DPE; (E) 30 $\mu\text{g/mL}$ DPE; or (F) 40 $\mu\text{g/mL}$ DPE for 3 hours then immunostained with TRITC-conjugated Phalloidin.



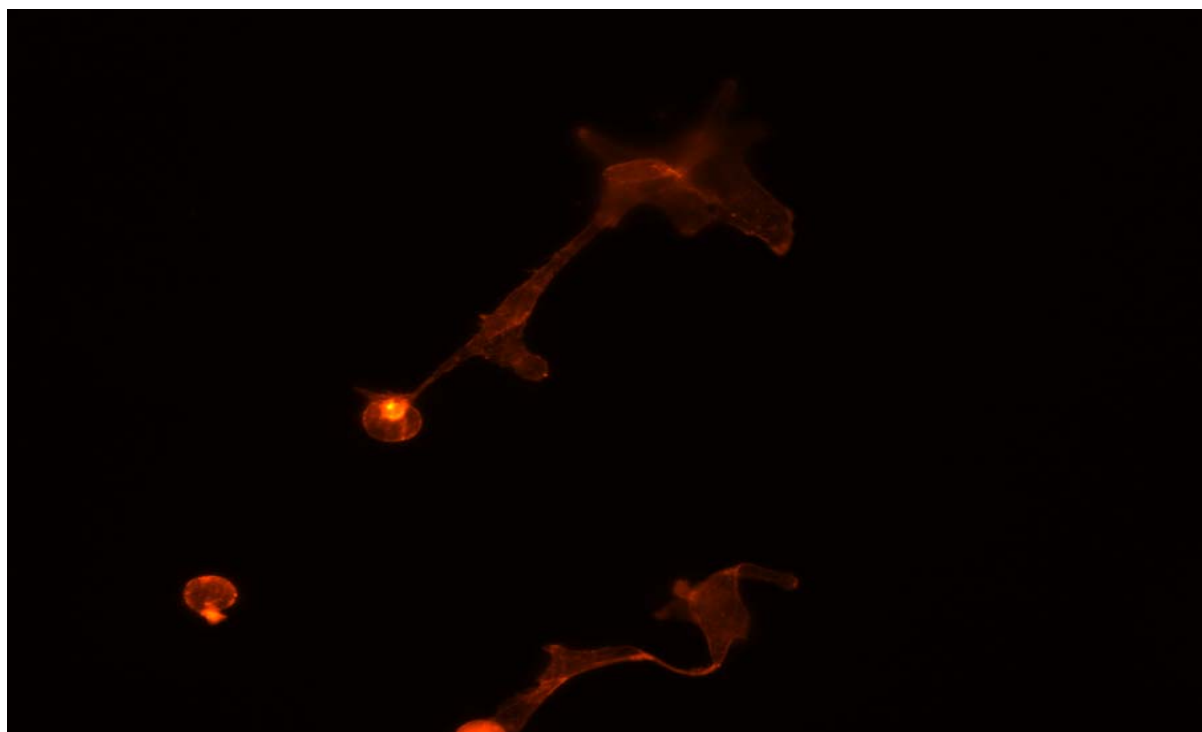
A - Media Control



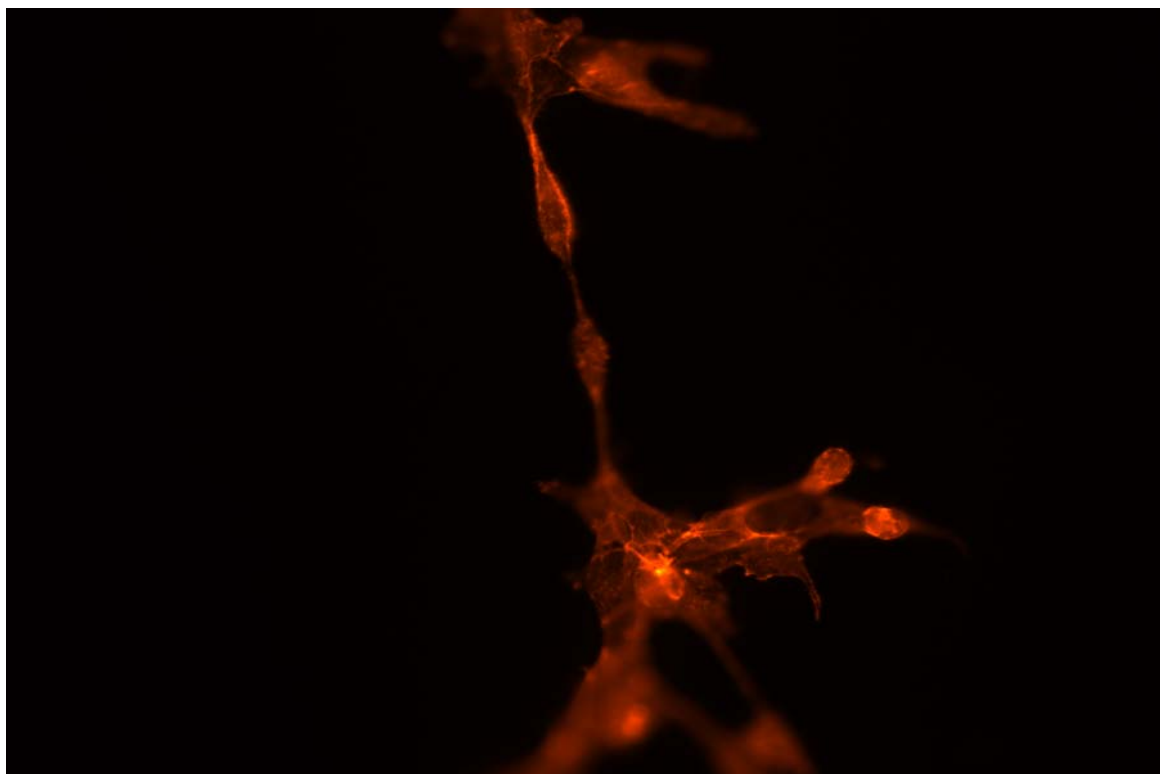
B - 0.1% DMSO



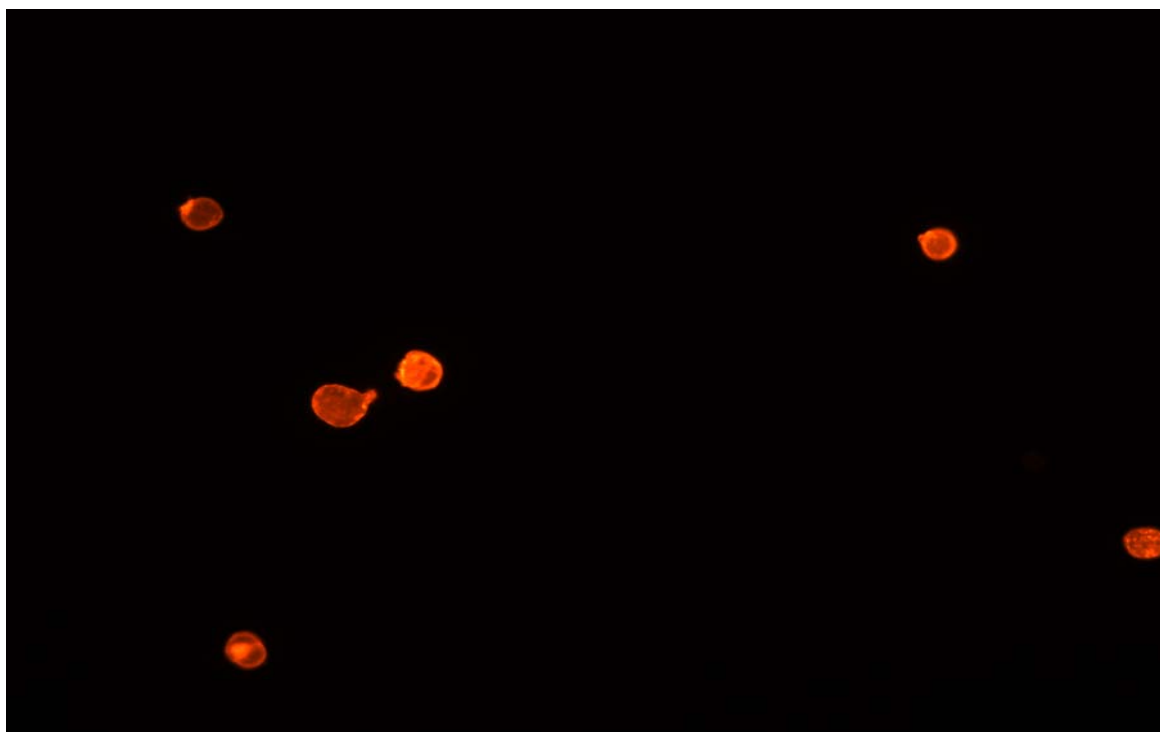
C - 10 $\mu\text{g/mL}$ DPE



D - 20 $\mu\text{g/mL}$ DPE

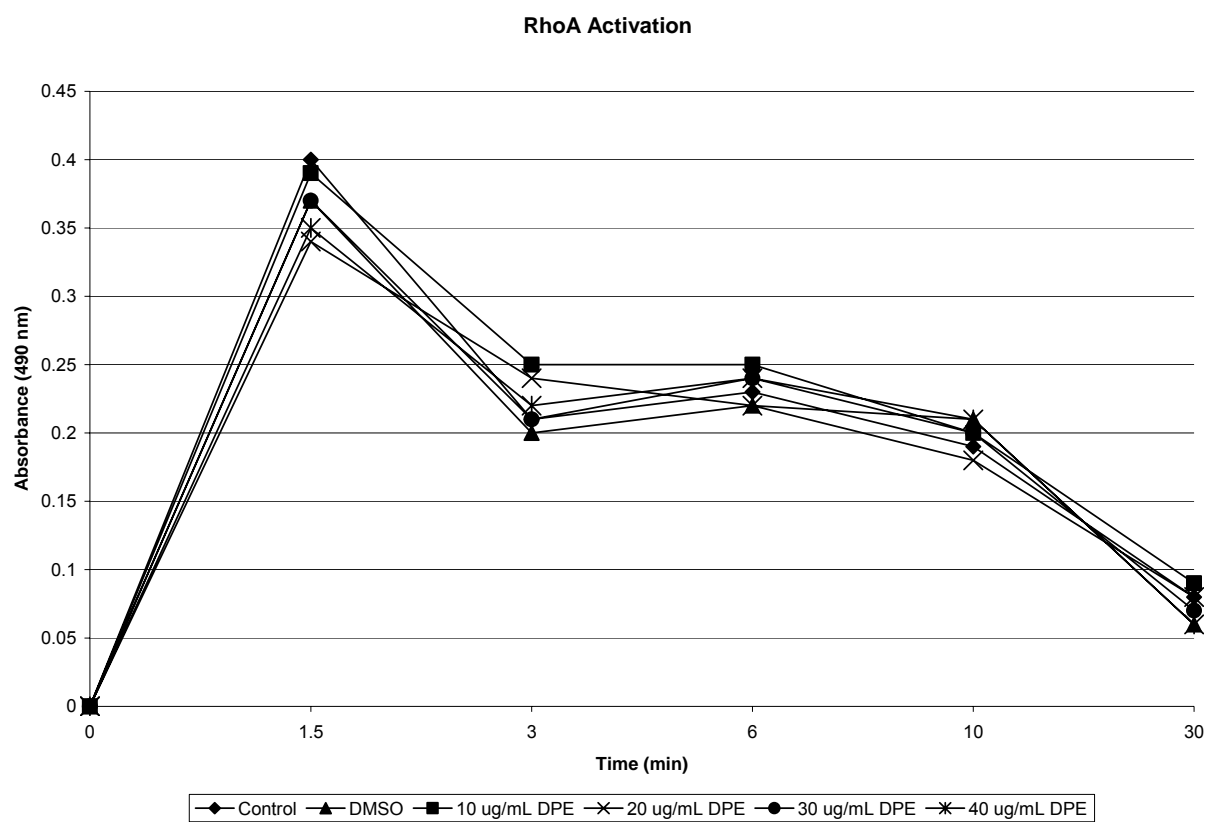


E - 30 $\mu\text{g/mL}$ DPE

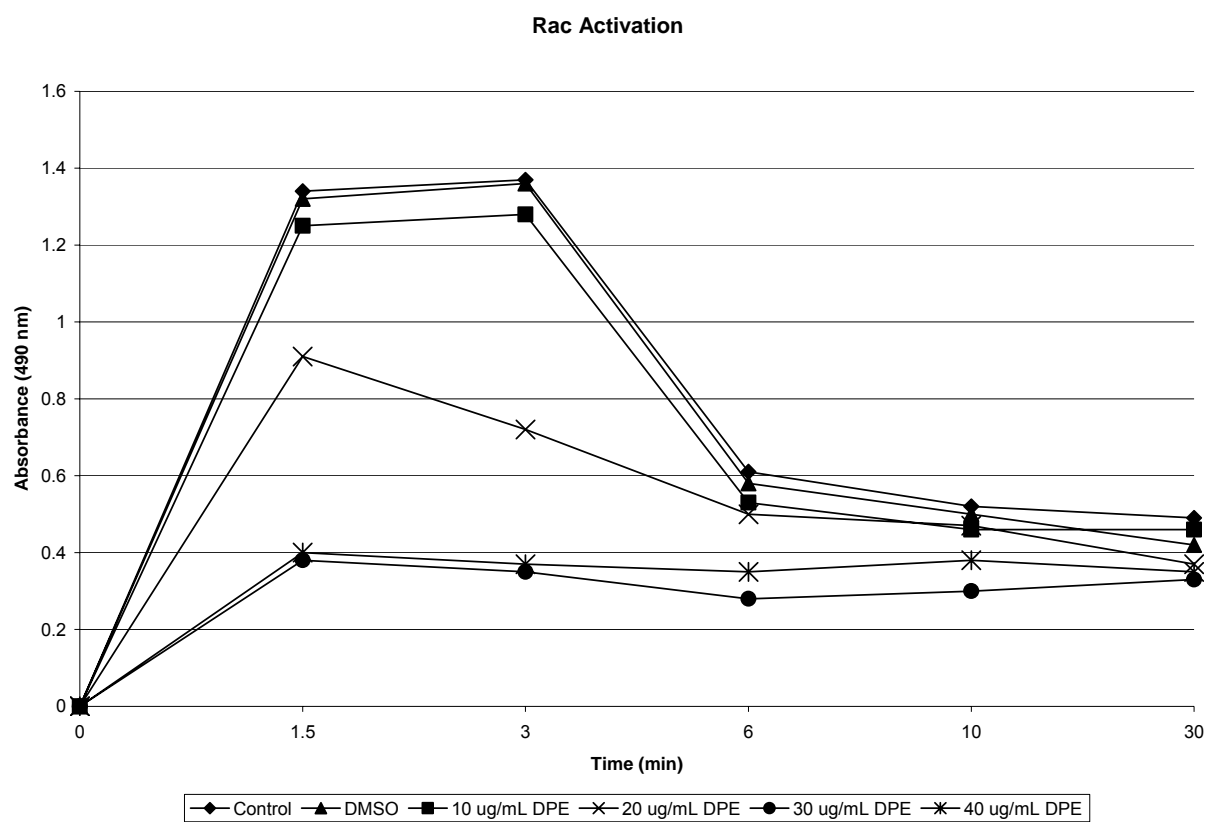


F - 40 $\mu\text{g/mL}$ DPE

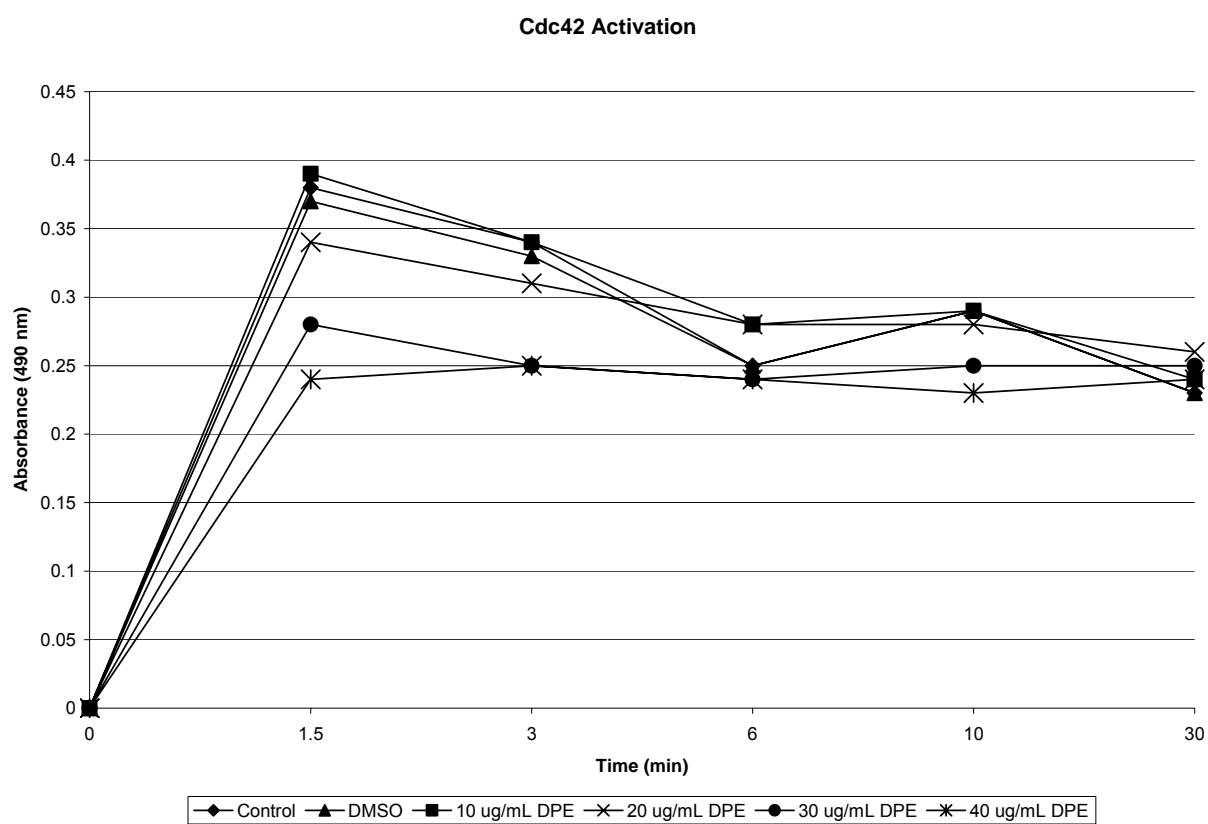
Figure 21. RhoA, Rac, and Cdc42 activity following exposure of HUVEC to 10, 20, 30, or 40 $\mu\text{g/mL}$ DPE: LDH activity as measured by ELISA. Statistical significance from untreated control was determined by Dunnett's Test.



A



B



C

DISCUSSION AND CONCLUSIONS

The developmental toxicity observed with exposure to MTBE or DEP may result from changes in vascular development. As a first step in the identification of possible effects these compounds have on developing vasculature and the determination of the mechanisms involved in these effects, MTBE was tested using an *in vitro* model of angiogenesis and three *in vivo* models, each utilizing a different species.

MTBE is a volatile organic compound used as an octane booster and oxygenating agent in gasoline. The principle route of exposure for humans is inhalation of fumes while refueling; however, oral routes of exposure also exist such as from groundwater contaminated by leaking underground storage tanks. Workers in the petroleum industry exposed to MTBE have reported a high incidence of neurologic symptoms, including headaches, dizziness, and nausea (Moolenaar, et al., 1994; Prah, et al., 1994). While these symptoms are suggestive of vascular involvement, little information is available on the direct effects of MTBE on vasculature. It is hypothesized that exposure to MTBE can induce vascular alterations and thus contribute to aberrations in vascular maintenance and development.

In a previous study in this laboratory, MTBE produced a unique lesion in the developing embryonic vasculature of the Japanese medaka. The embryonic vasculature failed to develop, while other, non-vascular tissues developed normally until vascularization became essential for further development (Kozlosky, et al., 1996). In the current study, exposure to MTBE produced a dose-dependent reduction in vascular tube formation in isolated Fisher-344 rat brain endothelial cells cultured on Matrigel and inhibited migration of endothelial cells into plugs of Matrigel implanted subcutaneously

in mice and in the CAM in the fertilized chicken egg. The mechanisms underlying these effects on the vasculature are unknown.

In the rodent developmental study, no changes in vascular development were observed in any of the rats following either gross or histological examination. It is believed that MTBE and any metabolites are eliminated too quickly under these experimental conditions for developmental vascular lesions to originate. In the piscine embryonic development study, the *in vitro* endothelial cell study, and both the CAM and Matrigel plug work described above, exposure to MTBE is continuous over the length of the experiment. In order for effects to be observed in a whole animal, a multiple daily dose regimen, a continuous infusion or oral intake (such as in the drinking water) of MTBE may be required to maintain adequate blood levels of MTBE over the length of the study.

Microcapillary formation, or angiogenesis, can be mediated by growth factor stimulation of endothelial cells. Activation of the VEGF growth factor receptors VEGFR-1 and VEGFR-2 lead to signal transduction in vascular endothelial cells. Of these two receptors, VEGFR-2 is a possible candidate to be involved in the mechanism of the inhibition of vascular development observed with MTBE. Mice lacking VEGFR-2 have little or no blood vessel formation, suggesting that many downstream effects of VEGF on endothelial cell blood vessel formation are mediated through this receptor (Shalaby, et al., 1995). The lack of vessel formation in the four current experiments, as well as the lesions previously described in the developing piscine embryonic vasculature are similar to those reported in the mice lacking VEGFR-2. Exposure of the developing vasculature to MTBE may inhibit VEGFR-2 function, resulting in loss of tyrosine kinase

activity and subsequent decreases in VEGFR-2 downstream effects such as cell migration and vascular formation. VEGFR-2 contains several autophosphorylation sites. Of these sites, Tyr⁹⁵¹ and Try⁹⁹⁶ both reside in the kinase insert. Tyr⁹⁵¹ was recently shown to be essential for VEGF-A-induced HUVEC migration (Zeng, et al., 2001).

Attempts to explore the ability of MTBE to inhibit phosphorylation of the VEGFR-2 receptor during the course of this investigation met with difficulty. Through the use of immunostaining techniques, several months were invested investigating the ability of MTBE to decrease levels of phosphorylated VEGFR-2. During immunocytochemical staining procedures, cells were very easily washed off the Matrigel. In addition, placement of a coverslip on the slides caused the cells to release from the Matrigel and move to the edges of the field. It appears that during the process of tube formation, HUVEC are not strongly attached to the soft Matrigel matrix. Several slides did produce encouraging results and are presented with the data; however, the time investment and logistical problems of the experiment overcame the value of the results using these techniques. Due to the similarity between the lesion observed in the embryo of the Medaka and those observed in mice lacking VEGFR-2 activity, further investigation into VEGFR-2 as a mechanism in MTBE inhibition of vascular development is warranted.

Microcapillary formation also relies on cell adhesion events mediated by cell surface receptors for extracellular matrix (ECM) proteins. Of these receptors, the integrins have a vital function in the process of angiogenesis. On the outside of the cell, integrins bind to ECM proteins while on the inside the cell, integrins bind elements of the cytoskeleton. (Vouri, 1998). Integrin $\alpha_v\beta_3$ is of special interest in the process of

angiogenesis. Integrin $\alpha_v\beta_3$ is a receptor for the ECM proteins vitronectin and fibrinogen (Cheresh, 1987; Leavesky, et al., 1992; Cheresh, 1993). Antagonists of integrin $\alpha_v\beta_3$ have been shown to selectively activate endothelial cell p53 and increase the expression of the p53-inducible cell cycle inhibitor p21^{WAF1/CIP1} (Stromblad, et al., 1996). Induction of p53 activity in cells undergoing DNA synthesis can lead to apoptosis. Administration of $\alpha_v\beta_3$ antagonists has also been shown to induce apoptosis in growth factor- or tumor cell-activated blood vessels (Brooks, et al., 1994b). These observations involving the inhibition of endothelial cell growth and the induction of apoptosis point to the potential involvement of integrin $\alpha_v\beta_3$ in the mechanism for the lesions reported in the developing embryo of the Japanese medaka and in those observed in the current studies.

In conclusion of the work with MTBE, the present studies indicate that exposure to MTBE can induce alterations in vascular development in several model systems if high enough vascular concentrations are obtained. However, in the rodent reproduction assay, no histological vascular lesions were observed which may reflect the inability to achieve high enough circulating MTBE levels. The data suggest that microvasculature may be a primary target of MTBE and that inhibition of vascular formation *in vitro* and angiogenesis *in vivo* by MTBE may be mediated through VEGFR-2.

In addition to exposure to MTBE, exposure to particulate pollution, especially particles with a diameter less than 2.5 μm , is a major health concern in occupational settings and for the population in general. DP are a major constituent of PM_{2.5} in urban and industrial areas. Studies suggest that exposure to DP during gestation may impair the early development of the placental boundary through the inhibition of blood vessel

formation or angiogenesis leading to various developmental toxicities. The results from these experimental studies can be linked with low term birth weight, intrauterine growth retardation, preterm birth, perinatal mortality, and birth defects observed in epidemiologic studies (Wang et al., 1997; Dejmek et al, 1999; Dejmek et al., 2000; Xu et al., 1995; Pereira et al., 1998; Ha et al., 2001; Loomis et al., 1999; Lipfert et al., 2000). Direct effects on endothelial cells may provide a partial explanation for this adverse effect on capillary growth.

DP are carbon-based particles that adsorb a variety of organic compounds, including PAHs, heterocyclic organic compounds, quinones, aldehydes, aliphatic hydrocarbons, and nitro-PAHs. Both the organic and particulate components of the DP could play a role in possible DP-induced effects on vascular formation. To explore the role of each of these components, varying concentrations of DP, CB, DPE, and WDP were tested for possible effects on HUVEC capillary tube formation on Matrigel.

Initial screening experiments demonstrated that exposure to DP resulted in a concentration-dependent inhibition of capillary tube formation in HUVEC grown on Matrigel. In addition, it was determined that the inhibition of capillary tube formation is due to the actions of the organic component of the particle. At DPE concentrations $\leq 40 \mu\text{g/mL}$, capillary tube formation was inhibited in a concentration-dependent manner with complete inhibition at $40 \mu\text{g/mL}$ and a NOEL of $10 \mu\text{g/mL}$. At $20 \mu\text{g/mL}$ DPE, individual cells began to be observed that were not involved in tube formation. At $40 \mu\text{g/mL}$ DPE, cells were still flattened to the Matrigel matrix; however, tube formation was completely inhibited. At $\geq 50 \mu\text{g/mL}$ DPE, tube formation was completely inhibited and all cells appeared ball-shaped and not flattened to the matrix.

DP have been shown to be endocytosed (Bao, et al., 2007). In that study, cellular granularity was increased by DP treatment in a dose-dependent manner. A similar pattern of granularity was observed in the current study. HUVEC treated with CB, WDP, or lower concentrations of DP show the particles concentrating along the same lines as the formation of the tube networks. This alignment of the particles may be indicative of the particles being endocytosed. Following endocytosis, DP organic compounds become directly available to the cells and affect cellular processes such as angiogenesis.

Using the information gained from the screening studies a series of experiments were run that were aimed at investigating a possible mechanism for the DPE-induced inhibition of HUVEC tube formation. Following treatment with DPE concentrations $\geq 50 \mu\text{g/mL}$, HUVEC appeared ball-shaped and had lost the flattened appearance normally observed when cells initially interact with the Matrigel matrix. Ball shape is one of the morphological changes indicative of apoptosis; therefore, apoptosis was explored as a possible mechanism.

Apoptosis is associated with chemical and morphological features that include enzyme activation, cell shrinkage, chromatin condensation, and nuclear fragmentation. The apoptotic process can be initiated by loss of growth factor binding, loss of adhesion to the ECM, or exposure to cytotoxic compounds (Xia, et al., 1995; Frisch and Francis, 1994; Re, et al., 1994; Zanke, et al., 1996; Lee, et al 1997). First evaluated was the potential for DPE to inhibit HUVEC binding to integrins. Inhibition of integrin binding has been shown to induce apoptosis (Stromblad, et al., 1996). The results of the experiments showed that treatment of HUVEC with DPE concentrations that inhibit

vascular formation (up to 40 $\mu\text{g/mL}$) does not affect the ability of the cells to attach to either fibronectin, vitronectin, collagen IV, or laminin I. Laminin I is a major component of Matrigel; therefore, the results indicate that the ball-shaped appearance of the HUVEC and the inhibition of tube formation upon exposure to DPE are not due to a lack of integrin binding to the ECM.

The next set of experiments explored the possible mechanism of DPE-induced inhibition of tube formation in HUVEC by examining various markers of apoptosis. The parameters investigated were activation of the apoptotic enzyme cascade through the use of caspase-9 and caspase-3 activation assays, changes in cell membrane structure and integrity through immunocytochemical staining using annexin-V and propidium iodide, condensation of chromatin using Hoechst staining, and fragmentation of nuclear material with a DNA fragmentation assay. Also explored was the possibility that the antiangiogenic effects of DPE exposure were due to generalized cell death by measuring LDH release. In all cases, the tests for apoptosis and cell death resulted in data that was comparable to untreated cells. Taken collectively, the results of these assessments support the idea that apoptosis is not the primary mechanism of tube inhibition in this system.

In an effort to directly relate the effects of DP with those observed with the organic extract, a Matrigel Tube Formation assay was run to evaluate the contribution of each component of the DP. Dry residue resulting from the dichloromethane extraction process was approximately 40% by weight of the whole particle. Based on this information, DPE doses of 40, 20, and 10 $\mu\text{g/mL}$ correlate to DP doses of 100, 50, and 25 $\mu\text{g/mL}$ and WDP doses of 60, 30, and 15 $\mu\text{g/mL}$, respectively. The results showed

treatment with 40 $\mu\text{g/mL}$ DPE resulted in a decrease in tube formation that correlated with the respective concentration of DP (100 $\mu\text{g/mL}$). At 50 $\mu\text{g/mL}$ DP/20 $\mu\text{g/mL}$ DPE and 25 $\mu\text{g/mL}$ DP/10 $\mu\text{g/mL}$ DPE, the inhibitory effect produced by the whole particle was greater than that observed with the equivalent fraction of organic extract. The levels of inhibition observed with exposure to 50 $\mu\text{g/mL}$ DP and 25 $\mu\text{g/mL}$ DP were more equivalent to the effects observed in the earlier screening studies where HUVEC were exposed to 40 $\mu\text{g/mL}$ DPE and 20 $\mu\text{g/mL}$ DPE, respectively. At both 50 $\mu\text{g/mL}$ DP and 40 $\mu\text{g/mL}$ DPE, cells were flattened to the Matrigel matrix, but complete inhibition of tube formation was observed. The WDP, which are largely devoid of organic compounds, had no effect on tube formation. These results indicate that there may be a component of the DP that is not extracted with dichloromethane, but is lost in the dichloromethane extraction process, that is responsible for part of the inhibitory effects on HUVEC tube formation observed with whole DP.

As an extension of the equivalent fraction experiment, HUVEC were examined for the ability to recover from the antiangiogenic effects of treatment with DP, DPE, and WDP. The only treatment not showing full recovery of the ability to form a network of capillary tubes on Matrigel were cells treated with 100 $\mu\text{g/mL}$ DP. HUVECs treated with 100 $\mu\text{g/mL}$ DP remained ball-shaped and did not show any signs of tube formation following 24 hr of exposure to fresh, untreated media, yet did recover following each of the correlative treatments. This lack of recovery lends support to the idea that, in addition to the organic fraction, there may be a water-soluble component of the DEP or a component lost or not recovered during the dichloromethane extraction that could potentially be involved in the inhibition of angiogenesis. As previously discussed, DP

adsorb a variety of compounds. From this collection of compounds, it is likely that more than one takes part in the effects observed in endothelial cells.

The final line of investigation into a possible mechanism for the effects of DP on HUVEC focused on the cytoskeleton. Results of the staining of the actin cytoskeleton show a disruption in the organization of actin into filaments in conjunction with the inhibition of tube formation observed with exposure to DPE. Cytoskeletal reorganization of actin microfilaments is regulated by the Rho family of GTPases. Proteins such as RhoA, Rac1, and Cdc42 are key contributors to this process (Chan, et al., 2000). At the leading edge of the cell, Rac1 regulates lamellipodia that pull the cell forward and Cdc42 regulates the formation of filopodia. RhoA is responsible for the formation and maintenance of focal adhesions (Nobes and Hall, 1999). The data show decreased activation of Cdc42 and Rac proteins including Rac1, but no change in activated RhoA when compared to control in HUVEC treated with DPE levels sufficient to inhibit HUVEC tube formation. It has previously been shown that DP and urban dust can cause cytoskeletal dysfunction in macrophages. The cytoskeletal dysfunction caused by these particles was reduced after washing the particles with dichloromethane (Moller, et al., 2002). These results directly correlate with what was observed in the equivalent fraction work. The inhibition of tube formation observed with exposure to DP and DPE was not observed in the equivalent fraction of WDP.

Chemical characterization studies have identified PAH and nitro-PAH in the extractable organic matter from diesel particles (Schuetzle and Lewtas, 1986; Claxton, 1983). PAHs have recently been shown to have a direct effect on HUVEC including the inhibition of tube formation on Matrigel (Andersson, et al., 2009; Chang, et al., 2009;

Kayashima, et al., 2009). In the case of 3-methylcholanthrene, the antiangiogenic effects were shown to be through regulation of Rho GTPases (Chang, et al., 2009). The human endothelium has also been shown to be a target tissue for PAH exposure associated with tobacco smoking (Zhang, et al., 1998). The inhibition of HUVEC tube formation observed with exposure to DP and DPE may be at least partly explained by the presence of PAHs on the surface of the particles.

In conclusion of the work with DP, the current study demonstrates that DP inhibit capillary tube formation *in vitro* and it appears to be the organic component of these particles, not the carbon core, producing this effect. However, the equivalent fraction study shows there may be a component of the whole DP not extracted, but lost in the extraction process, that is partly responsible for the observed inhibitory effects. These studies show that the inhibition of tube formation is not mediated through apoptosis or cell death, but may be caused by cytoskeletal toxicity mediated through the Rho GTPases Rac1 and Cdc42. In addition, results of the recovery assay indicate that the effects produced by DP and DPE are reversible. Further studies are necessary to determine the particle components responsible for these biological effects. The identification of implicated components will allow for a more thorough investigation into the pathways triggered by DP in endothelial cells and to assess the involvement of DP in the developmental effects observed *in vivo*.

Epidemiological and experimental studies have shown that exposure to DP increases the risk of cardiovascular and respiratory issues (Omori, et al., 2003; Pope, et al., 2002). Exposure to DP has also been linked with low term birth weight, intrauterine growth retardation, preterm birth, perinatal mortality, and birth defects in humans and

low uterine weights and decreases in offspring body weight in animals (Dejmek et al., 1999; Dejmek, et al., 2000; Xu, et al., 1995; Pereira, et al., 1998; Ha, et al., 2001; Loomis, et al., 1999; Lipfert, et al., 2000; Yu, et al., 2002; Tsukue, et al., 2002; Fujimoto, et al., 2005). Both DP and organic fractions extracted from particulate material have been shown to have direct effects on endothelial cells *in vitro* and *in vivo* (Bai, et al., 2001; Sumanasekera, et al., 2007; Hirano, et al., 2003; Ying, et al., 2009; Ichinose, et al., 1995). Exposure to MTBE has also been shown to induce developmental toxicity. Inhalation studies in mice indicate that exposure to MTBE can result in decreased pup viability, skeletal malformations and decreases in relative uterine and ovarian weight compared to controls (Conaway, et al., 1985; Moser, et al., 1998).

The vasculature is one of the first systems to form in the embryo and proper configuration is required to allow further development. Before these current studies, little information was available concerning the mechanism responsible for the developmental toxicity observed with exposure to MTBE or DP. This current body of work indicates both MTBE and DP can produce a direct effect on endothelial cells *in vitro* and that the effects observed with exposure to MTBE can also be observed in vascular development *in vivo* and across species. These direct effects lend support to the hypothesis that the developmental effects observed with exposure to MTBE or DP may be due to effects on developing vasculature. In the case of MTBE, the effects may be conveyed through inhibition of activation of the VEGFR-2 and these studies provide evidence that the Inhibition of vascular development by DP may be due to effects on cytoskeletal structure.

REFERENCES

- Akiyama, K. (2006) Gas chromatographic analysis and aerosol mass spectrometer measurement of diesel exhaust particles composition. *Talanta* 70, 178-181.
- Almeida, S. M., Pio, C. A., Freitas, M. C., Reis, M. A., and Trancoso, M. A. (2006) Approaching PM_{2.5} and PM_{2.5-10} source appointment by mass balance analysis, principal component analysis and particle size distribution. *Sci. Total Environ.* 368, 663-674.
- Andersson, H., Piras, E., Demma, J., Hellman, B., and Brittebo, E. (2009) Low levels of the air pollutant 1-nitropyrene induced DNA damage, increased levels of reactive oxygen species and endoplasmic reticulum stress in human endothelial cells. *Toxicol.* 262, 57-64.
- Ayotte, J.D., Argue, D.M., and McGarry, F.J. (2005) Methyl tert-butyl ether occurrence and related factors in public and private wells in southeast New Hampshire. *Environ. Sci. Technol.* 39, 9-16.
- Bai, Y., Suzuki, A. K., and Sagai, M. (2001) The cytotoxic effects of diesel exhaust particles on human pulmonary artery endothelial cells *in vitro*: role of active oxygen species. *Free Rad. Biol. Med.* 30, 555-562.
- Bao, L., Chen, S., Wu, L., Hei, T. K., Wu, Y., Yu, Z., and Xu, A. (2007) Mutagenicity of diesel exhaust particles mediated by cell-particle interaction in mammalian cells. *Toxicology* 229, 91-100.
- Bayless, K.J. and Davis, G.E. (2002) The Cdc42 and Rac1 GTPases are required for capillary lumen formation in three-dimensional extracellular matrices. *J. Cell Sci.* 115, 1123-1136.
- Bayona, J. M., Markider, K. E., and Lee, M. L. (1988) Characterization of polar polycyclic aromatic compounds in a heavy-duty diesel exhaust particulate by capillary column gas chromatography and high-resolution mass spectrometry. *Environ. Sci. Technol.* 22, 1440-1447.
- Becker, S., Mundandhara, S., Devlin, R.B., and Madden, M. (2005) Regulation of cytokine production in human alveolar macrophages and airway epithelial cells in response to ambient air pollution particles: further mechanistic studies. *Toxicol. Appl. Pharmacol.* 207, S269-S275.
- Behymer, T.D., and Hites, R.A. (1985) Photolysis of polycyclic aromatic hydrocarbons adsorbed on simulated atmospheric particulates. *Environ. Sci. Technol.* 19, 1004-1006.
- Behymer, T.D., and Hites, R.A. (1988) Photolysis of polycyclic aromatic hydrocarbons adsorbed on fly ash. *Environ. Sci. Technol.* 22, 1311-1319.

Benjamin, L.E., Hemo, I., and Keshet, E. (1998) A plasticity window for blood vessel remodeling is defined by pericyte coverage of the preformed endothelial network and is regulated by PDGF-B and VEGF. *Development* 125, 1591-1598.

Bennett, P.J. and Kerr, J.A. (1990). Kinetics of the reactions of hydroxyl radicals with aliphatic ethers studied under simulated atmospheric conditions: temperature dependences of the rate coefficients. *J Atmos Chem* 10: 29 – 38.

Beven, C., Neeper-Bradley, T.L., Tyl, R.W., Fisher, L.C., Panson, R.D., Kneiss, J.J., and Andrews, L.S. (1997) Two-generation reproductive toxicity study of methyl tertiary butyl ether (MTBE) in rats. *J. Appl. Toxicol.* 17 (Suppl1), S13-S19.

Biles, R.W.; Schroeder, R.E.; and Holdsworth, C.E. (1987) Methyl tertiary butyl ether inhalation in rats: a single generation reproduction study. *Toxicology and Industrial Health* 3, 519 – 534.

Borm, P. J., and Kreyling, W. (2004) Toxicological hazards of inhaled nanoparticles: potential implications for drug delivery. *J. Nanosci. Nanotechnol.* 4, 521-531.

Broman, M.T., Kouklis, P., Gao, X., Ramchandran, R., Neamu, R.F., Minshall, R.D., and Malik, A.B. (2006) Cdc42 regulates adherens junction stability and endothelial permeability by inducing α -catenin interaction with the vascular endothelial cadherin complex. *Circ. Res.* 98, 73-80.

Brooks, P., Clark, R., and Cheresh, P. (1994a) Requirement of vascular integrin $\alpha v \beta 3$ for angiogenesis. *Science* 264, 569-571.

Brooks, P., Montgomery, A., Rosenfeld, M., Reisfeld, R., Hu, T., Klier, G., and Cheresh, D. (1994b) Integrin $\alpha v \beta 3$ antagonists promote tumor regression by inducing apoptosis of angiogenic blood vessels. *Cell* 79, 1157-1164.

Brown, S.L. (1997) Atmospheric and potable water exposures to methyl tert-butyl ether (MTBE). *Regulatory Toxicology and Pharmacology* 25, 256-276.

Budavari, S., ed., (1996) *The Merck Index*, 12th edition. Whitehouse Station, NJ

Calvert, J.G. and Pitts, J.N.Jr. (1966). *Photochemistry*. John Wiley & Sons, NY. 441-442.

Carmeliet, P., Ferreira, V., Breier, G., Pollefeyt, S., Kieckens, L., Gertsenstein, M., Fahrig, M., Vandenhoek, A., Harpal, K., Eberhart, C., Declercq, C., Pawling, J., Moons, L., Collen, D., Risau, W., and Nagy, A. (1996) Abnormal blood vessel development and lethality in embryos lacking a single VEGF allele. *Nature* 380, 435-439.

Carmeliet, P. and Jain, R.K. (2000) Angiogenesis in cancer and other diseases. *Nature* 407, 249-257.

Cascone, I., Giraudo, E., Caccacari, F., Napione, L., Bertotti, E., Collard, J.G., Serini, G., and Bussolino, F. (2003) Temporal and spatial modulation of Rho GTPases during *in vitro* formation of vascular capillary network. *J. Biol. Chem.* 278, 50702-50713.

Chan, A.Y., Bailly, M., Zebda, N., Segall, J.E., and Condeelis, J.S. (2000) Role of cofilin in epidermal growth factor-stimulated actin polymerization and lamellipod protrusion. *J. Cell Biol.* 148, 531-542.

Chang, C., Tsai, S., Lin, H., Li, H., Lee, Y., Chou, Y., Jen, C., and Juan, S. (2009) Aryl-hydrocarbon receptor-dependent alteration of FAK/RhoA in the inhibition of HUVEC motility by 3-methylcholanthrene. *Cell. Mol. Life Sci.* 66, 3193-3205.

Cheresh, D. (1987) Human endothelial cells synthesize and express an Arg-Gly-Asp directed adhesion receptor involved in attachment to fibronectin and von Willebrand factor. *Proc. Nat'l. Acad. Sci. USA* 84, 6471-6475.

Cheresh, D. (1993) Integrins: structure, function and biological properties. *Advances in Molecular Cell Biology* 6, 225-252.

Claxton, L.D. (1983) Characterization of automotive emissions by bacterial mutagenesis bioassay: a review. *Environ. Mutagen.* 5, 609-631.

Conaway, C.C.; Schroeder, R.E.; and Snyder, N.K. (1985) Teratology evaluation of methyl tertiary butyl ether in rats and mice. *J Toxicol. Environ. Health* 16, 797 – 809.

Connolly, J.O., Simpson, N., Hewlett, L., and Hall, A. (2002) Rac regulates endothelial morphogenesis and capillary assembly. *Mol. Biol. Cell* 13, 2474-2485.

Davidson, J.; Parson, (1996) Remediating MTBE with current and emerging technology. *Proceedings of the Petroleum Hydrocarbons and Organic Chemicals in Groundwater Conference.* November 13 – 15. Houston: 15 – 29.

Davis, G.E. and Camarillo, C.W. (1995) Regulation of endothelial cell morphogenesis by integrins, mechanical forces, and matrix guidance pathways. *Exp. Cell Res.* 216, 113-123.

Davis, G.E., Black, S.M., and Bayless, K.J. (2000) Capillary morphogenesis during human endothelial cell invasion of three-dimensional collagen matrices. *In Vitro Cell. Dev. Biol. Anim.* 36, 513-519.

Davis, G.E., Bayless, K.J. and Mavila, A. (2002) Molecular basis of endothelial cell morphogenesis in three-dimensional extracellular matrices. *Anat. Rec.* 268, 252-275.

Dejmek, J., Selevan, S.G., Benes, I., Solansky, I., and Sram, R.J. (1999) Fetal growth an maternal exposure to particulate matter during pregnancy. *Environ. Health Perspect.* 107, 475-480.

Dejmek, J., Solansky, I., Benes, I., Lenicek, J., and Sram, R.J. (2000) The impact of polycyclic aromatic hydrocarbons and fine particles on pregnancy outcome. *Environ. Health Perspect.* 108, 1159-1164.

Dolske, DAc. and Gatz, D. (1985) A field intercomparison of methods for the measurement of particle and gas dry deposition. *J. Geophys Res.* 90, 2076-2084.

Dormond, O., Foletti, A., Paroz, C., and Ruegg, C. (2001) NSAIDs inhibit α v β 3 integrin-mediated and Cdc42/Rac-dependent endothelial cell spreading, migration, and angiogenesis. *Exp. Cell Res.* 269, 73-87.

Doron, D., Jacobowitz, D., Heldman, E., Feuerstein, G., Pollard, H., and Hallenbeck, J. (1991) Extracellular matrix permits the expression of von willebrand's factor, uptake of di-i-acetylated low density lipoprotein and secretion of prostacyclin in cultures of endothelial cells from rat brain microvessels. *In Vitro Cell. Dev. Biol.* 27A, 689-697.

Draper, W. M., (1986) Quantitation of nitro and dinitropolycyclic aromatic hydrocarbons in diesel exhaust particulate matter. *Chemosphere* 15, 437-447.

Dunan, L.J., Nagy, A., and Fong, G. H., (2003) Gastrulation and angiogenesis, not endothelial specification, is sensitive to partial deficiency in vascular endothelial growth factor-a in mice. *Biol. Reprod.* 69, 1852-1858.

Dunnett, C.W. (1955) A multiple comparison procedure for comparing several treatments with a control. *J. Am. Stat. Assoc.* 50, 1096-1121.

Elder, A. and Oberdorster, G. (2006) Translocation and effects of ultrafine particles outside of the lung. *Clin Occup. Environ. Med.* 5, 785-796.

Eliceiri, B. and Cheresh, D. (1998) The role of α v integrins during angiogenesis. *Molecular Medicine* 4, 741-750.

Etienne-Manneville, S. and Hall, A. (2002) Rho GTPases in cell biology. *Nature* 420, 629-640.

Ferrara, N., Carver-Moore, K., Chen, H., Dowd, M., Lu, L., O'Shea, K.S., Powell-Braxton, L., Hillan, K.J., and Morre, W.M. (1996) Heterozygous embryonic lethality induced by targeted inactivation of the VEGF gene. *Nature* 380, 439-442.

Folkman, J. (1995) Angiogenesis in cancer, vascular, rheumatoid and other disease. *Nat. Med.* 1, 27-31.

Fong, G-H., Rossant, J., Gertsenstein, M., and Breitman, M. (1995) Role of the Flt-1 receptor tyrosine kinase in regulating the assembly of vascular endothelium. *Nature* 376, 66-70.

Frisch, S.M., and Harris, H. (1994) Disruption of epithelial cell-matrix interactions induces apoptosis. *J. Cell Biol.* 124, 619-626.

Froines, J.R.; Collins, M.; Fanning, E.; McConnell, R.; Robbins, W.; Silver, K.; Kun, H.; Mutialu, R.; Okoji, R.; Taber, R.; Tareen, N.; and Zandonella, C. (1998) An evaluation of the scientific peer-reviewed research and literature on the human health effects of MTBE, it's metabolites, combustion products, and substitute compounds. The Center for Occupational and Environmental Health, USC-UCLA Southern California Environmental Health Sciences Center, and the UCLA School of Public Health, UC-Berkeley School of Public Health.

Fujimoto, A., Tsukue, N., Watanabe, M., Sugawara, I., Yanagisawa, R., Takano, H., Yoshida, S., and Takeda, K. (2005) Diesel exhaust affects immunological action in the placentas of mice. *Environ. Toxicol.* 20, 431-440.

Fujiwara, Y.; Kinoshita, T.; Sato, H.; and Kojima, I. (1984). Biodegradation and bioconcentration of alkyl ethers. *Yukagaku* 33: 111 – 114.

Geiser, M., Rothen-Rutishauser, B., Kapp, N., Schurch, S., Krelyling, W., Schulz, H., Semmler, M., Im, H., Heyder, V., and Gehr, J. (2005) Ultrafine particles cross cellular membranes by non-phagocytic mechanisms in lungs and in cultured cells. *Environ. Health Perspect.* 113, 155-1560.

Gerber, H.P., Hillan, K.J., Ryan, A.M., Kowalski, J., Keller, G.A., Rangell, L., Wright, B.D., Radtke, F., Aguet, M., and Ferrara, N. (1999) VEGF is required for growth and survival in neonatal mice. *Development* 126, 1149-1159.

Gerde, P., Muggenburg, B. A., Lundborg, M., Tesfaigzi, Y., and Dahl, A. R. (2001) Respiratory epithelial penetration and clearance of particle-borne benzo[a]pyrene. *Res. Rep. Health Eff. Inst.* 101, 5-25.

Gerhardt, H., Golding, M., Fruttiger, M., Ruhrberg, C., Lundkvist, A., Abramsson, A., Jeltsch, M., Mitchell, C., Alitalo, K., Shima, D., and Betsholtz, C. (2003) VEGF guides angiogenic sprouting utilizing endothelial tip cell filopodia. *J. Cell Biol.* 161,1163-1177.

Gerhardt, H., Ruhrberg, A., Abramsson, A., Fujisawa, H., Shima, D., Betsholtz, C. (2004) Neuropilin-1 is required for endothelial tip cell guidance in the developing central nervous system. *Dev. Dyn.* 231, 503-509.

Ha, E. H., Hong, Y. C., Lee, B. E., Woo, B. H., Schwartz, J., and Christiani, D. C. (2001) Is air pollution a risk factor for low birth weight in Seoul? *Epidemiology* 12, 643-648.

Hakansson, A., Stromberg, K., Pedersen, J., and Olsson, O. (2001) Combustion of gasolines in premixed laminar flames: European certified and California phase 2 reformulated gasoline. *Chemosphere* 44, 1243-1252.

Hakkola, M.A. and Saarinen, L.H. (2000) Customer exposure to gasoline vapors during refueling at service stations. *Appl. Occup. Environ. Hyg.* 15, 677-680.

Hansen, C.S., Sheykhzade, M., Moller, P., Folkman, J.K., Amtorp, O., Jonassen, T., and Loft, S. (2007) Diesel exhaust particles induce endothelial dysfunction in apoE^{-/-} mice. *Toxicol. Appl. Pharmacol.* 219, 24-32.

Hirano, S., Furuyama, A., Koike, E., and Kobayashi, T. (2003) Oxidative-stress potency of organic extracts of diesel exhaust and urban fine particles in rat heart microvessel endothelial cells. *Toxicology* 187, 161-170.

Hoang, M.V., Whelan, M.C., and Senger, D.R. (2004) Rho activity critically and selectively regulates endothelial cell organization during angiogenesis. *Proc. Natl. Acad. Sci. USA.* 101, 1874-1879.

Hong, Y.K., Lange-Asschenfeldt, B., Velasco, P., Hirakawa, S., Kunstfeld, R., Brown, L.F., Bohlen, P., Senger, D.R., and Detmar, M. (2004) VEGF-A promotes tissue repair-associated lymphatic vessel formation via VEGFR-2 and the alpha1beta1 and alpha2beta1 integrins. *FASEB J.* 18, 1111-1113.

Hubbard, C.E.; Barker, J.F.; and Vandegriendt, M. (1994) Transport and fate of dissolved methanol, methyl tertiary-butyl ether, and monoaromatic hydrocarbons in a shallow sand aquifer. Washington, D.C., Health and Environmental Sciences Department. American Petroleum Institute Publication No. 4601: 102 p.

Ichinose, T., Furuyama, A., and Sagai, M. (1995) Biological effects of diesel exhaust particle (DEP). II. Acute toxicity of DEP introduced into lung by intratracheal instillation. *Toxicology* 99, 153-167.

Kappos, A. D., Bruckmann, P., Eikmann, T., Englert, N., Heinrich, U., Hoppe, P., Koch, E., Krause, G. H. M., Kreyling, W. G., Rauchfuss, K., Rombout, P., Schulz-Klemp, V., Thiel, W. R., and Wichmann, H. E.. (2004) Health effects of particles in ambient air. *Int. J. Hyg. Environ. Health* 207, 399-407.

Kayashima, T., Mori, M., Yoshida, H., Mizushina, Y., and Matsubara, K. (2009) 1,4-Naphthoquinone is a potent inhibitor of human cancer cell growth and angiogenesis. *Cancer Letters* 278, 34-40.

Kim, D., Gautam, M., and Gera, D. (2002) Parametric studies on the formation of diesel particulate matter via nucleation and coagulation modes. *Aerosol Science* 33, 1609-1621.

Kiosses, W.B., Shattil, S.J., Pampori, N., and Schwartz, M.A. (2001) Rac recruits high-affinity integrin alphaVbeta3 to lamellipodia in endothelial cell migration. *Nat. Cell Biol.* 3, 316-320.

- Kittleson, D. (1998) Engines and nanoparticles: a review. *J. Aerosol Sci.* 29, 575-588.
- Kniazeva, E. and Putnam, A.J. (2009) Endothelial cell traction and ECM density influence both capillary morphogenesis and maintenance in 3-D. *Am. J. Physiol. Cell Physiol.* 297, C179-C187.
- Kolb, A., and Puttmann, W. (2006) Comparison of MTBE concentrations in groundwater of urban and nonurban areas in Germany. *Water Res.* 40, 3551-3558.
- Korff, T. and Augustin, H.G., (1999) Tensional forces in fibrillar extracellular matrices control directional capillary sprouting. *J. Cell. Sci.* 112, 3249-3258.
- Kozlosky, J., Longo, S., Cooper, K., and Philbert, M. A. (1996). Comparative studies of the acute toxicity of mtbe in japanese medaka and cultured rat brain microvessels. *Fundamental and Applied Toxicology* 30 (Suppl.), 193 (Abstract).
- Lamalice, L., Houle, F., Jourdan, G., and Huet, J. (2004) Phosphorylation of tyrosine 1214 on VEGFR2 is required for VEGF-induced activation of Cdc42 upstream of SAPK2/p38. *Oncogene* 23, 434-445.
- Leavesky, D., Ferguson, G., Wayner, E., and Cheresch, D. (1992) Requirements of integrin $\beta 3$ subunit for carcinoma cell spreading or migration on vitronectin and fibronectin. *J. Cell Bio.* 117, 1101-1107.
- Lee, J.U., Hosotani, R., Wada, M., Doi, R., Kosiba, T., Fujimoto, K., Mori, C., Nakamura, N., Shiota, K., and Imamura, M. (1997) Mechanism of apoptosis induced by cisplatin and VP16 in PANC-1 cells. *Anticancer Res.* 17, 3445-3450.
- Leuschner, U. (1986). Endoscopic therapy of biliary calculi. *Clinical Gastroenterology* 15, 333-358.
- Li, D., Yin, D., and Han, X. (2007) Methyl tert-butyl ether (MTBE)-induced cytotoxicity and oxidative stress in isolated rat spermatogenic cells. *J. Appl. Toxicol.* 27, 10-17.
- Li, D., Chuntao, Y., Gong, Y., Huang, Y., and Han, X. (2008) the effects of methyl tert-butyl ether on the male rat reproductive system. *food Chem. Toxicol.* 46, 2402-2408.
- Li, D., Liu, Q., Gong, Y., Huang, Y., and Han, X. (2009) Cytotoxicity and oxidative stress study in cultured rat Sertoli cells with methyl tery-butyl ether (MTBE) exposure. *Repro. toxicol.* 27, 170-176.
- Li, N., Venkatesan, M. I., Miguel, A., Kaplan, R., Gujuluva, C., Alam, J., and Nel, A. (2000) Induction of heme oxygenase-1 expression in macrophages by diesel exhaust particle chemicals and quinones via the anti-oxidant-responsive element. *J. Immunol.* 165, 3393-3401.

Lin, C.W., Chiang, S.B., Lu, S.J. (2005) Investigation of MTBE and aromatic compound concentrations at a gas service station. *Environ. Monit. Assess.* 105, 181-189.

Lindstrom, A.B. and Pleil, J.D. (1996). Alveolar breath sampling and analysis to assess exposures to methyl tertiary butyl ether (MTBE) during motor vehicle refueling. *Journal of the Air and Waste Management Association* 46: 676-682.

Lioy, P.J.; Weisel, C.P.; Jo, W.; Pellizzari, E.; and Raymer, J.H. (1994) Microenvironmental and personal measurements of methyl tertiary-butyl ether (MTBE) associated with automobile use activities. *Journal of Exposure Analysis and Environmental Epidemiology* 4(4), 427-441.

Lipfert, F. W., Zhang, J., and Wyzga, R. E. (2000) Infant mortality and air pollution: a comprehensive analysis of U. S. data for 1990. *J. Air Waste Manage. Assoc.* 50, 1350-1366.

Liu, Y. and Senger, D.R. (2004) Matrix-specific activation of Src and Rho initiates capillary morphogenesis of endothelial cells. *FASEB J.* 18, 457-468.

Loomis, D., Castillejos, M., Gold, D. R., McDonnell, W., and Borja-Aburto, V. H. (1999) Air pollution and infant mortality in Mexico City. *Epidemiology* 10, 118-123.

Ma, J.Y.C. and Ma, J.K.H. (2002) The dual effect of the particulate and organic components of diesel exhaust particles on the alteration of pulmonary immune/inflammatory responses and metabolic enzymes. *J. Environ. Sci. Health C Environ. Carcinogen. Ecotoxicol. Rev.* 20, 117-147.

Madden, M., Richards, J., Dailey, L., Hatch, G., and Ghio, J. (2000) Effects of ozone on diesel exhaust particle toxicity in rat lung. *Toxicol. Appl. Pharmacol.* 168, 140-148.

Maisonet, M., Bush, T.J., Correa, A., and Jaakkola, J.J. (2001) Relation between ambient air pollution and low birth weight in the northeastern United States. *Environ. Health Perspect.* 109 (Suppl),351-356

Maykut, N., Lewtas, J., Kim, E., and Larson, T. (2003) Source apportionment of PM_{2.5} at an urban IMPROVE site in Seattle, WA. *Environ. Sci. Technol.* 37, 5135-5142.

Moller, W., Hofer, T., Ziesenis, A., Karg, E., and Heyder, J. (2002) Ultrafine particles cause cytoskeletal dysfunctions in macrophages. *Toxicol. Appl. Pharmacol.* 182, 197-207.

Moolenaar, R., Hefflin, B., Ashley, D., Middaugh, J., and Etzel, R. (1994). Methyl tertiary butyl ether in human blood after exposure to oxygenated fuel in Fairbanks, Alaska. *Archives of Environmental Health* 49, 402-409.

Moore, K.A., Polte, T., Huang, S., Shi, B., Alsberg, E., Sunday, M.E., and Ingber, D.E. (2005) Control of basement membrane remodeling and epithelial branching morphogenesis in embryonic lung by Rho and cytoskeletal tension. *Dev. Dyn.* 232, 268-281.

Moran, M.J., Zogorski, J.S., and Squillace, P.J. (2005) MTBE and gasoline hydrocarbons in ground water of the United States. *Ground Water* 43, 615-627.

Moser, G.J.; Wolf, D.C.; Sar, M; Gaido, K.W.; Janszen, D.; and Goldsworthy, T.L. (1998) Methyl tertiary butyl ether-induced endocrine alterations in mice are not mediated through the estrogen receptor. *Toxicol. Sci.* 41(1), 77-87.

NSTC (1997). National Science and Technology Council Committee on Environment and Natural Resources, Interagency Assessment of Oxygenated Fuels.

Nemmar, A., Hoet, P.H., Vanquickenborne, B., Dinsdale, D., Thomeer, M., Hoylaerts, M. F., Vanbilloen, H., Mortelmans, L., and Nemery, B. (2002) Passage of inhaled particles into the blood circulation in humans. *Circulation* 105, 411-414.

Nemmar, A., Hoylaerts, M. F., Hoet, P. H., and Nemery, B. (2004) Possible mechanisms of the cardiovascular effects of inhaled particles: systemic translocation and prothrombotic effects. *Toxicol. Lett.* 149, 243-253.

Nobes, C.D., and Hall, A. (1999) Rho GTPases control polarity, protrusion, and adhesion during cell movement. *J. Cell Biol.* 22, 1235-1244.

Omori, T., Fujimoto, G., Yoshimura, I., Nitta, H., and Ono, P. (2003) Effects of particulate matter on daily mortality in 13 Japanese cities. *J. Epidemiol.* 13, 314-322.

Palmgren, F., Wahlin, P., Kildeso, J., Afshari, A., and Fogh, C. (2003) Characterization of particle emissions from the driving care fleet and the contribution to ambient and indoor particle concentrations. *Phys. Chem. Earth* 28, 327-334.

Pankow, J.F.; Rathburn, R.E.; and Zogorski, J.S. (1996). Calculated volatilization rates of fuel oxygenate compounds and other gasoline-related compounds from rivers and streams. *Chemosphere* 33: 921-937.

Pankow, J.F.; Thompson, N.R.; Johnson, R.L.; Baehr, A.L.; and Zogorski, J.S. (1997). The urban atmosphere as a non-point source for the transport of MTBE and other volatile organic compounds (VOC's) to shallow groundwater. *Environmental Science and Technology* 31: 2821-2828.

Passaniti, A., Taylor, R., Pili, R., Guo, Y., Long, P., Haney, J., Pauly, R., Grant, D., and Martin, G. (1992). Methods in laboratory investigation: a simple, quantitative method for assessing angiogenesis and antiangiogenic agents using reconstituted basement membrane, heparin, and fibroblast growth factor. *Laboratory Investigation* 67, 519-528.

Pereira, L. A., Loomis, D., Conceicao, G. M., Braga, A. L. F., Arcas, R. M., Kishi, H. S., Singer, J. M., Bohm, G. M., and Saldiva, P. H. N. (1998) Association between air pollution and intrauterine mortality in Sao Paulo, Brazil. *Environ. Health Perspect.* 106, 325-329.

Peters, A., Wichmann, H. E., Tuch, T., Heinrich, J., and Heyder, J. (1997) Respiratory effects are associated with the number of ultrafine particles. *Am. J. Resp. Crit. Care Med.* 155, 1376-1383.

Pitts Jr., J.N., Van Cauwenberghe, K.A., Grosjean, D., Schmid, J.P., Fitz, D.R., Belser Jr., W.L., Knudson, G.B., and Hynds, P.M. (1978) Atmospheric reactions of polycyclic aromatic hydrocarbons: facile formation of mutagenic nitro derivatives. *Science* 202, 515-519.

Pitts Jr., J.N., Lokensgard, D.M., riple, P.S., van Cauwenberghe, K.A., van Vaeck, L., Shaffer, S.D., Thill, A.J., and Belser Jr., W.L. (1980) Atmospheric epoxidation of benzo[a]pyrene by ozone: Formation of the metabolite Benzo[a]pyrene-4,5-oxide. *Science* 210, 1347-1349.

Pitts Jr., J.N., Sweetman, J.A., Zielinska, B., Winer, A.M., and Atkinson, R. (1985a) Determination of 2-nitrofluoranthene and 2-nitropyrene in ambient particulate organic matter: evidence for atmospheric reactions. *Atmos. Environ.* 19, 1601-1608.

Pitts Jr., J.N., Zielinska, B., Sweetman, J.A., Atkinson, R., and Winer, A.M. (1985b) Reaction of adsorbed pyrene and perylene with gaseous N_2O_5 under simulated atmospheric conditions. *Atmos. Environ.* 19, 911-915.

Pitts Jr., J.N., Sweetman, J.A., Zielinska, B., Atkinson, R., Winer, A.M., and Harger, W.P. (1985c) Formation of nitroarenes from the reaction of polycyclic aromatic hydrocarbons with dinitrogen pentoxide. *Environ. Sci. Technol.* 19, 1115-1121.

Pitts, Jr., J.N., Paur, H-R., Zielinska, B., Arey, J., Winer, A.M., Ramdahl, T., and Mejia, V. (1986) Factors influencing the reactivity of polycyclic aromatic hydrocarbons adsorbed on filters and ambient POM with ozone. *Chemosphere* 15, 675-685.

Pollard, T.D. and Borisy, G.G. (2003) Cellular motility driven by assembly and disassembly of actin filaments. *Cell* 112, 453-465.

Pope, C. A., III, Thun, M. J., Namboodiri, M. M., Dockery, D. W., Evans, J. S., Speizer, F. E., and Heath, C. W. (1995) Particulate air pollution as a predictor of mortality in a prospective study of U.S. adults. *Am. J. Respir. Crit. Care Med.* 151, 669-674.

Pope C.A., III, Burnett, R.T., Thun, M.J., Calle, E.E., Krewski, D., Ito, K., and Thurston, G.D. (2002) Lung cancer, cardiopulmonary mortality, and long-term exposure to fine particulate air pollution. *JAMA* 287, 1132-1141.

Pope, C. A., III, Burnett, R. T., Thurston, G. D., Thun, M. J., Calle, E. E., Krewski, D., and Godleski, J. J. (2004) Cardiovascular mortality and long-term exposure to particulate air pollution: epidemiological evidence of general pathophysiological pathways of disease. *Circulation*. 109, 71-77.

Poulsen, M.; Lemon, L.; and Baker, J.F.; (1992). Dissolution of monoaromatic hydrocarbons into groundwater from gasoline-oxygenate mixtures. *Env Sci Technol* 26: 2483-2480.

Prah, J., Goldstein, G., Devlin, R., Otto, D., Ashley, D., House, S., Cohen, K., and Gerrity, T. (1994). Sensory, symptomatic, inflammatory, and ocular responses to and the metabolism of methyl tertiary butyl ether in a controlled human exposure experiment. *Inhalation Toxicology* 6, 521-538.

Re, F., Zanetti, A., Sironi, M., Polentarutti, N., Lanfranccone, L., Dejana, E., and colotta, F. (1994) Inhibition of anchorage-dependent cell spreading triggers apoptosis in cultured human endothelial cells. *J. Cell Biol.* 127, 537-546.

Ren, X., Kiosses, W.B., and Schwartz, M.A. (1999) Regulation of the small GTP-binding protein Rho by cell adhesion and the cytoskeleton. *EMBO J.* 18, 578-585.

Rogers, J.F., Thompson, S.J., Addy, C.L., McKeown, R.E., Cowen, D.J., and Decoufle, P. (2000) Association of very low birth weight with exposures to environmental sulfur dioxide and total suspended particles. *Am. J. Epidemiol.* 151, 602-613.

Rogers, J.F., Thompson, S.J., Addy, C.L., McKeown, R.E., Cowen D.J., and Decoufle, P. (2000) Association of very low birth weight with exposures to environmental sulfur dioxide and total suspended particles. *Am. J. Epidemiol.* 15, 602-613.

Sagai, M., Saito, H., Ichinose, T., Kodama, M., and Mori, Y. (1993) Biological effects of diesel exhaust particles. I. *In vitro* production of superoxide and *in vivo* toxicity in mouse. *Free Radical Biology & Medicine*. 14, 37-47.

Salvi, S., Blomberg, A., Rudell, B., Kelly, F., Sandstrom, T., Holgate, S.T., and Frew, A. (1999) Acute inflammatory responses in the airways and peripheral blood after short-term exposure to diesel exhaust in healthy human volunteers. *Am. J. Respir. Care Med.* 159, 702-709.

Samet, V. M., Dominici, F., Curriero, F. C., Coursac, I., and Zeger, S. L. (2000) Fine particulate air pollution and mortality in 20 U.S. cities 1987-1994. *N. Engl. J. Med.* 343, 1742-1749.

Schauer, J., Rogge, W., Hildemann, L., Mazurek, M., Cass, G., and Simoneit, B. (1996) Source apportionment of airborne particulate matter using organic compounds as tracers. *Atmos. Environ.* 30, 3837-3855.

Schmidt, A. and Hall, A. (2002) Guanine nucleotide exchange factors for Rho GTPases: turning on the switch. *Genes Dev.* 16, 1587-1609.

Schuetzle, D., Lee, F. S., and Prater, T. J. (1981) The identification of polynuclear aromatic hydrocarbon (PAH) derivatives in mutagenic fractions of diesel particulate extracts. *Int. J. Environ. Anal. Chem.* 9, 93-144.

Schuetzle, D. (1983) Sampling of vehicle emissions for chemical analysis and biological testing. *Environ. Health Perspect.* 47, 65-80.

Schuetzle, D., and Lewtas, J. (1986) Bioassay-directed chemical analysis in environmental research. *Anal. Chem.* 58, 1060A-1075A.

Sgambato, A., Iavicoli, I., De Paola, B., Bianchino, G., Boninsegna, A., Bergamaschi, A., Pietroiusti, A., and Cittadini, A. (2009) Differential toxic effects of methyl tertiary butyl ether and tert-butanol on rat fibroblasts *in vitro*. *Toxicol. Indust. Health* 25, 141-151.

Shaffer, K.L. and Uchrin, C.G. (1997). Uptake of methyl tertiary butyl ether (MTBE) by groundwater solids. *Bull Environ Contamin Toxicol* 59: 744 - 749.

Shalaby, F., Rossant, J., Yamaguchi, T., Gertsenstein, M., Wu, X-F., Breitman, M., and Schuh, A. (1995). Failure of blood-island formation and vasculogenesis in Flk-1-deficient mice. *Nature* 376, 62-66.

Sieminski, A.L., Hebbel, R.P., and Gooch, K.J. (2004) The relative magnitudes of endothelial force generation and matrix stiffness modulate capillary morphogenesis *in vitro*. *Exp. Cell Res.* 297, 574-584.

Soga, N., Connolly, J.O., Chellaiah, M., Kawamura, J., and Hruska, K.A. (2001a) Rac regulates vascular endothelial growth factor-stimulated motility. *Cell Commun. Adhes.* 8, 1-13.

Soga, N., Namba, N., McAllister, S., Cornelius, L., Teitelbaum, S.L., Dowdy, S.F., Kawamura, J., and Hruska, K.A. (2001b) Rho family GTPases regulate VEGF-stimulated endothelial cell motility. *Exp. Cell Res.* 269, 73-87.

Squillace, P.J., Zogorski, J.S., Wilber, W.G., and Price, C.V., (1996) Preliminary assessment of the occurrence and possible sources of MTBE in groundwater in the United States, 1993 - 1994. *Environmental Science and Technology* 30(5), 1721-1730.

Squillace, P.J.; Pankow, J.F.; Korte, N.E.; and Zogorski, J.S. (1997) Review of the environmental behavior and fate of methyl tert-butyl ether. *Environmental Toxicology and Chemistry* 16(9), 1836 – 1844.

Stromblad, S., Becker, J., Yebra, M., Brooks, P., and Cheresch, D. (1996). Suppression of p53 activity and p21^{WAF1/CIP1} expression by vascular cell integrin $\alpha v\beta 3$ during angiogenesis. *J. Clin. Invest.* 98, 426-433.

Suflita, J.M. and Mormile, M.R. (1993) Anaerobic biodegradation of known and potential gasoline oxygenates in the terrestrial subsurface. *Environmental Science and Technology* 27, 976-978.

Sumanasekera, W. K., Ivanova, M. M., Johnston, B. J., Dougherty, S. M., Sumanasekera, G. U., Myers, S. R., Ali, Y., Kizu, R., and Klinge, C. M. (2007) Rapid effects of diesel exhaust particle extracts on intracellular signaling in human endothelial cells. *Toxicol. Lett.* 174, 61-73.

Tsukue, N., Tsubone, H., and Suzuki, A. K. (2002) Diesel exhaust affects the abnormal delivery in pregnant mice and the growth of their offspring. *Inhal. Toxicol.* 14, 635-651.

Uchirin, C.G.; Haus, K.; Katz, J.; Sabatino, T. (1992) Physical and mathematical simulation of gasoline component migration in ground water systems. *Journal of Exposure Analysis and Environmental Epidemiology* 2: 117 - 131.

U.S. Environmental Protection Agency (1993). Technical Information Review. Methyl tertiary Butyl Ether (CAS No. 1634-04-4). Office of Pollution Prevention and Toxics, U.S. EPA, Washington, D.C.

U.S. Environmental Protection Agency, (1997). Drinking Water Advisory – Consumer acceptability advice and health effects analysis on methyl tertiary-butyl ether (MTBE), EPA822-F-97-009, Office of Water.

U.S. Environmental Protection Agency, (1998). MTBE Fact Sheet #1 – Use and Distribution of MTBE and Ethanol. EPA Office of Solid Waste and Emergency Response. EPA 510-F-97-016.

U.S. EPA, Air Quality Criteria for Particulate Matter, US Environmental Protection Agency, Office of Research and Development, National Center for Environmental Assessment, Research Triangle Park Office, Research Triangle Park, North Carolina, 2004 (vol. I, EPA/600/P-99/002aF, and vol. II, EPA/600/P-99/002bF).

U.S. EPA, Health Assessment Document for Diesel Engine Exhaust, US Environmental Protection Agency, Office of Research and Development, National Center for Environmental Assessment, Washington, DC, 2002 (EPA/600/8-90/057F).

Vayghani, S.A. and Weisel, C.P. (1999) The MTBE air concentrations in the cabin of automobiles while refueling. *Journal of Exposure Analysis and Environmental Epidemiology* 9, 261-267.

Vainiotalo, S. and Ruonakangas, A. (1999) Tank truck driver exposure to vapors from oxygenated or reformulated gasoline during loading and unloading. *Am. Ind. Hyg. Assoc. J.* 60, 518-525.

van Nieuw Amerongen, G.P., Koolwijk, P., Versteilen, A., and van Hinsbergh, V.W. (2003) Involvement of RhoA/Rho kinase signaling in VEGF-induced endothelial cell migration and angiogenesis *in vitro*. *Arterioscler. Thromb. Vasc. Biol.* 23, 211-217.

Vernon, R.B. and Sage, E.H. (1995) Between molecules and morphology. Extracellular matrix and creation of vascular form. *Am. J. Pathol.* 147, 873-883.

Vogt, R., Kirchner, U., Scheer, V., Hinz, K. P., Trimborn, A., and Spengler, B. (2003) Identification of diesel exhaust particles at autobahn, urban, and rural locations using single-particle mass spectrometry during the SCOS97-NARSTO. *Atmospheric Environ.* 37, S239-S258.

Vuori, K. (1998). Integrin Signaling: Tyrosine Phosphorylation Events in Focal Adhesions. *J. Membrane Biol.* 165, 191-199.

Wang, C.H., Lin, S.S., and Chan H.L. (2002) Effects of oxygenates on exhaust emissions from two-stroke motorcycles. *J. Environ. Sci. Health A* 37, 1677-1685.

Wang, X, Ding, H., Ryan, L., and Xu, X. (1997) Association between air pollution and low birth weight: a community-based study. *Environ. Health Perspect.* 105, 514-520.

Watson, J., and Chow, J. (2001) Source characterization of major emission sources in the Imperial and Mexicali Valleys along the US/Mexico border. *Sci. Total Environ.* 276, 33-47.

Whelan, M.C. and Senger, D.R. (2003) Collagen I initiates endothelial cell morphogenesis by inducing actin polymerization through suppression of cyclic AMP and protein kinase A. *J. Biol. Chem.* 278, 327-334.

White, M.C.; Johnson, C.A.; Ashley, D.L.; Buchta, T.M.; and Pelletier, D.J. (1995) Exposure to methyl tertiary-butyl ether from oxygenated gasoline in Stamford, Connecticut. *Archives of Environmental Health* 50(3). 183-189.

Xia, Z., Dickens, M., Raingeaud, J., Davis, R.J., and Greenberg, M.E. (1995) Opposing effects of ERK and JNK-p38 MAP kinases on apoptosis. *Science* 270, 1326-1331.

Xu, X., Ding, H., and Wang, X. (1995) Acute effects of total suspended particles and sulfur dioxides on preterm delivery: A community-based cohort study. *Arch. Environ. Health* 50, 407-415.

Yamawaki, H. and Iwai, N. (2006) Mechanisms underlying nano-sized air-pollution-mediated progression of atherosclerosis - carbon black causes cytotoxic injury/inflammation and inhibits cell growth in vascular endothelial cells. *Circ. J.* 70, 129-140.

Ying, Z., Kampfrath, T., Thurston, G., Farrar, B., Lippmann, M., Wang, A., Sun, Q., Chen, L.C., and Rajagopalan, S. (2009) Ambient particulates alter vascular function through induction of reactive oxygen and nitrogen species. *Toxicol. Sci.* 111, 80-88.

Yu, F., Chapa, G., Fruin, S., Shaw, G., and Harris, J. (2002) Ambient air pollution and birth defects. *Am. J. Epidemiol.* 155, 17-25.

Yue, W., Li, X., Liu, J., Li, Y., Yu, X., Deng, B., Wan, T., Zhang, G., Huang, Y., He, W., Hua, W., Shao, L., Li, W., and Yang, S. (2006) Characterization of PM_{2.5} in the ambient air of Shanghai city by analyzing individual particles. *Sci. Total Environ.* 368, 916-925.

Zanke, B.W., Boudreau, K., Rubie, E., Winnett, E., Tibbles, L.A., Zon, L., Kyriakis, J., Liu, F.F., and Woodgett, J.R. (1996) The stress activated protein kinase pathway mediates cell death following injury induced by cis-platinum, UV radiation, or heat. *Curr. Biol.* 6, 606-613.

Zeng, H., Sanyal, S., and Mukhopadhyay, D. (2001) Tyrosine residues 951 and 1059 of vascular endothelial growth factor receptor-2 (KDR) are essential for vascular permeability factor/vascular endothelial growth factor-induced endothelium migration and proliferation, respectively. *J. Biol. Chem.* 276, 32714-32719.

Zeng, H., Zhao, D., and Mukhopadhyay, D. (2002) KDR stimulates endothelial cell migration through heterotrimeric G protein Gq/11-mediated activation of a small GTPase RhoA. *J. Biol. Chem.* 277, 46791-46798.

Zhang, Y.J., Weksler, B.B., Wang, L., Schwartz, J., and Santella, R.M. (1998) Immunohistochemical detection of polycyclic aromatic hydrocarbon-DNA damage in human blood vessels of smokers and non-smokers. *Atherosclerosis* 140, 325-331.

Zielinska, B. (2005) Atmospheric transformation of diesel emissions. *Exp and Toxicol. Path.* 57, 31-42.

Curriculum Vita

John Charles Kozlosky

Education:

- January 2010 Rutgers, The State University of New Jersey
New Brunswick, New Jersey
Doctor of Philosophy in Environmental Science
- May 1988 University of Medicine and Dentistry of New Jersey
New Jersey Medical School, Newark, New Jersey
Montclair State College, Upper Montclair, New Jersey
Joint Program in Toxicology
Bachelor of Science in Toxicology

Work Experience:

- January 2009 - Present
- Senior Research Scientist/Manager of Operations
Department of Toxicology
Bristol Myers Squibb Pharmaceutical Research Institute
New Brunswick, New Jersey
- September 2004 - January 2009
- Research Scientist II/Study Director
Department of Toxicology
Bristol Myers Squibb Pharmaceutical Research Institute
New Brunswick, New Jersey
- July 2002 - September 2004
- Research Scientist I/Study Director
Department of Toxicology
Bristol Myers Squibb Pharmaceutical Research Institute
New Brunswick, New Jersey

Work Experience (continued):

September 2000 - July 2002

Associate Research Scientist II/Study Director
Department of Toxicology
Bristol Myers Squibb Pharmaceutical Research
Institute
New Brunswick, New Jersey

November 1998 - September 2000

Associate Research Scientist II/Study
Supervisor
Department of Toxicology
Bristol Myers Squibb Pharmaceutical Research
Institute
New Brunswick, New Jersey

April 1992 - November 1998

Associate Research Scientist I/Study
Supervisor
Department of Toxicology
Bristol Myers Squibb Pharmaceutical Research
Institute
New Brunswick, New Jersey

November 1988 - April 1992

Assistant Research Scientist II/Study
Supervisor
Department of Toxicology
Bristol Myers Squibb Pharmaceutical Research
Institute
New Brunswick, New Jersey

May 1988 - November 1988

Associate Scientist
Cell Culture
Schering-Plough
Union, New Jersey

Publications:

Urine acidification has no effect on peroxisome proliferator-activated receptor (PPAR) signaling or epidermal growth factor (EGF) expression in rat urinary bladder urothelium. W. Achanzar, C. Moyer, L. Marthaler, R. Gullo, S.J. Chen, M. French, L. Watson, , J. Rhodes, **J. Kozlosky**, M. White, W. Foster, J. Burgun, B. Car, G. Cosma, and M. Dominick. Toxicology and Applied Pharmacology, 223 (2007) 246-256.